Oleg Zikanov¹

University of Michigan — Dearborn, Dearborn 48128-1491, MI e-mail: zikanov@umich.edu

Ivan Belyaev

Joint Institute for High Temperatures Russian Academy of Science, Izhorskaya Street 13, Building 2, Moscow 125412, Russia e-mail: bia@ihed.ras.ru

Yaroslav Listratov

Moscow Power Engineering Institute, National Research University, Krasnokazarmennaya Street 14, Moscow 111250, Russia e-mail: yaroslav.listratov@gmail.com

Peter Frick

Institute of Continuous Media Mechanics,
Russian Academy of Science,
Ac. Korolev Street 1,
Perm 614013, Russia;
Moscow Power Engineering Institute,
Krasnokazarmennaya Street 14,
Moscow 111250, Russia
e-mail: frick@icmm.ru

Nikita Razuvanov

Joint Institute for High Temperatures Russian Academy of Science, Izhorskaya Street 13, Building 2, Moscow 125412, Russia e-mail: nikita.razuvanov@mail.ru

Valentin Sviridov

Moscow Power Engineering Institute, National Research University, Krasnokazarmennaya Street 14, Moscow 111250, Russia

Mixed Convection in Pipe and Duct Flows With Strong Magnetic Fields

An imposed strong magnetic field suppresses turbulence and profoundly changes the nature of the flow of an electrically conducting fluid. We consider this effect for the case of mixed convection flows in pipes and ducts, in which unique regimes characterized by extreme temperature gradients and high-amplitude fluctuations (the so-called magneto-convective fluctuations) have been recently discovered. The configuration is directly relevant to the design of the liquid-metal components of future nuclear fusion reactors. This review presents the general picture of the flow transformation emerging from the recent studies, illustrates the key known facts, and outlines the remaining open questions. Implications for fusion reactor technology and novel experimental and numerical methods are also discussed. [DOI: 10.1115/1.4049833]

1 Introduction

The physical phenomena discussed in this review belong to the general area of magnetoconvection (also called magnetic convection), i.e., thermal convection occurring in an electrically conducting fluid in the presence of significant electromagnetic effects. Magnetoconvection is known to play an important role in many astrophysical and geophysical systems (e.g., in the dynamics of stellar convective shells and planetary cores [1]). It also appears in advanced technologies, such as the growth of semiconductor crystals [2] or the manufacture of high-quality metals [3].

The focus of this review is primarily on mixed convection flows of liquid metals in pipes and ducts. There are at least two good reasons for this choice. One is the complex, counterintuitive, and unique physics of the flows discovered in recent years. Another is the critical role of such flows in yet another application, namely,

nuclear fusion technology. As discussed, e.g., in Refs. [4-7], liquid metal components are promising and possibly unavoidable parts of the technical solutions for future commercial magneticconfinement (tokamak or stellarator) reactors. It is foreseen that such components will be parts of the inner structure of the reaction vessel. A circulating Li-containing metal (most likely, the eutectic PbLi alloy) will absorb the larger portion of the highly energetic neutrons generated in the fusion reaction as well as a portion of the radiative heat flux. The purpose of the liquid metal components will be three-fold. They will serve as a part of the heat exchange system, in which the energy produced by the fusion reaction is converted into heat and transported into an external power-generating unit. They will also shield the reactor's exterior, especially the superconducting magnets, from radiation. Finally, the interaction between the atoms of Li within the liquid metal and the absorbed neutrons will accomplish the crucial step of generating ("breeding") the tritium fuel for the fusion reaction.

Flows of liquid metals with strong effects of convection and magnetic field will play an especially important role in the blankets of tokamak reactors (see Fig. 1). Historically, the first liquid

¹Corresponding author.

Manuscript received September 30, 2020; final manuscript received January 17, 2021; published online February 18, 2021. Editor: Harry Dankowicz.

metal blanket systems presupposed the usage of only a liquid metal as a coolant and working medium (the self-cooled lead lithium (SCLL) concept [8,9], illustrated in Fig. 1(b)). Problems of extreme MHD pressure drop and electromagnetic interaction between channels have stopped the practical development and testing of this design.

Several competing concepts of blanket modules are currently being pursued [7]. In some, such as the LLCB (lead-lithium cooled ceramic breeder) module shown in Fig. 1(c) [10,11], breeding is done primarily in the solid phase, while liquid PbLi is responsible for cooling and shielding. In others, for example, in the HCLL (helium-cooled lithium-lead) module [12] (see Fig. 1(f)), heat transfer is primarily done by an auxiliary high-pressure He circuit, while slowly circulating PbLi is used mainly for breeding and shielding [13]. In the DCLL (dual coolant lithium-lead) module, shown in Fig. 1(d), PbLi flow is utilized for all three purposes [14]. The WCLL (water cooled lead-lithium) module [15], illustrated in Fig. 1(e), is a concept where water is mainly used for heat removal, while slowly moving liquid metal is a breeding medium and thermal interface.

At this moment, no preference can be given to any of the proposed concepts, since testing them in true reactor conditions is impossible and will not become possible until such reactors are built. First steps will be undertaken in the ITER experimental reactor [7], but further testing in the next generation FNSF (Fusion Nuclear Science Facility) and DEMO facilities [5,16] will certainly be required. It should also be mentioned that the current design of large-scale fusion experiments allows testing of the liquid-metal blanket concepts only in the form of modules of

moderate ($\sim 1\text{-}2\,\text{m}$) size (see Figs. 1(a)-1(f)). As we will discuss at the end of this review, this is a potentially critical limitation preventing the development of truly effective concepts.

Liquid metal flows with strong convection and magnetic field effects are found in other components of a fusion reactor, such as the divertor [17] and the first wall facing the plasma. Various schemes of a "curtain" of flowing liquid Li are currently considered for the latter [18,19].

At present, work on understanding the magnetohydrodynamic (MHD) behavior of liquid metal components is based on laboratory experiments and numerical simulations performed for simplified configurations (see Figs. 1(g) and 1(h) for illustrations). Neither of them leads to fully conclusive answers regarding the actual performance, because neither can approach the extreme conditions of a fusion reactor. Two aspects of these conditions are critically important. One is the extremely strong magnetic field (4) to 12 T is expected in the ITER and DEMO reactors). The field has a dominant toroidal component and a poloidal component, which is much weaker (about 5%) in tokamak reactors of the classical design, including ITER or DEMO (see Fig. 1), but can be up to 40% in more exotic concepts, such as spherical tokamaks. It has to be imposed in the fusion chamber to contain the plasma and inevitably permeates the blanket and divertor areas. Another factor is the very strong heat flux imposed by radiation from the plasma and by neutron absorption. The combined steady heat flux varies between 4 and 20 MW/m² depending on the location within the system and the type and size of the reactor. Much stronger (orders of magnitude higher) pulse loads are expected during plasma disruption events.

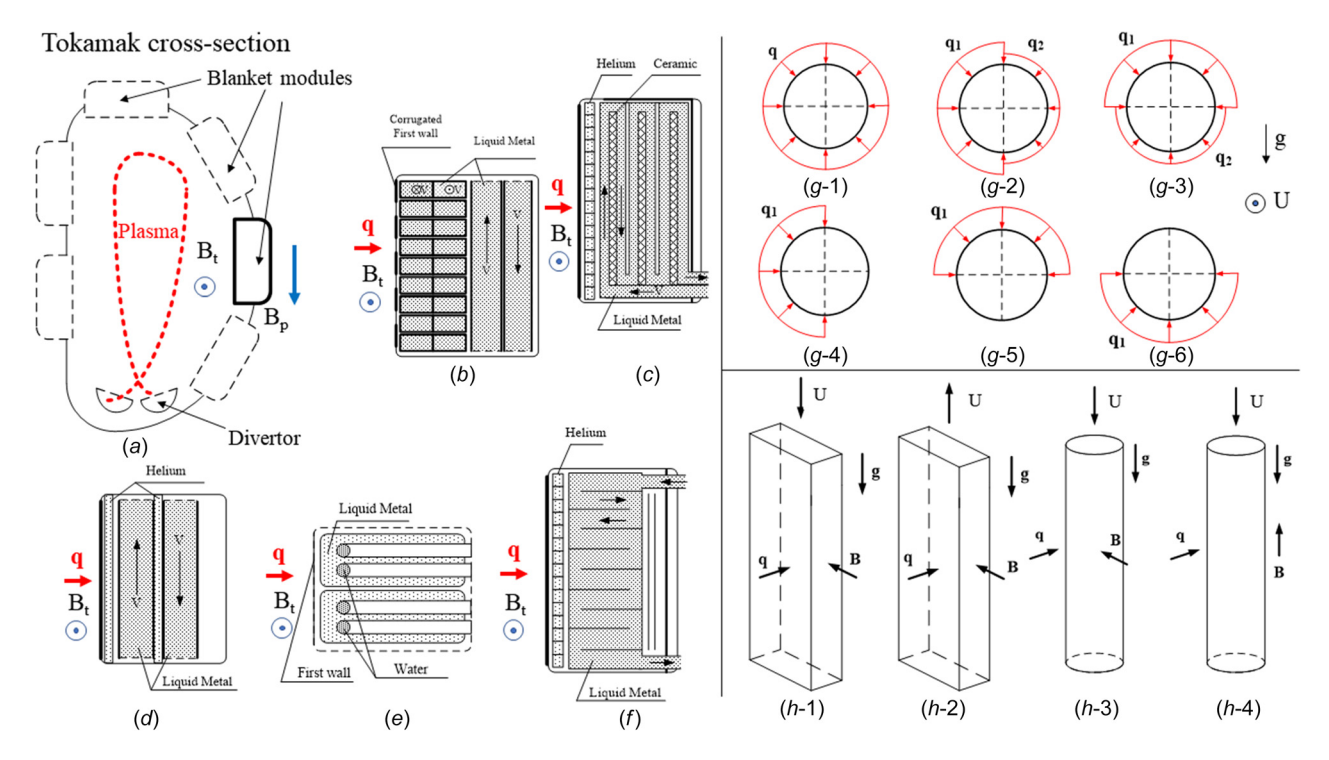


Fig. 1 (a) Schematic representation of the blanket and divertor of a tokamak nuclear fusion reactor. The structure is large (\sim 10 m in height). Blankets of experimental reactors will contain multiple testing modules, including those with a liquid metal circulating through ducts and manifolds. The energy flux in the form of neutrons produced by the fusion reaction and radiation heat flux propagates from the interior of the toroidal vessel. The magnetic field B imposed in the blanket-divertor domain has the dominant toroidal component B_t and the weaker (about 5% in classical tokamak designs) poloidal component B_p . (b–f) Various concepts of liquid-metal blanket modules shown here for the equatorial location (presented by the bold solid line in a). (b) Selfcooled lead-lithium module (SCLL) [8,9]; (c) lead-lithium ceramic breeder module (LLCB) [10,11]; (d) Dual cooled lead-lithium module (DCLL) [14]; (e) Water cooled lead-lithium module (WCLL) [15]; (f) Helium cooled module (HCLL) [12]; (g) Schematic illustration of various wall heating schemes applied in experiments and simulations. Flow in a horizontal pipe is used as an example, although the schemes can be applied to other configurations. (h) Schematic illustration of various combinations of the mean flow U, the imposed magnetic field B, and wall heat flux Q applied in experiments and simulations. Flows in a vertical duct and pipe are used as examples.

We can now present the specific subject of this review. In all the liquid-metal blanket concepts, but especially in those in which strong circulation of a liquid metal is required for the purpose of heat transfer (e.g., in the LLCB and DCLL modules mentioned above), there are flows of liquid metals in ducts and pipes subjected to very strong nonuniform heat fluxes and very strong imposed magnetic fields. The nature of these flows is unique and very different from the nature of the flows commonly studied in the context of heat transfer problems. One reason is the very low Prandtl number of liquid metals (see Sec. 5.2). This fact alone makes it impossible to use the results gathered for conventional fluids, such as water, and demands special approaches to research, in which only liquid metals can be used as model liquids. The very strong heat flux and magnetic field change the nature of the flow further. The recent results to be presented in this review show that these changes are:

- (1) Drastic and paradoxical
- (2) Impossible to predict on the basis of understanding of the effects of heating and magnetic field considered separately
- (3) Having a profound impact on the system's behavior

We must mention from the beginning that, while complex, often unsteady, and poorly understood, the flows considered in this review are very rarely turbulent in the usual sense of this term. The reason, as we explain in Sec. 4, is that turbulent velocity fluctuations are suppressed by strong magnetic fields. This is illustrated in Fig. 2, where the typical values of nondimensional parameters (the Reynolds (Re) and Hartmann (Ha) numbers, to be defined shortly) anticipated in flows within ducts of various liquid-metal blanket concepts are compared with the known range 200 < Re/Ha < 400 of the laminar-turbulent transition in isothermal duct, pipe, and channel flows [22]. We see that, with the exception of the molten salt concept, which we briefly address in Sec. 7.4, flows in all modern blanket concepts cannot generate turbulence by the conventional shear flow transition mechanism.

It must also be stressed that no particular flow configuration or several configurations are more practically relevant than the others and thus deserving to be the particular focus of our review. The multitude of proposed concepts of liquid metal modules and the three-dimensional shape of the blanket structure illustrated in Figs. 1(a)-1(f) imply that flows in a wide range of geometries (cross section shape and length of the tube), orientations with respect to gravity and the magnetic field, heating arrangements, and wall properties must be explored and understood.

The variety of relevant cross section shapes and of the ways the shapes interplay with the flow physics compel us to introduce a consistent and hopefully clear terminology. We will use the word

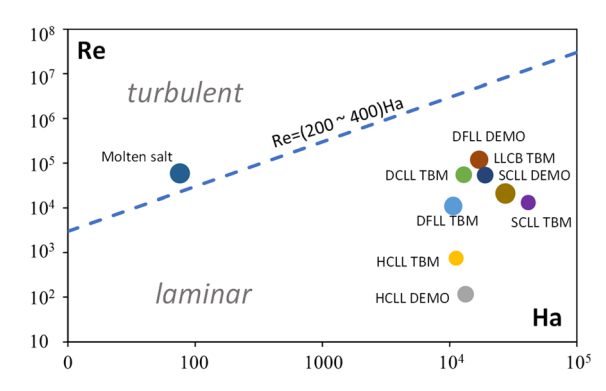


Fig. 2 Typical parameters (Re-and Ha are defined in section 2) of flows in channels of various liquid-metal blanket concepts [5,20,21]. The abbreviations TBM and DEMO indicate the parameters of, respectively, the ITER test reactor and the future commercial demonstration reactor. The range of laminar-turbulent transition in isothermal flows 200 < Re/Ha < 400 [22] is shown.

"pipe" for a pipe of circular cross section, the word "duct" to indicate that the cross section is rectangular, and the word "channel" as a general term applicable to all pipes, ducts, and planar (with infinite spanwise dimension) channels.

2 Governing Equations and Non-Dimensional Parameters

A flow of a single-phase, electrically conducting but not magnetizable liquid in a channel is considered. An externally generated magnetic field is imposed in the flow domain. Heating is applied to the wall, a part of the wall, or internally in the form of a nonuniformly distributed volumetric heating. In correspondence to technological applications, the focus is on the case of mixed convection, when there is a forced flow along the channel and the heating is applied with a constant heat flux. Natural convection is also considered insofar as it is important for understanding the general flow physics.

Three approximations are usually made in numerical and theoretical studies of liquid metal flows. One is the Oberbeck-Boussinesq approximation, according to which the variations of physical properties of the liquid with pressure and temperature are neglected, with the exception of density, for which linear variation with temperature is assumed in the buoyancy force term. One may question the validity of this approximation in the case of flows considered in this review, since, as we demonstrate below, temperature may vary by many tens of degrees within the flow domain (possible concerns and the theoretical framework are discussed in Refs. [23,24]). Analysis of physical data shows that such concerns are rarely justified. For example, considering the Pb-17%Li alloy and taking 870 K as a reference point, we find that an increase of temperature by 50 K results in acceptably low changes of all properties, except the dynamic viscosity and thermal conductivity, for which the change is, respectively, $\sim 10\%$ and \sim 5% [25,26]. The relative magnitude of thermal expansion remains much smaller than 1.

Another commonly used asymptotic approximation is the quasi-static (noninductive) model of the electromagnetic interactions. The approximation is described in books on magnetohydrodynamics, such as [27–30]. In the interesting situation in which the imposed magnetic field is steady and there are no imposed electric currents (the only currents flowing in the fluid are those induced by the moving fluid), the approximation amounts to two simplifications. The perturbations of the magnetic field induced by the electric currents are much weaker than the imposed field and can be neglected in the expressions of Ohm's law and the Lorentz force. As a result of these simplifications, the flow can be described without taking the induced magnetic field into account, in the framework of the model of the one-way effect of the magnetic field on fluid velocity. Furthermore, the electric currents are assumed to adjust instantaneously to changes of velocity field.

As derived in, e.g., [30,31] and validated in many experimental and numerical studies, the quasi-static approximation is accurate when the magnetic Reynolds and Prandtl numbers are both small:

$$\operatorname{Re}_{\mathrm{m}} \equiv \frac{Ud}{\eta} \ll 1, \quad \operatorname{Pr}_{\mathrm{m}} \equiv \frac{\nu}{\eta} = \frac{\operatorname{Re}_{\mathrm{m}}}{\operatorname{Re}} \ll 1$$
 (1)

Here U and d are the typical velocity and length scales, ν is the kinematic viscosity, and $\eta=(\sigma\mu_0)^{-1}$ is the magnetic diffusivity, σ and $\mu_0=4\pi\times 10^{-7}$ H/m being the fluid's electrical conductivity and the magnetic permeability of vacuum.

As we show in Sec. 5.2, liquid metals, molten salts, and electrolytes are characterized by very small values of $Pr_{\rm m}$. Small values of $Re_{\rm m}$ can be found and the quasi-static approximation can be applied for flows with Reynolds numbers as high as $Re \sim 10^5$.

It must be stressed that an increase of Re_m above 1 means that the quasi-static approximation must not be used. As an example, experiments with sodium flows in a closed channel show that the

turbulent magnetic diffusivity (turbulent magnetic viscosity) becomes essential if Re_m , defined through the velocity fluctuations, reaches the order of unity [32]. At the same time, simplifications are still possible at moderate Re_m . Numerical analysis [33] shows that the quasi-linear approximation based on the linearized magnetic induction equation is applicable when $Pr_m \ll 1$ and $Re_m \sim 1-10$.

The third approximation is also routinely used in studies of liquid metal flows. The heat sources corresponding to the Joule and viscous dissipations are neglected in the energy equation. This is justified by the typically very low $(\sim 10^{-7})$ values of the Eckert numbers $\text{Ec} \equiv U^2 (c_p \Delta T)^{-1}$ and/or by high applied thermal load. The thermoelectric Thomson, Peltier, and Seebeck effects can also be neglected with exception of the applications characterized by extreme temperature gradients (see, e.g., [18]).

With these three approximations, the nondimensional governing equations are:

$$\frac{\partial \mathbf{u}}{\partial t} + (\mathbf{u} \cdot \nabla)\mathbf{u} = -\nabla p + \frac{1}{\text{Re}} \nabla^2 \mathbf{u} + \mathbf{F}_{\text{b}} + \mathbf{F}_{\text{L}}$$
 (2)

$$\nabla \cdot \boldsymbol{u} = 0 \tag{3}$$

$$\frac{\partial T}{\partial t} + \boldsymbol{u} \cdot \nabla T = \frac{1}{\text{Pe}} \nabla^2 T + q \tag{4}$$

where u, p, and T are the fields of velocity, pressure, and perturbation of temperature with respect to a reference value. There can be internal heating of volumetric rate q. The nondimensional buoyancy and Lorentz forces are:

$$\mathbf{F}_{b} = -GrRe^{-2}T\mathbf{e}_{g} \tag{5}$$

$$\mathbf{F}_{L} = \mathrm{Ha}^{2} \mathrm{Re}^{-1} \mathbf{j} \times \mathbf{B} \tag{6}$$

where e_g is the unit-length vector in the direction of gravity and B is the nondimensional imposed magnetic field. The density of induced electric currents j can be found via the nondimensionalized Ohm's law

$$\mathbf{i} = -\nabla \mathbf{o} + \mathbf{u} \times \mathbf{B} \tag{7}$$

The electric potential ϕ is a solution of the Poisson equation expressing the electric neutrality of the liquid

$$\nabla^2 \phi = \nabla \cdot (\boldsymbol{u} \times \boldsymbol{B}) \tag{8}$$

One can also use the quasi-static approximation model in the form of the reduced MHD induction equation [29,34]. The electric currents are determined as $\mathbf{j} = \nabla \times \mathbf{b}$, where \mathbf{b} is the field of perturbations of magnetic field caused by the induced currents. \mathbf{b} can be found as a solution of an elliptic equation. The model is physically and mathematically equivalent to the potential-based model introduced above but may lead to different computational approaches [35].

The imposed magnetic field \boldsymbol{B} is generally a three-dimensional field, which may in many cases be accurately approximated as two-dimensional. This has to be reflected by the numerical models in which large flow domains (e.g., entire test sections of experiments), are considered. Reasonably accurate analytical approximations of \boldsymbol{B} (see, e.g., [36]) are available for this purpose. At the same time, experimental and technological systems often have long zones in which the magnetic field is well approximated by a single uniform component. We will refer to it as the main component of the magnetic field or simply as the magnetic field where it is justified by the context.

The discussion in this review will assume the following typical scales leading to the nondimensional system (2)–(8). For forced convection, the typical velocity U and length d are the mean

streamwise velocity and channel width. The latter is determined differently by different researchers, which calls for care in interpreting and comparing the results. In this review, we use the diameter for pipes, the side for duct of square cross section, and the shorter side for rectangular ducts. The nondimensional parameters of other studies mentioned in the discussion are recalculated to these units where necessary.

Different scales – the free-fall velocity $U \equiv (g\beta\Delta Td)^{1/2}$ and the distance d between the hot and cold walls – are utilized for natural convection flows.

A physically relevant definition of the typical temperature scale ΔT in the case of mixed or forced convection is based on the heating rate. For example, when heating is applied to the wall with the typical rate per unit area $q_{\rm w}$, we use

$$\Delta T \equiv \frac{q_{\rm w}d}{\kappa} \tag{9}$$

where κ is the thermal conductivity of the fluid. In the case of volumetric heating, q_0 is the typical rate per unit volume, and the expression is

$$\Delta T \equiv \frac{q_0 d^2}{\kappa} \tag{10}$$

The symbol q is used in the following discussion for the spatial distribution of the nondimensional heat flux in both the wall-heating and internal heating configurations.

The definition of ΔT as the temperature difference between the hot and cold walls is applied for natural convection flows.

The maximum magnetic field strength B_0 is used for the magnetic field. The derived values ρU^2 , $\sigma U B_0$, and $d U B_0$ are used as the typical scales of pressure, current density, and electric potential.

The nondimensional parameters are:

$$Re \equiv \frac{Ud}{\nu} - Reynolds number$$
 (11)

$$Pr \equiv \frac{\nu}{\gamma} - Prandtl number \tag{12}$$

$$Ha \equiv B_0 d \left(\frac{\sigma}{\rho \nu}\right)^{1/2} - \text{Hartmann number}$$
 (13)

$$Gr \equiv \frac{g\beta\Delta Td^3}{v^2} - Grashof number$$
 (14)

$$Pe \equiv RePr = \frac{Ud}{\chi} - Peclet number.$$
 (15)

Here, χ and β are the thermal diffusivity and thermal expansion coefficients. The Rayleigh number

$$Ra \equiv GrPr$$
 (16)

can be used instead of Gr.

The strength of the magnetohydrodynamic effect is evaluated by the Hartmann number. More specifically, Ha², which is sometimes referred to as the Channdrasekhar number, estimates the typical ratio between the Lorentz and viscous forces. Alternatively, one can use the Stuart number (also called the magnetic interaction parameter)

$$N \equiv \frac{\mathrm{Ha}^2}{\mathrm{Re}} = \frac{\sigma B_0^2 d}{\rho U} \tag{17}$$

estimating the ratio between the Lorentz and inertial force.

Similarly, the ratio between the buoyancy and inertia force is estimated by the Richardson number

$$Ri \equiv \frac{Gr}{Re^2} = \frac{g\beta\Delta Td}{U^2}$$
 (18)

Finally, we mention the Reynolds number based on the thickness of the Hartmann boundary layer as the typical length

$$Rh \equiv \frac{Re}{Ha} = \frac{U\delta_{H}}{\nu}$$
 (19)

This parameter is known to largely determine the hydrodynamic laminar-turbulent transition in parallel shear flows with electrically insulating walls and a strong magnetic field effect [22].

The Prandtl number is typically very low for liquid metals (between 0.01 and 0.1). The values of the other parameters vary, but the most interesting and technologically relevant effects are observed at moderate $10^3 \le \text{Re} \le 10^5$ and large $10^8 \le \text{Gr} \le 10^{12}$, $200 \le \text{Ha} \le 10^4$.

The standard boundary conditions at solid walls are those of no slip for velocity (the effect of partial slip in MHD duct flows with high Ha is explored in Ref. [37]).

For electric potential and temperature, the easiest approach is to assume the idealized conditions of perfectly conducting (constant ϕ or T) or perfectly insulating (zero wall-normal derivatives of ϕ or T) walls. A conjugate transport problem for heat or electric charges has to be solved when these asymptotic approximations are invalid. The effect of wall conductance is further discussed in Sec. 7.1.

For the electric potential, the commonly used control parameter is the wall conductance ratio

$$C_{\rm w} \equiv \frac{\sigma_{\rm w} d_{\rm w}}{\sigma d} \tag{20}$$

where $\sigma_{\rm w}$ and $d_{\rm w}$ are the electric conductivity and thickness of the wall. $C_{\rm w}=0$ and $C_{\rm w}=\infty$ correspond, respectively, to a perfectly insulating and perfectly conducting wall. We note that the high values of σ typical for liquid metals mean that $C_{\rm w}$ can be quite small even when walls are made of electrically conducting materials. In many cases, this justifies use of the insulating wall model in numerical and theoretical analysis.

As an example, excellent quantitative agreement is found between the majority of the experiments reviewed in Sec. 6 and the results of computations conducted at $C_{\rm w}=0$. The experiments are performed with mercury as a working fluid and stainless steel walls, and have $C_{\rm w}<0.05$. No accurate estimates are available for the possible contribution of the contact resistance between the liquid metal and the wall, but it is clear that it increases the cumulative electric resistivity of the wall and, thus, further improves the accuracy of the insulating wall approximation.

If $d_{\rm w} \ll d$, the thin-wall model relying on the transport equations integrated across the wall is applicable [28,34].

Mixed convection flows in channels evolve downstream under the action of heating and magnetic field. This means that in many cases the entire domain of interest, for example, the entire test section of an experiment or the entire straight portion of a duct of a blanket, has to be considered in the analysis. The typically chosen inlet and exit conditions are those of a prescribed \boldsymbol{u} and T and a zero streamwise gradient of φ at the inlet and some soft (zero streamwise gradient or convective) conditions at the exit. In blanket design, complex and yet poorly understood 3D effects of entry into the channel from a connecting manifold (see Figs. 1(b)-1(e)) may need to be considered. Further discussion of inlet and exit conditions and their impact on the flow can be found in Sec. 7.3 of this review.

An alternative approach based on the modified version of the governing Eqs. (2)-(4) is helpful in numerical and theoretical

analysis of mixed convection flows. In addition to being convenient, it reflects fundamental features of flow physics, some of which, as we will see later, are particularly pronounced in flows strongly affected by magnetic fields. The modification is based on the separation of the mean flow fields, which are functions of the streamwise coordinate, from fluctuations that, in the case of a fully developed flow, are statistically uniform along this coordinate and therefore suitable for simulations in a channel's segment with cyclic inlet-exit conditions.

The first step of the modification is standard. We separate the pressure field $\hat{p}(x)$, which is a linear function of x and whose gradient drives the flow. The second step is commonly used in studies of heat transfer in channels. Applying the energy balance to a segment, we find that unless there are perfectly conducting walls, the energy flux supplied by the wall or internal heating must be balanced by the streamwise convection heat transfer. The average and mean-mixed temperatures defined as

$$\bar{T}(x) \equiv \frac{\int_A T dA}{A}, \quad T_m(x) = \frac{\int_A u_x T dA}{\int_A u_x dA}$$
 (21)

where A is the channel's cross section, grow downstream. The standard decomposition is

$$T = T_{\rm m}(x) + \theta(x, t), \tag{22}$$

where θ is the field of temperature fluctuations, which are statistically uniform in the streamwise direction.

There is a nontrivial consequence of (22) for flows in nonvertical channels. The buoyancy force associated with $T_{\rm m}$

$$\mathbf{F}_{\rm bm} = -\text{GrRe}^{-2}T_{\rm m}(x)\mathbf{e}_{\rm g} \tag{23}$$

has a nonzero curl and thus modifies the velocity field. As discussed in Refs. [38–41], its action on the flow can be described by introducing the pressure field \tilde{p} , such that its vertical component of its gradient balances $\emph{\textbf{F}}_{bm}$. $\tilde{\emph{p}}$ is a two-dimensional function increasing with the streamwise coordinate x and vertical coordinate z' (see Fig. 3). Its z-dependent gradient $\partial \tilde{p}/\partial x$, which appears in the respective momentum equation, generates a flow in the positive x-direction in the lower part of the channel and in the negative x-direction in the upper part. The result is a top-bottom asymmetry of the streamwise velocity profile and of the associated convection heat flux. Recent numerical studies [40-43] show that this may have a remarkably profound effect on flows with strong heating and strong magnetic fields. We should note that a similar effect has been known for a long time for natural convection systems. A horizontal temperature gradient in horizontally extended systems generates a near-bottom flow in the direction of the

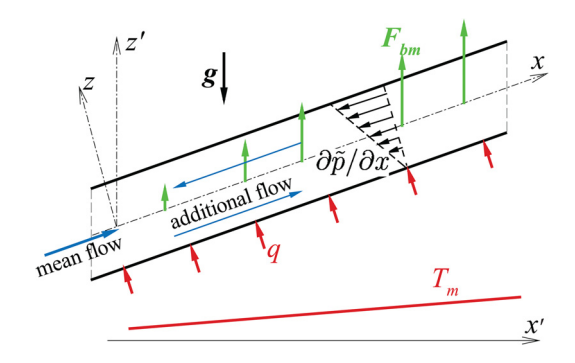


Fig. 3 Illustration of the effect on flow in nonvertical channels of the buoyancy force associated with the mean temperature. A typical distribution of the mean-mixed temperature $T_{\rm m}$ (see (21)) is also shown. See text for notation.

gradient and a reversed flow above, providing a stable stratification [44].

The pressure field is thus decomposed as

$$p = \hat{p} + \tilde{p} + p'(\mathbf{x}, t), \tag{24}$$

where p' is the fluctuation field, which is statistically uniform in the streamwise direction. The fields \hat{p} and \tilde{p} are determined by the mean flow parameters.

As an example, we will write the modified equations for a fully developed channel in a horizontal tube with a part of the wall heated at a uniform constant rate and the rest of the wall perfectly thermally insulated [40–43]. In nondimensional units

$$\frac{dT_{\rm m}}{dx} = \frac{d\bar{T}}{dx} = \frac{P}{APe} = \text{const}$$
 (25)

where P is the nondimensional perimeter of the heated portion. The field \tilde{p} is expressed as

$$\tilde{p}(x,z) = \frac{Gr}{Re^2} \frac{dT_m}{dx} xz$$
 (26)

The governing equations become

$$\frac{\partial \mathbf{u}}{\partial t} + (\mathbf{u} \cdot \nabla)\mathbf{u} = -\nabla p' - \nabla \hat{p} - \nabla \tilde{p} + \frac{1}{\text{Re}} \nabla^2 \mathbf{u} + \mathbf{F}_{\text{b}} + \mathbf{F}_{\text{L}}$$
 (27)

$$\nabla \cdot \boldsymbol{u} = 0, \tag{28}$$

$$\frac{\partial \theta}{\partial t} + \boldsymbol{u} \cdot \nabla \theta = \frac{1}{\text{Pe}} \nabla^2 \theta - u_x \frac{dT_{\text{m}}}{dx} + q \tag{29}$$

with the forces

$$\mathbf{F}_{b} = -GrRe^{-2}\theta \mathbf{e}_{g} \tag{30}$$

$$\mathbf{F}_{L} = \mathrm{Ha}^{2} \mathrm{Re}^{-1} \mathbf{j} \times \mathbf{B} \tag{31}$$

and the electric currents computed as in (7)–(8). All the solution variables $(u, \theta, p', \text{ and } \phi)$ can now be considered as statistically uniform along the channel and modeled in a relatively short segment with cyclic inlet-exit conditions.

3 Convection at Low Prandtl Numbers

We will foreword the main discussion by a brief review of the general effects of low values of Pr on convection flows. Some of the effects are obvious. The temperature field has much weaker gradients and thicker boundary layers than the velocity field. The contribution of conduction to heat transfer is higher than in liquids with larger Pr. Other effects are less evident and appear in specific configurations.

3.1 Natural Convection at Low Pr. Our discussion will focus on the classical and most thoroughly studied system, namely, the Rayleigh-Bénard convection (RBC). For fully turbulent regimes ($\sqrt{Gr}\gg 1$), one of the key questions is that of the dependence of the dimensionless heat flux, characterized by the Nusselt number Nu, on the parameters of the convective flow (Ra and Pr) and the geometry of the cavity. An analysis of experimental data shows that one can identify up to ten regions in the parameter plane (Ra, Pr) differing from each other by the character of the heat and mass transfer in the boundary layers and in the core, and, as a result, by different power laws in the form Nu $\sim Ra^{\gamma} Pr^{\alpha}$ [45]. As these pure regimes intermix, and the observational regime is rather small in Ra and/or Pr, in practice only effective scaling exponents are observed.

The peculiarity of liquid metal convection is primarily due to the typically low values of the Prandtl number. This means that the viscous length scale is much smaller than the heat conduction length scale. This affects both the bulk turbulence (the Reynolds number is much higher than the Peclet number) and boundary layers, because the thermal boundary layer at low Pr is considerably thicker than the kinetic boundary layer. The Grossmann-Lohse theory [45] predicts a regime at moderate Rayleigh numbers (Ra $\leq 10^9-10^{10}$) in which most of the kinetic energy is dissipated in the turbulent core and the heat dissipation dominates in the boundary layers. In this regime

$$Nu \sim Ra^{1/5}Pr^{1/5}$$
 (32)

With further growth of Ra, most of the energy of the temperature fluctuations is also dissipated in the turbulent core. The theory predicts a regime with

$$Nu \sim Ra^{1/2}Pr^{1/2}$$
 (33)

Note that in both the low-Pr regimes $\alpha = \gamma$.

Among the numerous experiments on turbulent RBC, there are not many experiments with liquid metals. The RBC in sodium has been investigated in a set of *short* vertical cylinders with $0.03 \le$ $H/D \le 0.22$ and Pr = 0.006 [46], where a power law Nu \sim Ra^{0.25} was observed for $2 \times 10^4 \le Ra \le 10^6$. There are some liquid metal experiments with $H \approx D$. Turbulent convection of mercury (Pr ≈ 0.025) in a cylinder with H = D provided $\gamma =$ 0.26 ± 0.02 (for $7 \times 10^6 < \text{Ra} < 5 \times 10^8$) [47,48] and $\gamma =$ 0.20 ± 0.02 (for $5 \times 10^8 \le \text{Ra} \le 2 \times 10^9$) [48]. Experiments with gallium (Pr ≈ 0.025) gave $\gamma \approx 0.25$ for $2 \cdot 10^6 < Ra < 10^8$ [49] and experiments with GaInSn (Pr ≈ 0.029) provide $\gamma =$ 0.27 ± 0.02 (for $4 \times 10^6 \le \text{Ra} \le 6 \times 10^7$) [50]. Experiments with mercury in cylinders with H = D and H = 2D revealed a power law relation with $\gamma = 2/7 \approx 0.286$ over the range $10^5 < \text{Ra} <$ 10^{11} [51]. Recent experiments with liquid sodium (Pr = 0.0094) in a cell of unit aspect ratio (H = D) showed a slightly lower value of the scaling exponent: $\gamma \approx 0.22$ for $4 \times 10^6 < \text{Ra} < 2 \times 10^7$

Direct numerical simulations of liquid metal RBC have been limited to moderate Ra, with the exception of the recent study [53] where $Ra \le 10^9$ were considered. They demonstrate consistent results with good agreement with experiments in terms of the Nu versus Ra scaling [52,54,55]. At the same time, the experimentally measured values of Nu tend to be lower than those obtained in computations. This can be partially attributed to the difficulties of convection experiments with liquid metals discussed in Sec. 5.2. One should also mention the difficulties of numerical simulations of turbulent convection flows in low-Pr fluids (see, e.g., [56]) and flows with strong magnetic field effects (see the discussion in Sec. 5.3).

The elongation of the convective cell changes the heat transport and the dependence Nu(Ra). Confining ourselves to the case of RBC in liquid sodium, we note that in a channel with L=5D the effective heat flux displays a law Nu \sim Ra^{0.43} [57], while in a cylinder L=20D the scaling exponent γ increased further, to Nu \sim Ra^{0.77} [58].

3.2 Mixed convection at Low Pr. If both forced and natural convection exist in the flow, their relative importance is determined by the magnitude of the Richardson number Ri. The extreme cases of $Ri \ll 1$ or $Ri \gg 1$ are characterized by the dominance of, respectively, forced or natural convection, in which only one of these effects needs to be considered. More interesting and important for us is the case of a true mixed convection, in which Ri is neither very large nor very small, so both effects play significant roles. The impact of natural convection is highly case-specific in that case. One example is the effect of natural convection on turbulent heat transfer. In the majority of turbulent

flows, the heat transfer is mainly provided by turbulent mixing. Depending on the configuration, the buoyancy either enhances or suppresses the turbulence and thus either increases or decreases the heat transfer [59–61]. The situation is different in liquids with very low Pr (e.g., in liquid Na). The molecular conductivity remains essential in such liquids, even when the flow is turbulent, and the influence of buoyancy can be similar to that in laminar flows [62].

The role of buoyancy in mixed convection typically increases with decreasing Pr. While not universal, this statement is certainly true for flows in channels because of the thicker thermal boundary layers. Zones of significant gradient of mean temperature and thus significant buoyancy force are not limited to near-wall regions but penetrate into the bulk of the flow.

In vertical or inclined channels, the buoyancy force can act downstream (an upward forced flow) or upstream (a downward forced flow), transforming the velocity profile (see Fig. 4 for an illustration). The transformation can include generation of inflection points, which in turn leads to instability and transition to turbulence at lower Re. In upward flows, the velocity increases near the heated walls and, at a given mean flowrate, decreases in the central part of the duct (Figs. 4(c) and 4(d)), possibly with formation of an M-shaped profile (Fig. 4(d)). In downward flows, the velocity is reduced or even reversed near the heated walls (Figs. 4(a) and 4(b)). The peculiar physical effect of the so-called "elevator modes" may appear in such configurations. The modes have been observed in both natural and mixed convection [63-65]. They are exact solutions of the Boussinesq equations in vertically unbounded systems, where they have the form of exponentially growing pairs of streamwise-uniform ascending/ descending jets with the possibility of nonlinear saturation at high amplitudes. Albeit not as exact solutions, physically similar flow regimes are possible in long finite ducts. The critical role of the elevator modes in flows with strong magnetic fields will be discussed in Sec. 6.2.

The buoyancy forces also strongly affect flows in horizontal channels. Stable stratification suppresses turbulence and can laminarize the flow [66,67]. Note that the stable stratification may appear not only in channels heated from above. As discussed in Sec. 2, the downstream growth of mean-mixed temperature, which occurs, e.g., at constant-rate heating applied internally or to a wall, results in a significant top-bottom asymmetry of streamwise velocity. The forced streamwise heat flux is stronger in the bottom than in the top part of the channel. At large Ri, this may result in stable stratification, even when the imposed heat flux is not directed downwards. Examples of such behavior are found, e.g., in a duct heated from the side [42] or volumetrically [68].

The general case of unstable stratification can be identified with its best known representative – the Poiseuille-Bénard problem,

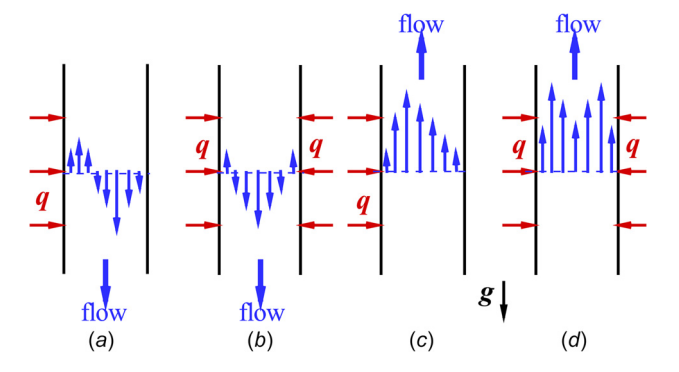


Fig. 4 Schematic illustration of the effect of buoyancy forces on mixed convection in vertical channels. Laminar velocity profiles in the cases of downward ((a) and (b)) and upward ((c) and (d)) mean flow and with asymmetric ((a) and (c)) and symmetric ((b) and (d)) constant-rate heating of the walls are shown. See text for discussion.

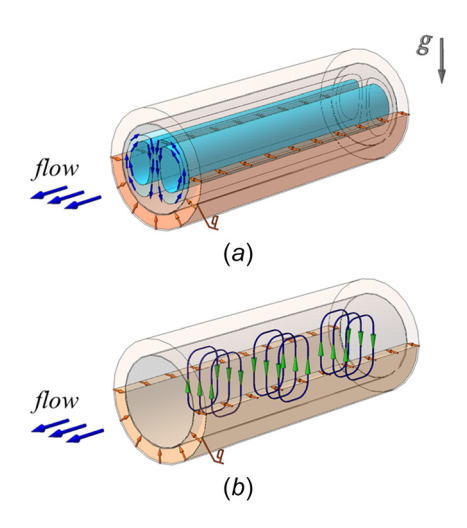


Fig. 5 Schematic illustration of convection instability modes in a horizontal pipe with unstable stratification. Longitudinal (a) and transverse (b) modes are shown. See text for discussion.

i.e., a flow in a channel with a heated bottom. A laminar flow loses its stability to longitudinal (oriented along the duct), transverse, or oblique rolls (see Fig. 5) depending on the values of Ra and Re, the shape of the transverse cross section, and the boundary conditions (see, e.g., [69] and references therein). Instability to longitudinal rolls is not affected by the streamwise velocity and usually occurs at lower Ra than to transverse or oblique rolls (we will see in Sec. 6.1 that the situation is drastically different in flows with strong transverse magnetic fields). In ducts of moderate aspect ratio and round pipes, longitudinal rolls with liquid rising along sidewalls (see Fig. 5(a)) persist in turbulent states as elements of the mean flow

4 Effects of Magnetic Field

The principal physical mechanisms by which an imposed magnetic field transforms a flow of an electrically conducting fluid are relatively well understood. We briefly survey them in this section, while focusing on the aspects critical for the central subject of this review. It has to be stressed that the discussion is limited to flows satisfying the quasi-static (low Re_m and Pr_m) approximation described in Sec. 2.

4.1 Suppression of Turbulence and Development of Anisotropy. These effects are directly related to the Joule dissipation of the electric currents that are induced when an electrically conducting fluid flows in a magnetic field. The dissipation serves as an additional (to the viscous dissipation) mechanism of conversion of the flow's kinetic energy into heat. As a result, MHD flows are found in a laminar or transitional state at much higher control parameters (, e.g., Re or Ra) than hydrodynamic flows of the same type.

The Joule dissipation has an important property that is the key source of the special nature of MHD flows. Unlike its viscous counterpart, the Joule dissipation is anisotropic. Its rate is proportional to the square of the velocity gradient in the direction of the magnetic field [70,71]. Flow structures with largest such gradients generate the strongest currents and experience the strongest suppression due to the Joule dissipation. Structures that are uniform along the field lines generate no electric currents and no Joule dissipation and thus are not affected by the magnetic field. The flow as a whole becomes anisotropic, with its structures elongated along the magnetic field lines.

It must be stressed that the term anisotropy is used here with the meaning of dependence of velocity gradients and typical length scales of the flow on the spatial direction. The anisotropy of magnitude of velocity components (and the Reynolds stresses) usually follows, but it is not caused directly by the magnetic field and has a nonuniversal nature, strongly influenced by initial conditions, boundaries, and other specific flow features [72–75].

The degree of the flow transformation is largely determined by the value of the Stuart number N. At moderate N, $(N \sim 1)$ if the definition (17) is based on the rms velocity and integral length scale), the flow remains turbulent, but acquires noticeable anisotropy and modified statistical properties (e.g., a steeper inertial-range slope of the energy spectrum) [72,73,76,77].

At large N, the flow's transformation is more profound. It includes (i) full suppression of turbulence and (ii) quasi-two-dimensionality. The latter term describes the state of the flow in which all its variables are uniform (or nearly uniform with very weak gradients) along the magnetic field lines in the core of the flow. The uniformity ceases within the boundary layers at the walls crossing the field lines, where sharp gradients appear to satisfy the boundary conditions. Pure two-dimensionality is possible in systems without such walls [68,72,78,79].

4.2 Transformation of Flows in Channels. The geometry and electric conductivity of walls affect the distribution of electric currents and Lorentz forces in the flow domain. The resulting modification of flow structure and properties can be very strong if Ha and N are large. A detailed discussion can be found in books [28,29,34] or in the recent review [22]. Only the facts critical for our following discussion are stated here.

The classical configuration is that of a flow in a rectangular duct with a uniform magnetic field parallel to one set of walls [80–82]. The mean flow crossing the magnetic field lines generates spanwise (perpendicular to the flow and the magnetic field) electric currents. If the duct's walls are electrically conducting, the currents close within the walls. The Lorentz force due to the currents crossing the field lines opposes the mean flow. The resulting additional pressure drop is very large in flows at high Ha. For example, a drop of several MPa is predicted for a typical blanket of a fusion reactor cooled directly by PbLi flowing in ducts of a $\sim\!10\,\mathrm{cm}$ side [5]. The resulting additional energy demand and technical problems are so challenging that no such direct cooling systems are currently considered [5].

If the walls are perfectly electrically insulating, the electric currents close within the fluid. The net Lorentz force is zero, but its distribution transforms the mean velocity profile so that it acquires a nearly flat core and MHD boundary layers: Hartmann layers of thickness \sim Ha⁻¹ at walls perpendicular to the magnetic field lines and Shercliff layers of thickness \sim Ha^{-1/2} at walls parallel to these lines. At high Ha (e.g., at Ha $\approx 10^4$ typical for fusion reactor blankets), the layers are very thin and with extremely strong velocity gradients, which implies strong wall friction and proneness to shear-layer instabilities [22].

Flows in round pipes subject to a transverse magnetic field are transformed in a physically similar but geometrically different manner [22,83]. A more complex transformation is found in flows with finite or strongly varied electric conductivity of walls or when the imposed magnetic field is not uniform [28,29,34,84,85].

Finally, we note that configurations with a uniform magnetic field not crossing any walls (e.g., fully developed flows in channels with a purely streamwise field or flow in an unbounded plane channel with a spanwise field) have zero gradients of mean velocity along the field lines. The magnetic field does not interact with the mean flow directly. It does, however, have an indirect effect via suppression and anisotropization of velocity fluctuations [86].

4.3 Instabilities and Complex Dynamics of MHD Flows. The additional anisotropic dissipation mechanism (the Joule dissipation) changes the instabilities and dynamics of common flows. In systems with a strong magnetic field effect, the modification is strong to such a degree that the flow's behavior changes in a profound and often counterintuitive way. We will fully illustrate this statement on the example of mixed convection flows in Sec. 6.

Here, we briefly discuss the principal physical mechanism and briefly present several examples.

Only the instability modes that have significant nonzero velocity gradients along the magnetic field lines are suppressed by the Joule dissipation. Modes with zero or weak gradients (purely two-dimensional or quasi-two-dimensional, hereafter referred to as 2D or Q2D) are either not influenced at all or influenced only slightly. This has serious implications for systems in which geometry and physics permit the existence of such modes. The typical situation is when a conventional hydrodynamic instability is suppressed, but the flow does not retain its base form. Instead, it becomes unstable to 2D or Q2D modes at higher control parameters.

Several examples of such a behavior were discovered recently. We can mention the instability of a free shear layer [87], a bypass transition to turbulence in a duct or a plane channel with insulating walls [88,89] (see [22] for a review) or a duct with conducting walls [84,85], the instability of an elliptic vortex [78], etc. An indepth theoretical discussion can be found in Ref. [78].

When Ha and N are large, growth of 2D or Q2D modes and the subsequent evolution of resulting flow structures occur on the background of fully suppressed conventional 3D turbulence. Moreover, secondary 3D instabilities of the 2D or Q2D structures are either fully or partially suppressed by the magnetic field. The result is flow regimes dominated by large-scale 2D or Q2D coherent structures. The manifestations of their dynamics may appear unusual, counterintuitive, or even paradoxical. For example, the so-called large-scale intermittency, i.e., the state of the flow in which long periods of laminar Q2D behavior are inter-rupted by short 3D turbulent bursts, is found in periodic boxes with artificial forcing [72] or channels with spanwise magnetic fields [90–92]. Localized turbulent zones are observed in wall-bounded shear flows [91,93–95].

An important example for us is the still not fully understood effect of an imposed magnetic field on the Rayleigh-Bénard convection. The principal physical mechanisms described earlier in this section remain valid. Their specific manifestation depends on Ra, Ha, orientation of the magnetic field, and presence of sidewalls. The instability threshold Rac increases with Ha. For example, $Ra_c \sim Ha^2$ in a horizontal layer with vertical field [96]. At $Ra > Ra_c$, flow is dominated by large-scale 2D or Q2D convection modes aligned with the field lines. For example, horizontal rolls are found when the field is horizontal [97-99], and vertical cells or columns are detected when the field is vertical [100]. Further increase of Ra at a given Ha leads to complex and sometimes spectacular dynamics of these modes [97,99] and then to turbulence modified by the magnetic field [53,98]. The large-scale convection modes are often a vehicle for an unusually strong heat transfer. For example, in flows with a vertical magnetic field, this leads to the Nusselt number Nu growing with Ra much faster than in conventional turbulent Rayleigh-Bénard convection (as Nu ~ Ra or even faster) [53,101–103]. Another peculiar feature of flows with a vertical magnetic field is the exceptional role of sidewalls. Similarly to flows with strong rotation, a large portion of heat transfer is provided by wall modes – vertical jets located near the sidewalls [53,104-106]. Weaker but still noticeable wall modes are found at Ra \sim Ra_c, including the range Ra < Ra_c [107,108].

5 Methods of Exploration

5.1 Asymptotic Models. When $N\gg 1$, one may formally derive asymptotic approximations based on the assumption that the Lorentz force is much stronger than the inertia force. In fact, much of the MHD development in its early years (the 1960s to 1980s) was based on such models.

One popular model simply ignores inertia. This leads to linearized momentum equations and to solutions in which the driving force (e.g., the pressure gradient) is balanced by the Lorentz force and, in boundary layers, by viscous friction [28,29,34,109–111]. The solutions are inevitably laminar and, under stationary external

Table 1 Physical properties of selected liquid metals, molten salts and electrolytes. Values corresponding to temperature $T_{\rm w}$ are shown. Liquid metals (the top part of the table) are listed in the order of decreasing melting point temperature. The properties shown are the fluid's density ρ , electric conductivity σ , kinematic viscosity ν , coefficient of thermal expansion β , thermal conductivity λ , temperature diffusivity χ , and specific heat $C_{\rm p}$. Values of the Prandtl number Pr and magnetic Prandtl number Pr_m are also shown.

Liquid	T_{melt} $^{\circ}\mathrm{C}$	$^{T_{ m w}}_{\circ m C}$	$\begin{array}{c} \rho \cdot 10^{-3} \\ \text{kg/m}^3 \end{array}$	$\frac{\sigma \cdot 10^{-6}}{1/(\Omega \cdot m)}$	$\begin{array}{c} \nu \cdot 10^7 \\ \text{m}^2/\text{s} \end{array}$	$\frac{\beta \cdot 10^3}{1/K}$	$\overset{\lambda}{W/mK}$	$\begin{array}{c} \chi \cdot 10^5 \\ m^2/s \end{array}$	$\frac{C_{\mathrm{p}}}{\mathrm{J/kg\cdot K}}$	Pr	$Pr_m \cdot 10^6$
Pb [129]	327	350	10.6	1.05	2.1	0.12	17	1.1	147	0.022	0.28
PbLi [129]	235	300	9.4	0.79	2.1	0.09	13.2	0.76	183	0.028	0.21
Sn [130,131]	232	300	6.9	2.0	2.4	0.11	31.6	1.8	255	0.014	0.6
Li [129]	181	220	0.51	3.8	10.6	0.20	44.2	2.0	4340	0.053	5.1
Na [132]	98	170	0.91	8.3	5.5	0.26	83	6.7	1360	0.0082	5.8
Ga [130]	29.8	60	6.04	3.5	3	0.12	30	1.2	390	0.025	1.3
GaZnSn [133]	15	25	6.15	2.6	2.9	0.11	20.1	0.88	300	0.035	0.95
NaK [129]	-12.6	80	0.85	2.6	5.7	0.23	23.1	2.9	942	0.020	1.9
GaInSn [134]	-19	20	6.44	3.5	3.7	0.12	16.5	0.87	296	0.043	1.6
Hg [129]	-39	30	13.5	1.0	1.1	0.18	8.6	0.46	139	0.024	0.13
FLiNaK [135,136]	454	600	2.05	$2 \cdot 10^{-4}$	23.5	0.32	0.86	0.022	1905	10.7	0.0006
FLiBe [137,138]	460	600	1.99	$2 \cdot 10^{-4}$	43.8	0.25	1.1	0.023	2385	18.9	0.0011
KOH 30% [139–141]	-62	40	1.26	$1 \cdot 10^{-4}$	11.9	0.38	0.61	0.016	3000	5.9	0.0001

conditions, steady-state. The model can be criticized on two accounts. Firstly, liquid metal flows often have large Re, so N > 1 but not $\gg 1$, even when the imposed magnetic field is strong. Inertia is not negligible. Secondly, the logic of the model is invalidated by the development of Q2D structures, which have weak or zero gradients along the field lines and for which, therefore, the Lorentz force is greatly reduced. Recent experimental and computational work, including the studies reviewed below, show that inertia is active in the majority of MHD flows and often leads to instabilities and unsteady behavior. The inertialess model must be considered as irrelevant in all such cases.

It should be mentioned that the results accumulated via the use of the intertialess model during the early years of MHD influenced the later work, in which inertia was taken into account. It is still assumed sometimes that liquid-metal flows at high Ha are inevitably steady-state and laminar even if the effective Reynolds number is large (see, e.g., [112–114]). As demonstrated in recent works, such as, e.g., [115–117], and extensively illustrated below, the approach often brings misleading results.

Another important asymptotic model is SM82, named so after the 1982 Sommeria and Moreau paper [71]. The model explicitly utilizes the Q2D character of flows in strong magnetic fields. The approximation uses purely two-dimensional governing equations to describe the flow variables, such as velocity or temperature integrated wall-to-wall in the magnetic field direction and produces good results (see, e.g., [118–122]). The original model is

Table 2 Values of nondimensional parameters (the Hartmann, Grashof, and Reynolds numbers) for a typical example of an experimental flow (a duct with width $d=20\,\mathrm{mm}$, mean velocity $U=0.25\,\mathrm{m/s}$, imposed heat flux $q=30\,\mathrm{kW/m^2}$ and magnetic field $B=1\mathrm{T}$). Values of physical properties corresponding to temperature T_w are used.

Liquid	$T_w, {}^{\mathrm{o}}\mathrm{C}$	На	$Gr_q \cdot 10^{-7}$	$\text{Re} \cdot 10^{-3}$
Pb	350	410	1	21.7
PbLi	300	390	1	23.5
Sn	300	770	0.7	25
Li	220	1170	0.02	4.7
Na	170	2650	0.1	14.2
NaK	80	1430	0.2	8.1
Ga	60	830	0.3	19.2
Hg	30	540	9	49.1
FliNaK	600	2	1.7	3.1
FLiBe	600	1	0.4	1.7
KOH(30%)	40	4	3.4	4.2

valid only for a limited class of problems, namely, for flows in domains with perfectly electrically insulating walls, uniform magnetic fields perpendicular to one set of walls and parallel to the other, and constant wall-to-wall distance along the field lines. Similar limitations apply to the corrections of the model that account for weak deviations from quasi-two-dimensionality [123,124]. An extension of the model to the case of electrically conducting walls was proposed in Ref. [125].

We conclude that the asymptotic models based on the assumption of a very strong magnetic field effect must be applied only with utmost care and after full validation. In many cases, their use may lead to incorrect predictions even though N and Ha are large.

Yet another class of 2D models was introduced for MHD flows in shallow layers [126,127]. These models are based on locally exact solutions for nonisothermal rotating layers of conductive fluids, which are substituted into the full 3D equations and integrated across the layer. The models were shown not only to work for strong magnetic fields, but also revealed reach and unexpected dynamics of turbulent MHD flows under both perpendicular [127] and parallel [126] magnetic fields.

5.2 Experimental Methods. We will start with a discussion of liquids interesting in the context of this review either because they are found in technological applications or because they are used as working fluids in laboratory experiments. The focus will be primarily on liquid metals, although processes in electrolytes can also be affected by the magnetic field, as discussed below. The key physical properties of the liquids are presented in Table 1 together with the two nondimensional material parameters: the Prandtl number (12) and the magnetic Prandtl number (1).

The list includes two metals with very different properties used as cooling liquids in advanced nuclear fission reactors: lead (Pb) and sodium (Na). Two lead alloys have been widely studied and tested in laboratories: Pb-Bi and Pb-Li, the latter being interesting as a tritium breeding medium in nuclear fusion applications [4–6,10,11,13,128]. Besides sodium, two other alkaline metals, lithium (Li) and sodium-potassium alloy (NaK), are of interest for the cooling systems of fission and fusion reactors and for laboratory experiments. Liquid metals with low melting points, such as mercury (Hg), gallium (Ga), and eutectic gallium alloys (GaInSn and GaZnSn) are widely used in laboratories and thus are indispensable for studying MHD phenomena. Finally, our list includes two molten salts, FLiNaK and FLiBe, which are considered as possible working fluids in fission and fusion reactors, and the water solution of potassium hydroxide (KOH), which is used in the laboratory as a low-temperature imitator of such salts and technological electrolytes.

The main challenge of experimental research into liquid metal flows and heat transfer in fusion reactors is that the extreme conditions of very strong magnetic fields and very high heat loads cannot be reproduced in existing laboratories. Reaching realistically high values of Gr and Ha will only be possible in future experimental reactors or specialized facilities [5,6,10,16]. Experiments are currently performed for simplified models of the reactor components and at values of Gr and Ha that are high but still orders of magnitude lower than in the reactor. Various metals are used, such as technologically similar Pb, Pb-Bi [142], Pb-Li [143–148], Li [149], and Na [150,151] or model liquids, such as Ga and its alloys [152,153], NaK [154–156], and Hg [157]. A recent review of operating experimental facilities can be found in Ref. [158].

While obviously interesting and sometimes unavoidable, experiments with technologically similar liquid metals are difficult and expensive to perform, since they require high temperatures and handling of aggressive fluids. In particular, work at high temperature implies complex maintenance, long periods between experimental sessions, and limited available diagnostics. Model liquid metals are easier and less expensive to work with due to their lower working temperature and their compatibility with other materials.

Therefore, it is interesting to compare the ranges of governing parameters that can be reached using different liquids. High values of Ha and Gr can be achieved if σ/μ and $\beta/(\lambda \cdot \nu^2)$ are large. Small values of $C_{\rm p}$ are desirable, since this results in greater temperature gradients and thus higher accuracy of temperature measurements. There is no universal optimal solution of this problem, but in order to demonstrate the opportunities, Table 2 shows estimates of Ha, Gr, and Refor a typical duct flow in a laboratory setting.

We see that the highest values of Ha are achieved with alkali metals, in particular with Na, which makes them the best candidates for studying MHD effects, which do not involve heat transfer. Usage of mercury gives the highest value of Gr (one or two orders of magnitude higher than with other metals) and Re. Mercury, therefore, allows us to perform heat transfer experiments at the lowest heat fluxes and liquid metal volumes. Molten salts experience a barely noticeable MHD effect ($\text{Ha} \sim 1-10$). It should also be mentioned that direct experimental work with molten salts is extremely difficult [159], so studies are typically done with model fluids (aqueous solutions of potassium hydroxide or sulfuric acid of different concentrations) providing close values of the MHD parameters and Pr [160].

Experiments with liquid metals are substantially more complex than with conventional fluids such as water. Liquid metals are opaque and in many cases chemically active, toxic, and hot media, which limits the choice of measuring techniques. Further significant complications are related to the use of high-field magnets and high-intensity heaters and to maintenance of liquid metal loops [28].

Different devices used to perform velocity measurements in liquid metals are reviewed in the chapter by Eckert, Cramer, and Gerbeth in Ref. [161] and in Refs. [162–164]. These comprehensive reviews can be supplemented by such methods as fiber-optic sensors [165,166], optomechanical sensors [167], and temperature correlation velocimetery [168]. However, velocity measurements under high magnetic fields and high heat fluxes are technically difficult. Velocity sensors are bulkier and less accurate than the ones used to measure temperature. The experimental data presented below in this review were gathered predominantly using temperature measurements.

Methods of pressure measurements in liquid metals are basically the same as in other liquids. Complications arise in high temperature systems, which require special organization of pressure lines to sensors to make it possible to use standard equipment. Furthermore, oxides may complicate the operation of small pneumatic systems.

Temperature measurements, which are critically important for the problems under discussion, face strong challenges but also

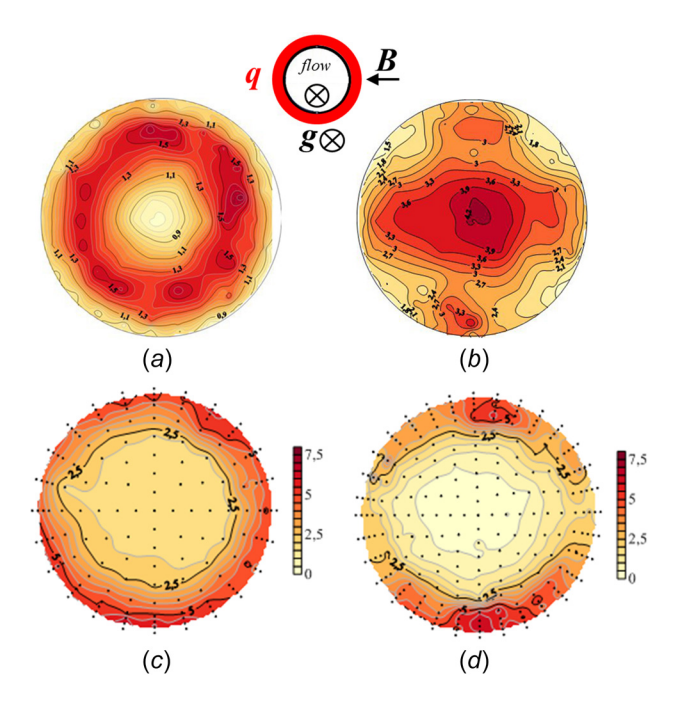


Fig. 6 Intensity of temperature fluctuations in the downward flow of mercury at $Re = 10^4$, $Gr = 1.2 \cdot 10^7$ (a,b) [177] and KOH(30%) water solution at $Re = 3 \cdot 10^3$, $Gr = 1.1 \cdot 10^7$ (c,d) [178] in a vertical pipe with uniformly heated walls and transverse magnetic field (see the diagram at the top). (a,c) Ha = 0, (b) Ha = 350, (d) Ha = 15.

have advantages in liquid metals. One serious challenge is that the ideal boundary conditions of constant temperature at the walls cannot be easily implemented in the experiments with liquid metals due to their high thermal conductivity and capacity. The second common challenge is the formation of oxide layers [169] causing additional thermal resistance and thus poor accuracy of the methods based on the temperature measured on the outer side of the domain's walls. The effect can be significant for some liquid and wall materials and flow conditions. For example, steady-state oxide layers (both from the wall oxidation and liquid metal oxidation) can be up to $100~\mu m$ in lead [169,170] and $10~\mu m$ in sodium [171].

At the same time, temperature measurements in liquid metals are a very powerful tool of flow diagnostics. This statement contradicts the common and somewhat naive preconception that high thermal conductivity makes such measurements ineffective due to smoothing of temperature inhomogeneities. The fact is that in flows of liquid metals the high mobility (low viscosity) of the medium becomes an important factor. To illustrate this statement, we show in Fig. 6 the distributions of temperature fluctuations in the cross–sections of pipe flows of a liquid metal and an electrolyte at similar heating and flow rates. In the absence of a magnetic field (left panels), the temperature fluctuations penetrate much deeper inside the pipe in liquid metal than in the electrolyte. With a magnetic field (left panels), the difference becomes even stronger because the Lorentz forces are much higher in liquid metal.

Some popular and powerful diagnostic tools cannot be used in liquid metal flows. One example is the PIV technique. Another is the hot-wire anemometry, for which problems are created by the high thermal conductivity of metals. At the same time, high electric and thermal conductivity of liquid metals enables other measurement tools (we note that not all of them can be used under strong external magnetic fields). The presence of external magnetic fields opens the possibility of noninvasive methods based on the measurement of electric potential or magnetic field perturbations. The classical example of such methods uses the measurements of the electric potential at the walls of the flow domain to

evaluate the integrated velocity. We note that this method works well in the conditions of high temperature and high temperature gradients. Other more modern noninvasive methods are the Lorentz force velocimetery [172,173] and inductive tomography [174]. The ultrasonic Doppler velocimetery (UDV) technique was recently developed to be capable of measuring two-dimensional velocity distributions in even unsteady flows [175].

In general, the noninvasive measurement techniques are preferable as they affect the flow only slightly if at all. These methods are, however, limited by such factors as high temperatures and strong magnetic fields, which often leads to special shielding requirements, as well as limited working space around the flow domain. Furthermore, the information provided by the noninvasive techniques is typically limited to spatially integrated quantities. Therefore, immersion sensor techniques, which are more reliable and provide more detailed information, are often a better and sometimes the only meaningful approach. The probes can be installed at certain points of the flow domain or on its surface, but the most detailed information is provided by scanning techniques producing 3D and 2D fields of the measured quantity. A recent review of the scanning probe method can be found in Ref. [176].

5.3 Numerical Methods. It may appear that the numerical solution of the governing equations of quasi-static MHD (2)–(8) requires only a slight modification of conventional techniques, namely, solution of the additional Poisson Eq. (8). This is certainly true for flows with a moderately strong magnetic field effect, i.e., with moderate values of Ha and N. The task is substantially more challenging in the more interesting for us case of Ha $\gg 1$, N $\gg 1$ (values as high as Ha $\sim 10^4$, N $\sim 10^4$ are typical for a fusion reactor blanket).

The main reason is the numerical stiffness of the problem. The smallest typical time scale is the Joule damping time $\tau_J \equiv \rho/\sigma B^2$, which characterizes the typical time of suppression of velocity gradients by the Joule dissipation. It is related to other typical time scales of the flow, namely, the turnover time $T_v \equiv d/U$ and the times of viscous dissipation and temperature diffusion $\tau_v \equiv d^2/\nu$ and $\tau_\chi \equiv d^2/\chi$, as $\tau_J = T_v N^{-1} = \tau_v H a^{-2} = \tau_v H a^{-2} P r^{-1}$.

In space, one has to deal with very thin boundary and internal shear layers. For example, in a duct flow with electrically insulating walls and transverse magnetic field, one finds the Hartmann boundary layers of thickness $\delta_{Ha} = d \mathrm{Ha}^{-1}$ forming at walls normal to the magnetic field and Shercliff boundary layers of thickness $\delta_{Sh} = d \mathrm{Ha}^{-1/2}$ at walls parallel to it. Another example is the Hunt flow in a duct with conducting walls, where thin and dynamically active jets develop near the field-parallel walls [84]. Internal shear layers of comparable thickness are often associated with Q2D structures. Experience (see, e.g., [40]) and common sense suggest that each such layer has to be resolved by at least 8-10 grid points. At high Ha, this implies the requirement of large and extremely nonuniform grids.

Numerical analysis of mixed convection flows is associated with other not always fully appreciated difficulties. One is the requirement of an unusually large length of the time interval of the simulations. As we will see in Sec. 6, such flows often demonstrate slow dynamics with irregular fluctuations on the typical time scale of tens of convective time units. Simulation of hundreds or even thousands such units is necessary to fully understand the flow's behavior and to accumulate data for accurate evaluation of the statistical properties.

Another difficulty is related to the fact that even when the mean and fluctuating flow fields are separated from each other in the analysis (see Sec. 2), some of the key physical mechanisms are impossible to represent in the framework of a model, in which a segment of the duct with periodic inlet/exit conditions is considered. A good example is the flow in vertical ducts discussed in Sec. 6.2, for which evolution along the duct is essential. The only accurate approach to numerical analysis of such cases is to simulate the entire test section of the experiment or the entire duct of a

module of a reactor blanket. This typically requires an exceptionally large number of grid points or cells in the streamwise direction.

The numerical stiffness of the problem implies that many conventional computational methods are not suitable for flows with strong magnetic field effects. This includes spectral and spectralelement methods, and finite difference schemes not adapted to the MHD flow transformation. The finite-element method also has not been shown to be effective, although this approach may need further exploration [179,180]. Rather unfortunately for the efforts on the design of fusion reactor components, serious problems arise when one utilizes general-purpose CFD tools, such as Ansys Fluent, COMSOL, ANES, or OpenFOAM. Attempts at such simulations [112,113,115,181-192] have shown that convergence and reasonable accuracy are possible only for steady-state regimes at moderate values of Ha and Gr. Accurate simulations of unsteady high-Ha flows are either impossible or inefficient, since the low efficiency and slow convergence of such tools typical in the case of stiff problems inevitably leads to excessive computational

An interesting contribution to the question of applicability of general-purpose codes is the recent code-comparison study [193]. The mixed convection flow in a vertical duct with horizontal heating and magnetic field and the mean velocity directed downward was solved using the finite volume code HIMAG [194], COMSOL Multiphysics, ANSYS Fluent, ANSYS CFX, and OpenFOAM. As we discuss in Sec. 6.2, the flow is characterized by strong convection-induced deformation of the streamwise velocity profile and, in a broad range of parameters, including the parameters considered in Ref. [193], a secondary instability leading to highamplitude temperature fluctuations. It has been found that all five codes represent the deformation of the velocity profile reasonably well. The predictions of the time-dependent flow behavior, however, vary greatly between the codes. Two of them - ANSYS Fluent and ANSYS CFX - fail to detect the fluctuations altogether, apparently due to the excessive numerical dissipation of their second-order upwind schemes.

Development of accurate and effective numerical models for high-Ha flows has recently been an area of active research (see [195] for a review). The focus has been primarily on finite volume and finite difference schemes with good conservative properties [196–202]. In addition to the mass, momentum, and energy balances, the conservation of electric charges (exact reproduction of the zero divergence of electric currents (8)) has to be fulfilled by the discretized solution.

As an example of this approach, we mention the family of finite volume (with finite difference versions on structured grids) schemes originating in Refs. [196,197]. In these two works, the principles of conservative discretization based on interpolation of velocity to staggered velocity fluxes [203] were extended to solution of the potential Eq. (8) and calculation of electric currents (7) and Lorentz forces (6). Further developments of the method included its extensions to various discretization approaches (e.g., simulations on staggered and unstructured grids) and adaptations to various physical effects, such as heat transfer and thermal convection or walls of finite electric conductivity [40,93,199, 200,202,204-206]. The method has been validated in comparison with experimental data (see, e.g., [40,195]) and has shown accuracy and efficiency in simulations of high-Ha flows, including flows with strong instabilities and unsteady behavior (see, e.g., [40,41,53,68,79,93,107,205,207,208]).

Another problem appears in numerical analysis of turbulent MHD flows at moderately high Ha. The modification of velocity field described in Sec. 4.1 (suppression of turbulence intensity and development of anisotropy), if it is sufficiently strong, implies that commonly used LES and RANS models become inaccurate. The models have to be adjusted to account for the effect of the magnetic field.

The question of accurate LES modeling has been actively researched and to a large degree answered in recent studies, such

as [73,77,86,209–213]. It has been found that the key to accuracy is the model's ability to adjust to the local anisotropy-related suppression of energy transfer to small length scales and to the drop of subgrid-scale dissipation. The dynamic Smagorinsky and coherent structure models have shown good results [73,77, 86,209–213]. An interesting and promising approach was taken in Ref. [214], where it was shown that the proper value of the constant of the Smagorinsky model strongly correlates with a measure of local anisotropy.

Adjusting RANS models to the MHD flow transformation has also been attempted with a good degree of success. We will mention the models based on the local anisotropy coefficient [215,216] and the more complex models [217–220].

6 Mixed Convection in Channels With Strong Imposed Magnetic Field

This section presents the central topic of the review, namely, that of mixed convection in channels under the simultaneous action of strong heating and magnetic field (high values of Gr and Ha). The topic is directly relevant to the design of liquid metal blankets for nuclear fusion reactors introduced in Sec. 1. Interestingly, the effect of thermal convection was largely ignored during the long (about two decades) first period of work on blanket design (see [161] for a review). It was assumed that velocity fluctuations at such high Ha would be fully suppressed by the magnetic field and the flow would be laminar, steady-state, and with passive heat transfer (see, e.g., [149]). Much effort was given to finding a way to raise the heat transfer rate above its laminar flow value by, e.g., reaching very high values of Re ($\sim 10^5$) or using turbulence promoters. The first experimental indications that nonisothermal flows may avoid full laminarization even in very strong magnetic fields [166,221,222] were argued to be results of experimental imperfections, flow structures developing at the entrance into the magnetic field, or other such secondary effects, rather than the thermal convection.

It is now clear that thermal convection plays an important, often even critical role by completely changing the flow's internal structure and causing high-amplitude fluctuations of velocity and temperature in systems with strong magnetic field effects. Experimental and computational results proving this statement are presented below in this section.

The mechanisms and outcomes of the interaction between the liquid metal flow, convection, and magnetic field strongly depend on the orientation of the channel with respect to gravity, the direction of the mean flow, the orientation of the magnetic field, and the arrangement of applied heating. Accordingly, the discussion is structured by principal configurations: horizontal, vertical, and inclined channels with a transverse magnetic field presented in, respectively, Secs. 6.1, 6.2, and 6.4, and flows with a longitudinal magnetic field presented in Sec. 6.3. Various versions of the cross-sectional geometry, such as rectangular ducts and round pipes, are discussed in parallel, since the differences between them are typically limited to quantitative albeit significant aspects. The key physical mechanisms are usually the same in all such channels.

The flow behavior is expected to be also affected by the electric and thermal conductivities of the walls. The majority of available data are for systems, in which the walls are either assumed to be perfectly insulating (in computational studies) or can be approximately considered as such (in experiments). The results reviewed in this section are for such systems, with a few exceptions clearly indicated in the text. A more detailed discussion of the effects of wall conductivity is provided in Sec. 7.1.

Following the terminology recently proposed in Ref. [223], the high-amplitude low-frequency fluctuations of velocity and temperature that appear in flows with strong convection and magnetic field effects (high values of Gr and Ha) are called magnetoconvective fluctuations (MCFs) in the following discussion.

The presentation of the results largely follows the conventional ways established in the reviewed literature on the subject. In particular, experimental temperature measurement data are shown in dimensional units. The results of numerical simulations are presented in the nondimensional form, except where direct comparison between simulations and experiments is made. In every case, the information necessary for conversion between dimensional and nondimensional units can be found in the cited literature.

6.1 Horizontal Channels. Horizontal or nearly horizontal channels are elements of many concepts of the cooling systems of a fusion reactor including both blanket (see Figs. 1(b), 1(e), and 1(f)) and divertor. Also they appear in blanket modules located in the top and bottom portions of the blanket (see Fig. 1(a)). Among the possible configurations, we will focus on the one with imposed heat flux from the bottom (see Fig. 1(g)-6 for the round pipe version) and the main component of the magnetic field in the transverse horizontal direction. This configuration is directly relevant to the design of upper divertor [224] and top blanket modules. It is also the most thoroughly studied and interesting from the historical perspective as the first configuration in which the effect of MCFs was described and explained. To demonstrate the diversity of possible flow regimes, we will also present examples of flows with other heating schemes at the end of this section.

Mixed convection in pipes and ducts with heating from below and transverse magnetic field was studied in experiments [225–228] and numerical simulations and linear stability analyses [40,41,228–230]. We will illustrate the typical behavior observed at moderately large Re-and large Gr by the results obtained for a pipe flow. Experiments such as [227,228] and numerical analysis [41,228,230] demonstrate that the behavior and the physical mechanisms presented below are also found in horizontal ducts of square and rectangular cross section.

The effect of a magnetic field on the flow's behavior is illustrated by the single-point temperature signals in Fig. 7 and the visualizations of the same flow regimes in Fig. 8. A turbulent flow with a clearly visible mean-field structure in the form of two axial rolls (see the scheme in Fig. 5(a)) is found at Ha = 0 (see Figs. 7(a) and 8(a)). The same flow structure with reduced turbulent fluctuations remains under a weak magnetic field (see Figs. 7(b) and 8(b) for Ha = 50). A moderate magnetic field suppresses the turbulence (see Figs. 7(c) and 8(c) for Ha = 100). The flow becomes laminar and steady soon after entering the magnetic field zone and remains such until its exit from this zone. Axial convective rolls still exist in the heated segment.

The flow's behavior changes spectacularly at higher Ha (see Figs. 7(d), 7(e) and 8(d), 8(e)). Temperature fluctuations reappear, but in a form clearly different from that in a turbulent flow. They have an order-of-magnitude larger amplitude and a quasi-regular pattern with dominating low frequencies. The flow structure in Figs. 8(d) and 8(e) shows that the streamwise convection rolls are replaced by transverse rolls, illustrated schematically in Fig. 5(b).

Temperature signals similar to those in Figs. 7(*d*) and 7(*e*) observed in the experiments [225,226] were the first examples of high-amplitude low-frequency fluctuations appearing in magneto-convection at high Ha. Named "anomalous fluctuations" at that time, they are now viewed as one of many manifestations of the phenomenon of MCFs.

The physical mechanism causing MCFs in horizontal unstably stratified channels was hypothesized in Refs. [225,226] and later revealed in the linear stability analysis [40,41,230] and direct numerical simulations [40,41,228,229]. Remarkably good quantitative agreement between the predictions of the typical amplitude, frequency, and pattern of the temperature signal and the experimental data was found (a similar agreement can be seen if we compare the red and black curves in Fig. 7).

The mechanism can be explained by the effect of magnetic damping caused by the Joule dissipation of the electric currents induced by the flow moving in a magnetic field (see Sec. 4.1). At a sufficiently strong magnetic field the dissipation suppresses the turbulence, so the flow becomes laminar. At an even stronger

field, the dissipation changes the balance between the two types of convection modes shown in Fig. 5. The streamwise rolls of Fig. 5(a), which dominate a nonmagnetic flow or a flow with moderate magnetic field (see Figs. 8(a)-8(c)), experience strong damping because the velocity field of such rolls has significant gradients along the magnetic field lines. The growth of this mode is suppressed, and the instability threshold is shifted to a higher Gr. At a sufficiently large Ha, the effect becomes so strong that the first instability occurs in the form of growth of the transverse rolls shown in Fig. 5(b), which have much weaker gradients along the magnetic field lines and thus are much less susceptible to suppression by the Joule dissipation. The growth of this instability mode

leads to nonlinear saturation in the form of Q2D rolls (see Figs. 8(d) and 8(e)), which implies alternating zones of upward and downward flows and, respectively, higher and lower temperature. Transport of the rolls by the streamwise flow generates the anomalous (magnetoconvective) fluctuations of temperature at a given location detected in experiments and simulations (see Figs. 7(d) and 7(e)).

Linear stability studies and direct numerical simulations of the flow have shown that in addition to this universally valid general scenario, there are other features of MCFs related to specific configurations and parameter values. In particular, simulations [41] show that in a broad range of parameters the convection instability

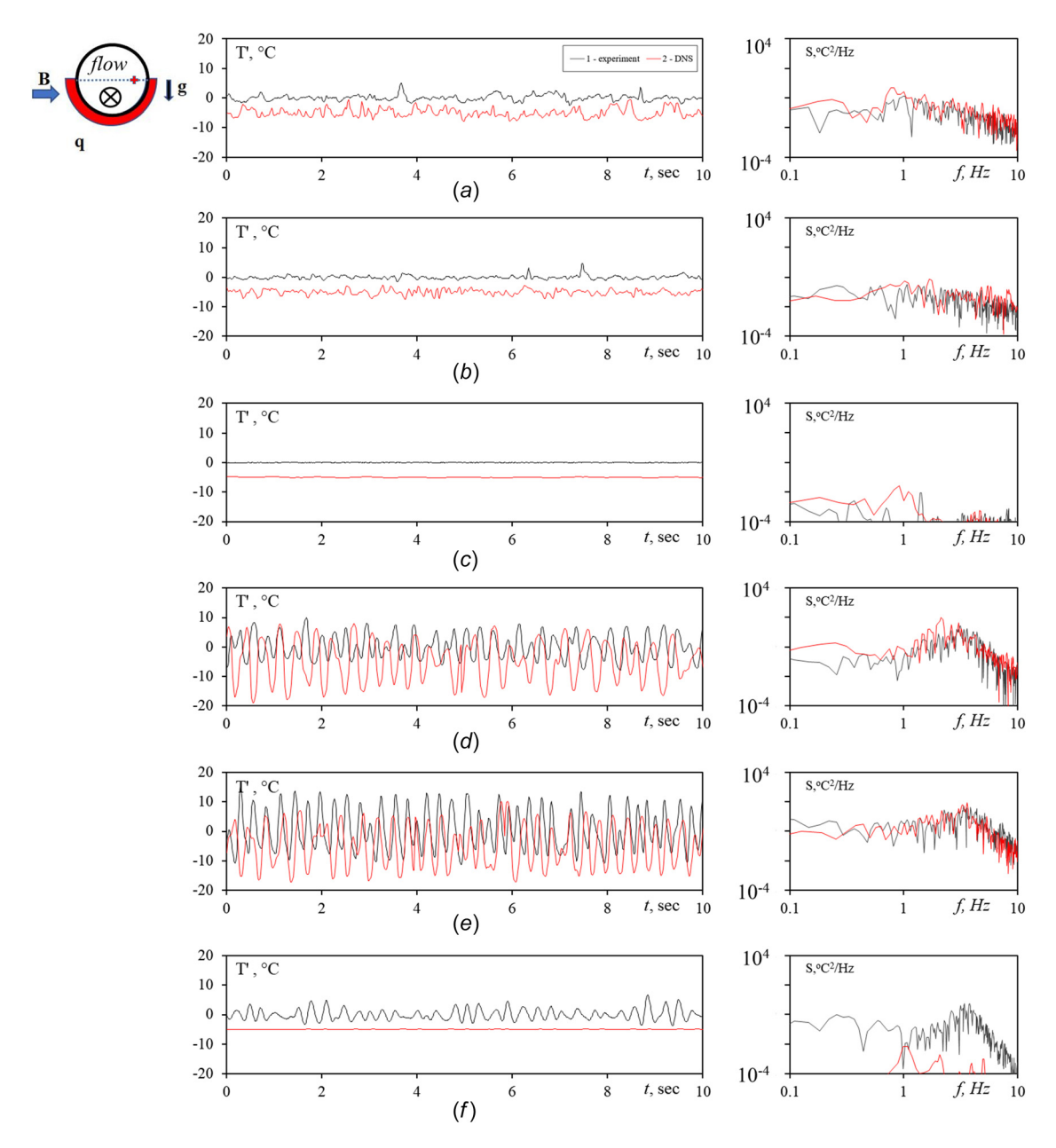


Fig. 7 Time signals and power spectra of temperature fluctuations in a horizontal pipe heated from the bottom and affected by a transverse horizontal magnetic field (see the diagram at the top) at Re = 10^4 , Gr = $8.5 \cdot 10^7$, and Ha = 0, 50, 100, 300, 700, and 1000. Measured and simulated centered signals of temperature at the point indicated by a cross in the diagram and located at the axial distance of 37 pipe diameters from the beginning of the heated portion are shown. The same scales and axis limits are used in all cases for better comparison. The spectrum values smaller than 10^{-4} are below the measurement sensitivity level and, therefore, not shown. The numerical data are recalculated into the dimensional units of the experiment and shifted by 5 degrees for better visibility. Unpublished experiments and three-dimensional simulations of the entire experimental test sections performed by the authors of this review using the techniques described, respectively, in Refs. [227] and [40] are shown. See Figure 8 for visualizations of the simulated flow fields.

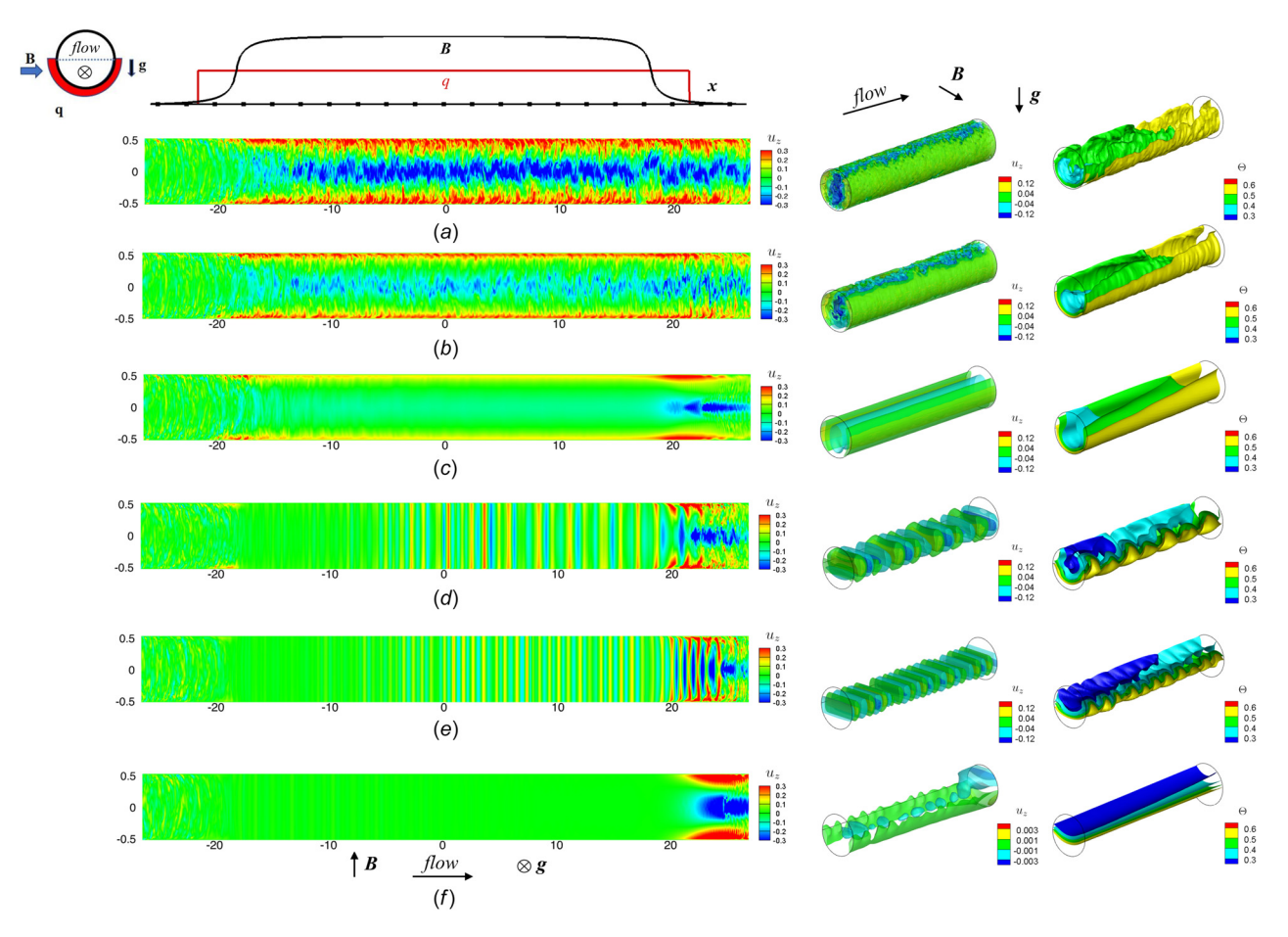


Fig. 8 Liquid metal flow in a horizontal pipe (numerical simulations performed by the authors of this review using the technique are described in Ref. [40]). The entire test section of the experiment with true distributions of the main component of the magnetic field and bottom heating as shown at the top of the left-hand side panel is modeled. The flow arrangements and parameters are as in Fig. 7. Left-hand side panel: instantaneous distributions of nondimensional vertical velocity in the horizontal cross section along the pipe's axis. Note that the axial and radial coordinates, which are nondimensionalized using the pipe's diameter, are plotted with strongly different scales. Right-hand side panel: Isosurfaces of vertical velocity and temperature in the segment between 27 and 37 pipe's diameters measured from the beginning of the heated portion.

results in a combination of streamwise and transverse rolls. The domain of existence of this regime (the high-Gr regime in the terminology of [41]) at a given Re has been determined as the range of the parameter ${\rm Gr/Ha^2}$ exceeding a threshold value by about several hundreds.

Another effect anticipated in flows with large Gr is that of reduced or even reversed streamwise velocity in the upper part of the channel caused by the buoyancy forces associated with the growth of the mean-mixed temperature. As we discuss in Sec. 3.2, this may lead to stable stratification in the upper part of the channel. The effect is poorly understood due to the difficulties in reaching sufficiently high (10⁹ and higher) values of Gr in experiments and simulations, but it is plausible that the MCF instability still occurs but the rolls are limited to the lower part of the channel, have shorter wavelength, and manifest themselves as temperature oscillations of higher typical frequencies.

The instability is influenced by inlet conditions: the amplitude and type of perturbations and the formation of an M-shaped profile of streamwise velocity at the entrance into the magnetic field [228,229]. It must be stressed that the inlet conditions affect only the inception stage of the instability. The Q2D rolls and MCFs are features of a fully developed flow. This is confirmed by the linear stability analysis of streamwise-homogeneous flow [40,41,230], where the parametric range of the instability as well as the shape and typical wavelength of the unstable perturbations are found to be in quantitative agreement with the experimental data. Furthermore, numerical simulations [40,41,228,229] and experiments

[227,228] show that once formed, Q2D rolls occupy, without much change of their properties, the entire remaining length of the segment of the channel, where heating and magnetic field are applied.

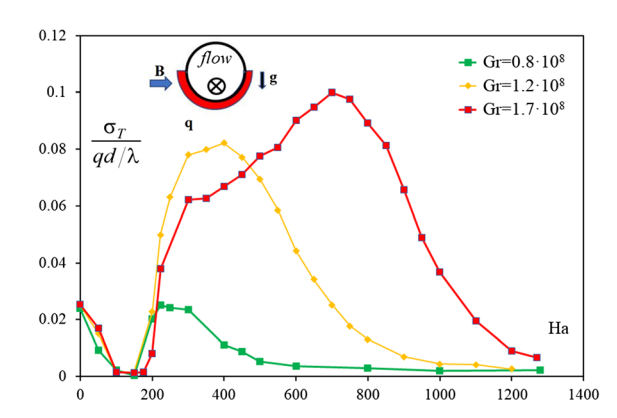


Fig. 9 Maximum standard deviation of nondimensional temperature fluctuations measured in the pipe cross section at the distance x/d = 37 from the beginning of the heated section at Re = 10000. The flow configuration is as in Figs. 7 and 8. Unpublished results of experiments performed by authors of this review using the technique are described in Ref. [227].

The parametric range of existence of the MCF regime is poorly known. The experiments and numerical simulations show that the range is substantial but do not provide sufficient information on its boundaries.

The critical question is if MCFs exist at high values of Gr and Ha, namely, at $Gr \sim 10^9 - 10^{12}$, $Ha \sim 10^4$ typical for components of a fusion reactor. The question cannot be answered directly since neither experiments nor 3D simulations are currently possible at such parameters. We see in Figs. 7(e) and 8(f)that at Re = 10^4 , Gr = 8.5×10^7 , and Ha = 1000, MCFs are substantially suppressed in the experiment and fully in DNS (we attribute the difference to the difficulty of accurate simulations at such high Ha). Further information is provided in Fig. 9, which shows the nondimensionalized standard deviation σ_T of the temperature fluctuation measured as in Fig. 7. We see that the intervals of Ha in which MCFs are observed (the intervals of large σ_T at Ha > 100) become broader at larger Gr. This indicates the possibility that MCFs exist at very high Gr and Ha. One can also hypothesize that the region of existence is likely to be larger in ducts than in the pipes primarily studied so far, since ducts are less restrictive for the Q2D flow states expected at high Ha.

The boundaries at low Gr and Ha are accessible in experiments and simulations but are still largely unexplored. Preliminary conclusions can be drawn from the numerical simulations of pipe flows [229]. In agreement with experiments and general physical arguments, the simulations show that MCFs appear only when the effect of natural convection is significant and the magnetic field is strong enough to suppress turbulence. For the pipe, the conditions are approximately quantified as the requirements that, respectively, Ri > 0.1 and N > 1.

We will now briefly review the results obtained for other heating arrangements. Only few studies are known to the authors: the experiments [231,232] in pipes with variously heated walls and numerical simulations [42] of a flow in a duct with one sidewall heated. A horizontal transverse magnetic field was imposed in all these studies. No MCFs were found. This can be viewed as an indication of a rather evident statement that the physical mechanism described above becomes less powerful in the absence of strong unstable stratification produced by bottom heating. One should not, however, consider this as a proof due to the scarcity of data and because the possibility of an MCFs-producing instability in other heating configurations cannot be excluded on the basis of physical arguments.

An example of a typical flow transformation in a homogeneously heated pipe under a transverse magnetic field is presented in Fig. 10. In the absence of a magnetic field (Ha = 0), a pair of convection rolls create the downward flow in the vertical central plane, distorting the mean temperature field and shifting the zone of lower temperature downward. The applied transverse magnetic

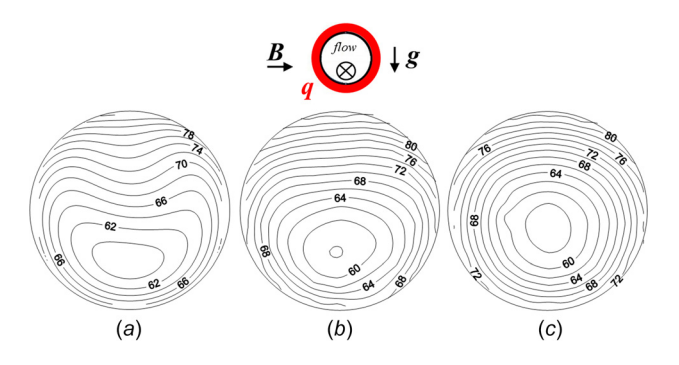


Fig. 10 Results of experiments [231] for the flow in a pipe with uniform heating of the walls (the configuration of Fig. 1(g)-1) and transverse horizontal magnetic field. Time-averaged temperature fields in a cross section located at the downstream portion of the test section are shown for Re = 10^4 , Gr = $7.6 \cdot 10^7$, Ha = 0, 100, 300 (left to right). Image copyright of the Begell House Inc. Reproduced with permission.

field suppresses both turbulent fluctuations and axial rolls. At Ha = 300, the mean temperature distribution approaches that of a laminar flow. No fluctuations are registered in the temperature signals at Ha = 200 (not shown) and Ha = 300.

Interesting results were obtained in numerical simulations of fully developed flows in a square duct with one sidewall heated so that the imposed heat flux was parallel to the imposed magnetic field [42]. Flows with Re = 10,000, Gr \leq 1.6 × 10¹⁰, and Ha \leq 1600 were considered. It has been found that with exception of the cases with Gr = 1.6 × 10¹⁰ and low Ha, the flow is two-dimensional.² Suppression of turbulence and absence of the MCF instability result in a state of the flow that is not just laminar and steady-state, but also uniform in the streamwise direction. At high Gr and Ha, the flow demonstrates prominent features: strong jets near the heated and both horizontal walls and deformation of the streamwise velocity profile $u_x(z)$.

The first of these features is typical for natural convection flows subjected to strong horizontal magnetic fields (see, e.g., [201]). The suppression of velocity gradients along the magnetic field lines leads to convection circulations dominated by strong nearwall jets. The second feature is, as we discussed in Sec. 2, the result of the buoyancy force associated with the mean-mixed temperature growing in the streamwise direction. Due to the strong magnetic field, u_x is nearly uniform in the y-direction (see Fig. 11(d)), with very thin Hartmann boundary layers (invisible to the eye) forming at the vertical walls. In summary, the buoyancy together with the magnetic field provides a stably stratified, uniform in x and nearly-uniform in y-directions flow with an accelerated cold near-bottom stream.

6.2 Vertical channels. Vertical channels, typically ducts, are a common feature of many concepts of liquid metal blankets of fusion reactors [5,21,233]. Such channels are of special interest, since they appear in the modules located in the blanket's equatorial area (see Fig. 1(a)), i.e., exactly where liquid metal blanket concepts will be tested in the ITER experiment [6].

In such modules, a liquid metal will circulate through a network of vertical ducts with upward and downward flows. Due to the geometry of a tokamak reactor, the ducts are inevitably arranged so that the horizontal heat flux created by volumetric and wall heating is perpendicular to the main (horizontal, toroidal) component of the magnetic field (see Fig. 1(a)). Various models representing this configuration (see Fig. 1(h)) have been at the focus of thermo- and hydrodynamic research and, therefore, are primarily discussed in this section.

Two interrelated effects of thermal convection already introduced in Sec. 3.2 are essential for understanding the physics of flows in vertical channels. One is the temperature stratification caused by the growth of mean-mixed temperature $T_{\rm m}$ in the streamwise direction: stable in upward flows and unstable in downward flows. Another is the deformation of the streamwise velocity profile, often leading to the formation of inflection points and zones of reversed flow (see Fig. 4). We will see shortly that the role of these effects increases dramatically when turbulence is suppressed by the magnetic field.

We will start with the configuration of downward mean flow with asymmetric heating (see Figs. 1(*a*)–1, 1(*h*)-3), in which the most spectacular phenomena have been observed. This configuration is also most thoroughly studied, with a large body of data being provided by the experiments [177,223,234–238] performed at strong magnetic fields (Ha up to 1500). MCFs are detected in a wide range of Re, Gr, and Ha. Their properties and range of existence vary with the channel's geometry and heating arrangements, but the phenomenon itself is quite robust. In particular, MCFs are observed in pipes [177,234] and rectangular ducts [235,237]. The amplitude of temperature fluctuations can be remarkably high,

 $^{^{2}}$ We emphasize that two-dimensionality is understood here and throughout the review as the independence of all three velocity components from one coordinate, in this case, from x.

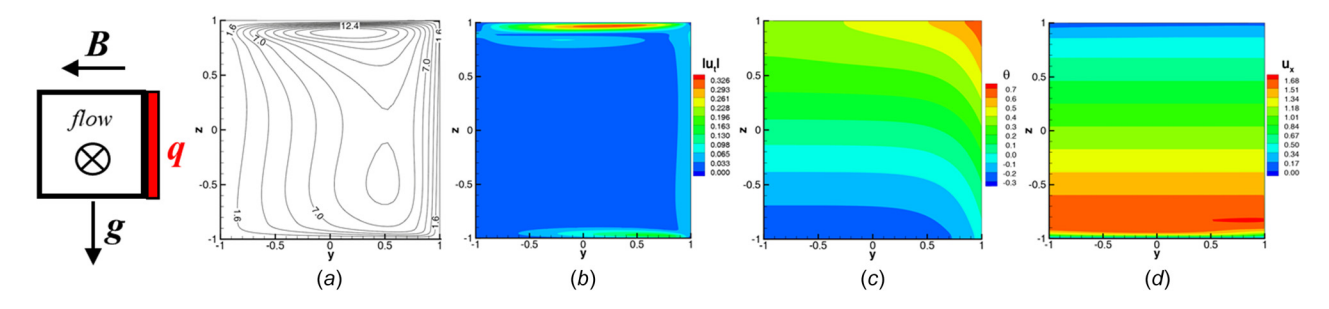


Fig. 11 Results of numerical simulations [42] for the flow in a square duct with horizontal magnetic field and heating applied to the right sidewall at Re = 10^4 , Gr = $1.6 \cdot 10^{10}$, Ha = 1600 (parameters are recalculated according to the definitions used in this review). The flow is laminar, steady-state, and streamwise-uniform at these parameters (see text). From left to right: streamlines of transverse circulation, and distributions of the amplitude of transverse velocity u_t , temperature θ in excess of the mean-mixed value, and streamwise velocity u_x . Image copyright of the American Institute of Physics (2014). Reproduced with permission.

much higher than in other configurations. As an example, amplitudes as high as 50° C are found at a moderate applied heating load ($\sim 50 \text{kW/m}^2$) in the experiments [223,234,235,237].

As an illustration, Fig. 12 shows signals and power spectra of the fluctuations of temperature in a downward flow in a pipe with

half of the wall heated [234]. The Reynolds and Grashof numbers are fixed (Re = 2×10^4 and Gr = 6×10^7), while the Hartmann number varies to illustrate the effect of the magnetic field. At Ha = 0 and Ha = 150, the fluctuations are typical for turbulent flows – the spectra are smooth without a dominating frequency.

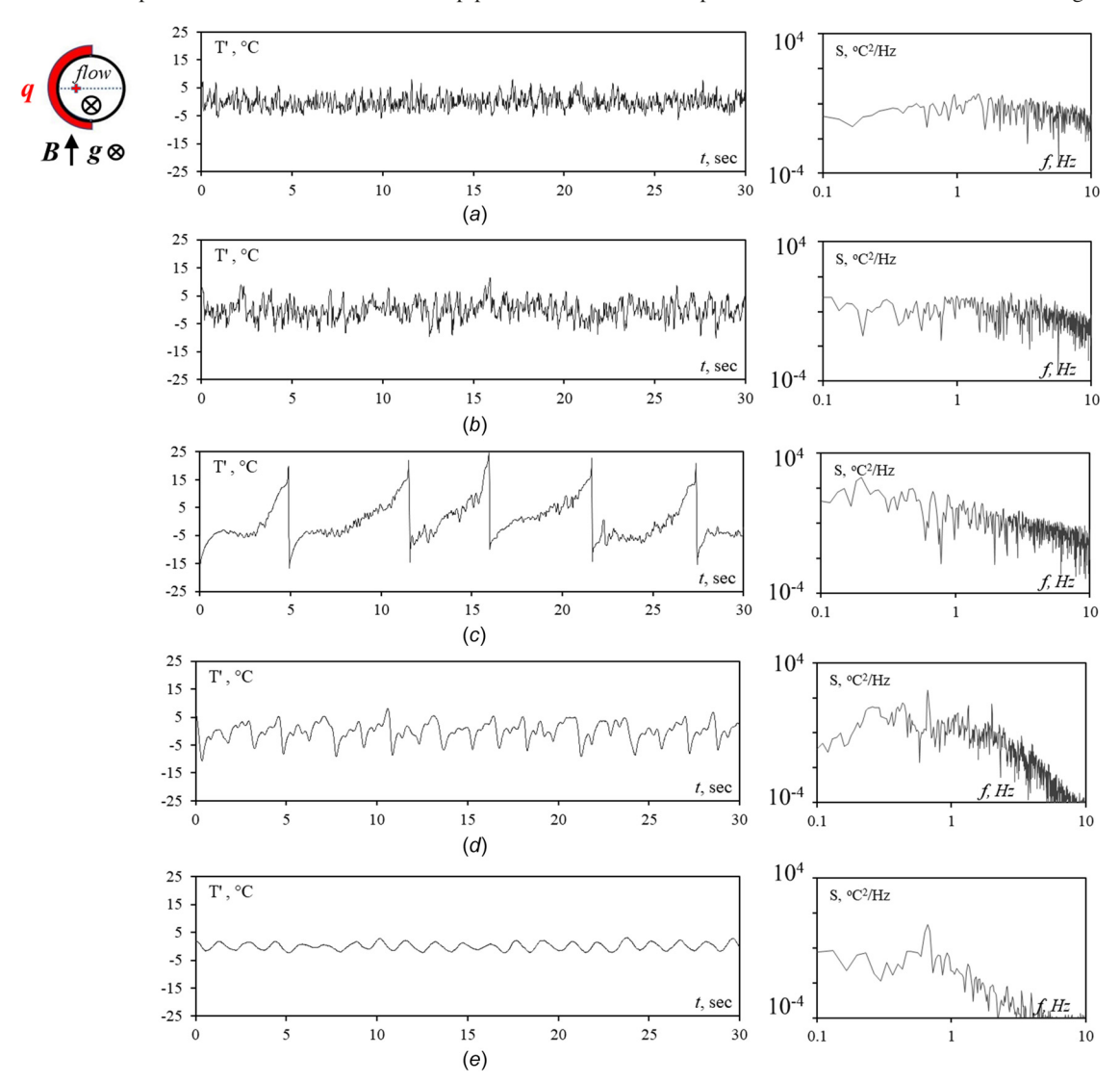


Fig. 12 Signals and power spectra of temperature fluctuations in the downward flow in a vertical pipe with half of the wall heated (see the diagram at the top) [234]. The centered signals recorded at the point of the cross section indicated by the cross in the diagram and at the axial location 37 pipe diameters downstream from the beginning of the heated section are shown for $Re = 2 \cdot 10^4$ and $Gr = 6 \cdot 10^7$ and various values of Ha.

MCFs characterized by dominance of low frequencies are found at higher Ha. The signal at Ha = 200 in Fig. 12(c) is a typical "sawtooth," also called a "tear-off/peak" signal, characterized by very large amplitude and quasi-cyclic evolution consisting of long periods of gradual increase of temperature inter-rupted by abrupt drops. Smooth quasi-harmonic oscillations are found at Ha = 575 (see Fig. 12(e)). An example of a mixed-type signal combining quasi-harmonic and sawtooth features is shown for Ha = 500 (see Fig. 12(d)).

The physical mechanism causing MCFs has been demonstrated in recent computational and theoretical studies [122,207,239]. Briefly, we observe an inflection point instability generating Q2D vortices. In this sense, the phenomenon is analogous to the instabilities found earlier in isothermal MHD flows with M-shaped velocity profiles, which appear, e.g., in ducts with nonuniform electrical conductivity of walls or nonuniform magnetic fields [84,85,120,240–242]. The formation of the inflection points in our case is, however, caused by a completely different effect – thermal convection.

The validity of this explanation is confirmed by the general consistency between numerical and experimental results and by good qualitative agreement in one case for which direct comparison was accomplished (see Fig. 13).

The mechanism has two main components. One is that the unstable stratification and horizontal heat flux lead to growth of long and strong ascending (near the heated wall) and descending jets. In the asymptotic limit of an infinitely long channel, the jets are not just long and strong, but exponentially growing streamwise-uniform exact solutions of the Boussinesq equations – the elevator modes [63–65], which we already mentioned in Sec. 3.2.

The second component is the stabilizing effect of the magnetic field. In systems with zero or weak effect of the magnetic field, the jets, with their thin shear layers and inflection points, are prone to secondary instabilities and typically disintegrate into turbulence before growing to significant amplitudes. The situation is changed by a strong magnetic field. Firstly, the transverse field modifies the jets by flattening their profiles and forming MHD boundary layers. Secondly and more importantly, the magnetic field suppresses three-dimensional fluctuations and stabilizes the jets, so that they maintain their undisturbed structure and continue to grow to very large velocity amplitudes while retaining the inflections points and zones of strong shear [65]. Eventually, the jets become unstable to Q2D perturbations, which can grow in a strong magnetic field since their velocity fields are nearly uniform along the field lines in the bulk of the channel (see Sec. 4).

The transient nature of the jets is a critical element of the instability at high Gr. This is illustrated by the linear stability analysis of flows in infinitely long channels. The steady-state streamwise-uniform solutions always exist but become unphysical (consisting of multiple ascending/descending pairs) at Gr higher than approximately 10^8 [65,239]. On the contrary, transient solutions retain physically plausible form and lead to the secondary instability, consistent with experimental data at all the values of Gr tested so far.

The entire instability scenario described above has been demonstrated computationally for three configurations: a flow in a pipe segment reproducing the test section of the experiment [207,234], a duct flow simulated in the 2D asymptotic limit corresponding to Ha $\gg 1$, N $\gg 1$ [239], and another 2D duct flow at much higher values of Ha and Gr [122].

As an example, Fig. 14 shows the results of the 3D DNS of the pipe flow [207]. Three consecutive snapshots illustrate the typical evolution of the pattern developing as a result of the instability. We see segments of ascending and descending jets growing for a long time and thus extending for a long distance along the pipe. Once their amplitude and thus the strength of the inflection points become high, the stability is lost and a local Q2D vortex is generated. Strong mixing in the vortex area destroys the jets and initiates the new process of their growth. The downward transport of the entire pattern by the mean flow produces the saw-tooth signal of temperature shown in Figs. 12 and 13. In this signal, periods of gradual increase of temperature correspond to the stages of growing jets, while abrupt drops manifest arrivals of well-mixed vortex zones.

The spatio-temporal flow behavior presented in Figs. 13 and 14 is not the only possible realization of the MCF instability. Flow regimes characterized by different patterns and typical frequencies and amplitudes of the temperature signal are possible. As examples, we mention the quasi-harmonic temperature fluctuations of higher frequency and lower amplitude detected in experiments and computations (such as shown in Fig. 12 for Ha = 550) [122,177,207,223,234–238]. Numerical simulations, in particular [122], demonstrate that different types of signals correspond to different spatial forms and characteristics of unstable perturbations.

The map of possible instabilities and underlying physical mechanisms remains poorly known. The available data show that the specific scenario of flow evolution and the spatio-temporal structure of MCFs are determined by the channel's geometry, configuration of heating, and values of all three independent governing parameters, Gr, Re, and Ha. It is, however, plausible to assume that the principal mechanism of the instability outlined above is universally valid.

The boundaries of existence of MCFs in the parameter space is an important and not yet fully answered question. Before presenting the data, we will discuss the anticipated impact of each independent parameter on the instability mechanism.

Gr is the key parameter determining the buoyancy forces and thus the strength of the instability. Increase of Gr causes faster growth of the ascending/descending jets and development of the inflection points. This results in shorter distances between the secondary vortices and provides fluctuations of higher typical frequency and amplitude.

The influence of Re-and Pe has two main aspects. Evidently, this parameter determines the suppression of instability by viscous friction and conduction. Since values of Re-are typically large, this effect is expected to be weak. The other more important effect is that larger Re means weaker unstable stratification along the channel. The growth of jets is slower, and the instability either

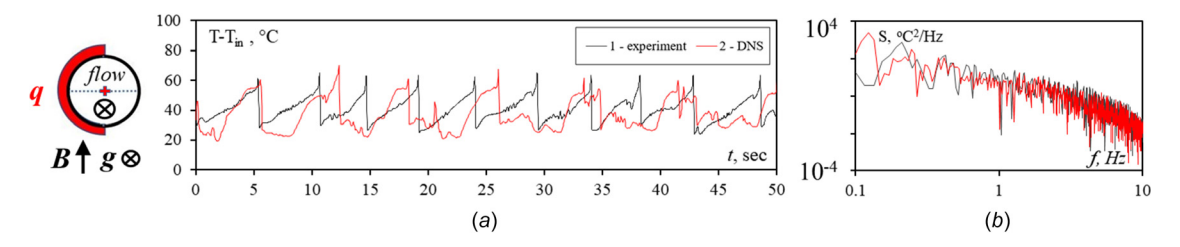


Fig. 13 Comparison between experimental [234] and numerical [207] results for a downward flow in a vertical pipe (see the diagram on the left). Signals and power spectra of temperature fluctuations measured at the center of the pipe 37 diameters downstream from the beginning of the heated section are shown for $Re = 10^4$, $Gr = 6 \times 10^7$, Ha = 300.

does not occur at all or leads to weaker fluctuations with lower frequency. This effect is usually taken into account by describing the results in terms of the Richardson number $Ri = GrRe^{-2}$ in lieu of Gr.

The role of Ha is also complex. On the one hand, a certain strength of magnetic damping is required to suppress turbulence, which is a necessary condition of MCFs. This is usually identified as a critical value of the Stuart number $N=\mathrm{Ha^2/Re}$ or the Hartmann-length based Reynolds number $Rh=\mathrm{Re/Ha}$, although in our case the role of Re as a measure of the strength of inertia is debatable. On the other hand, when turbulence is suppressed and Q2D MCFs appear, higher Ha implies stronger damping of these structures by friction in the Hartmann boundary layers.

Some information on the domain of existence of MCFs is provided by experiments and simulations [122,177,207,223, 234–239]. A more detailed picture available for the pipe flow from the experiments [223] and for a flow in a square duct from

the 2D simulations [122] is summarized in Fig. 15. It allows us to identify the following limits of the MCFs' existence domain.

There is the limit Ri ≈ 0.08 , below which no MCFs can appear in the pipe flow. The reason for that was revealed in the simulations [207] conducted at Ri = 0.049 (see the left plot of Fig. 16). The buoyancy forces are weak, so the jets never become sufficiently strong to trigger the instability. It must be mentioned that the specific value of this threshold depends on the length of the channel's segment with active heating and magnetic field. The data in Fig. 15 are for a fairly long segment (more than 40 pipe diameters). A longer segment would allow the jets to grow over a larger distance and possibly cause instability at lower Ri. An opposite effect is anticipated in a shorter segment.

There is also the limit of a weak magnetic field. The right plot in Fig. 16 illustrates the state of the flow when the magnetic field is not strong enough to suppress turbulence. Coherent ascending/descending jets do not form, so the inflection point instability

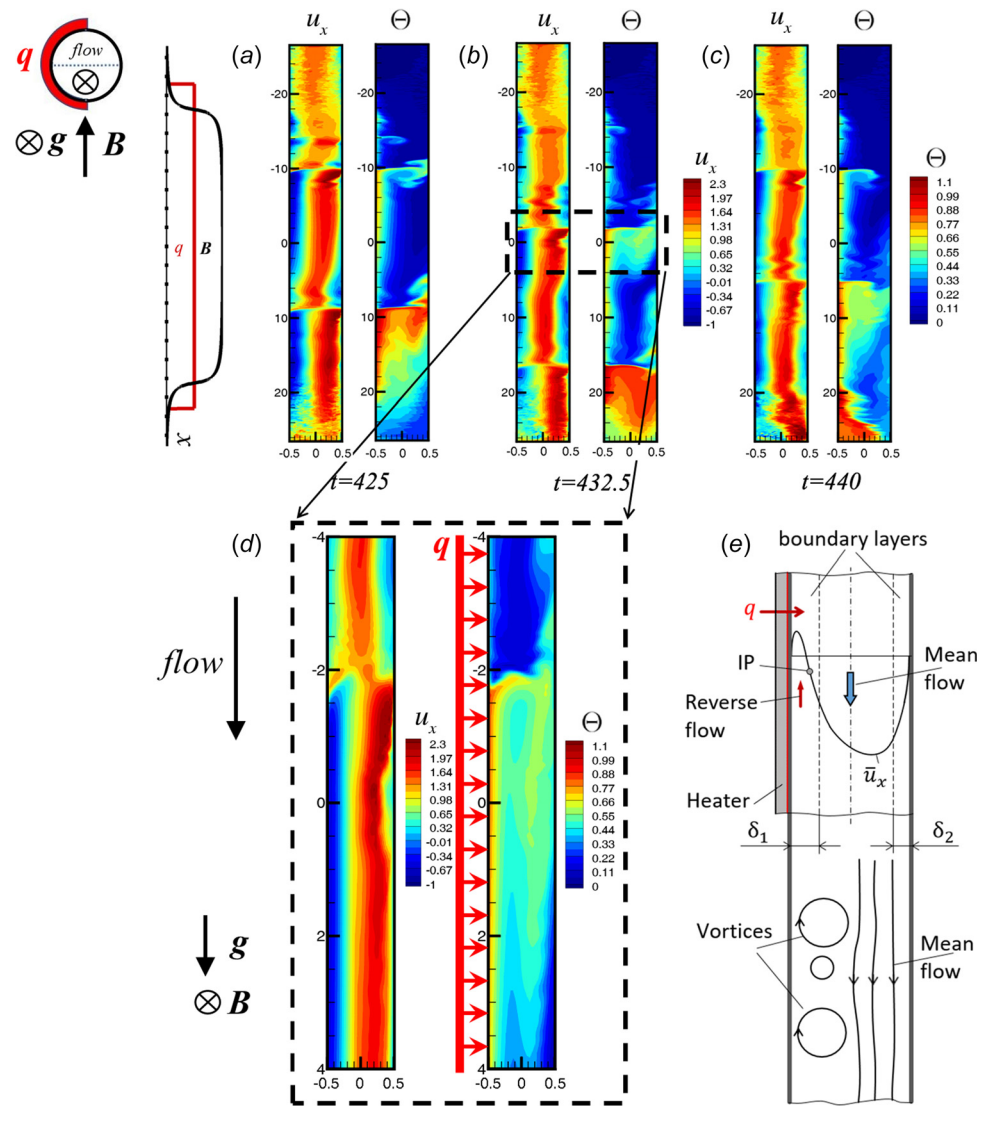


Fig. 14 Results of simulations [207] of downward flow in a pipe with a half of the wall heated (see the diagram at the top) at Re = 10^4 , Gr = 6×10^7 , and Ha = 300. (a)–(c) Snapshots of distributions of streamwise velocity u_x and temperature θ in the vertical plane indicated by the dashed line in the diagram are shown for three consecutive time moments taken with the step of 7.5 nondimensional time units. Note, that positive u_x correspond to the downward direction and that the coordinates x and z are plotted with different scales. Distributions of the main component of the magnetic field and wall heating rate used in the simulations are shown on the left. (d) A part of the fields in (b) plotted with equal x and z scales. (e) A schematic illustration of the instability mechanism. Plots (a)–(d)—Image copyright of the Elsevier (2016). Reproduced with permission. Plot (e)—courtesy of Yu. Kolesnikov.

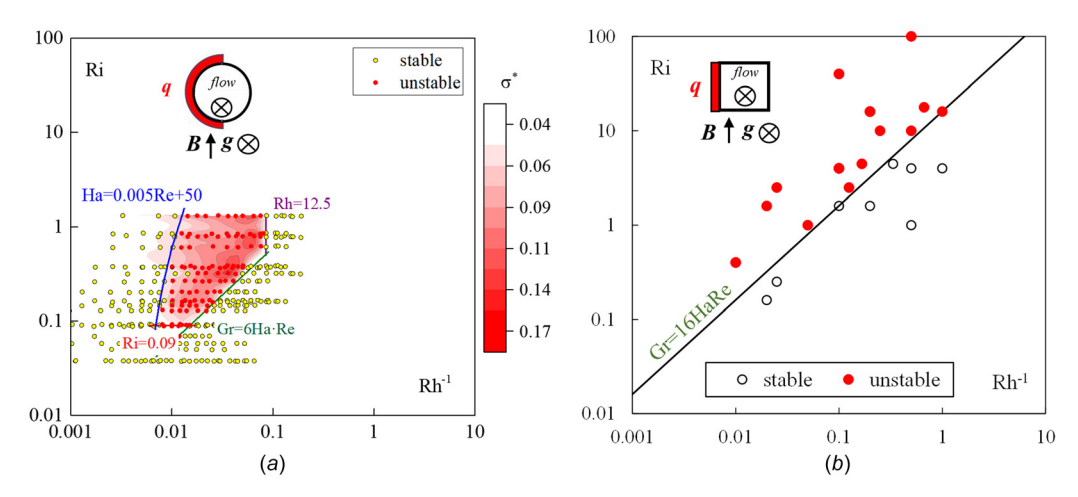


Fig. 15 Domain of existence of MCFs in downward flows in vertical channels with asymmetric heating. (a) Experimental data of [223] for the flow in a pipe with a half of the wall heated and the magnetic field perpendicular to the imposed heat flux. The maximum value of the standard deviation of temperature in a pipe's cross section is shown in the (Rh $^{-1}$, Ri) plane. Approximate boundaries of the domain of existence of MCFs are indicated. (b) Data of 2D (in the asymptotic model valid at Ha \gg 1, N \gg 1) simulations of [122]. Computed flow states with (unstable) and without (stable) MCFs are shown. Parameters are recalculated according to the definitions used in this review.

does not occur. The data of [223] suggest two possible definitions of this limit, both consistent with the understanding of how turbulence is suppressed by the magnetic field. One is that N must be larger than approximately 1.5. Another is that Ha is larger than 0.005Re + 50 (see Fig. 15(a)). Apart from the additive term, the latter expression is consistent with the well-established range of laminar-turbulent transition $200 \le Rh \le 400$ in isothermal duct and pipe flows with strong transverse magnetic fields [22]. The lower boundary of this range Rh ≈ 200 is recovered in Ref. [223] because of the deformation of the velocity profile and strong perturbations introduced by thermal convection effects.

We note that the low-end limits were not detected in the simulations of the duct flow shown in Fig. 15(b). The limit of a weak magnetic field could not appear because the asymptotic 2D model

presumes a very strong magnetic field effect. The limit at low Ri was not identified because no simulations were made in the range of small Rh (Rh < 0.01) where this limit could be found.

There is also a boundary of the MCF existence domain at strong magnetic fields, although the situation is less clear. The pipe flow experiments [223] show that at moderate Ri the limit is defined as Gr = 6HaRe or Ri = 6/Rh (see Fig. 15(a)). This is consistent with the results of the duct flow simulations [122], which show a similar limit at Gr = 16HaRe (see Fig. 15(b)). The difference between the slopes can be plausibly attributed to different geometries of the two systems. There is another significant difference in the behavior at large Ri. The pipe flow shows a cutoff at Rh \approx 12.5. No such cutoff is found for the duct flow. The difference can be attributed to the difference between the two

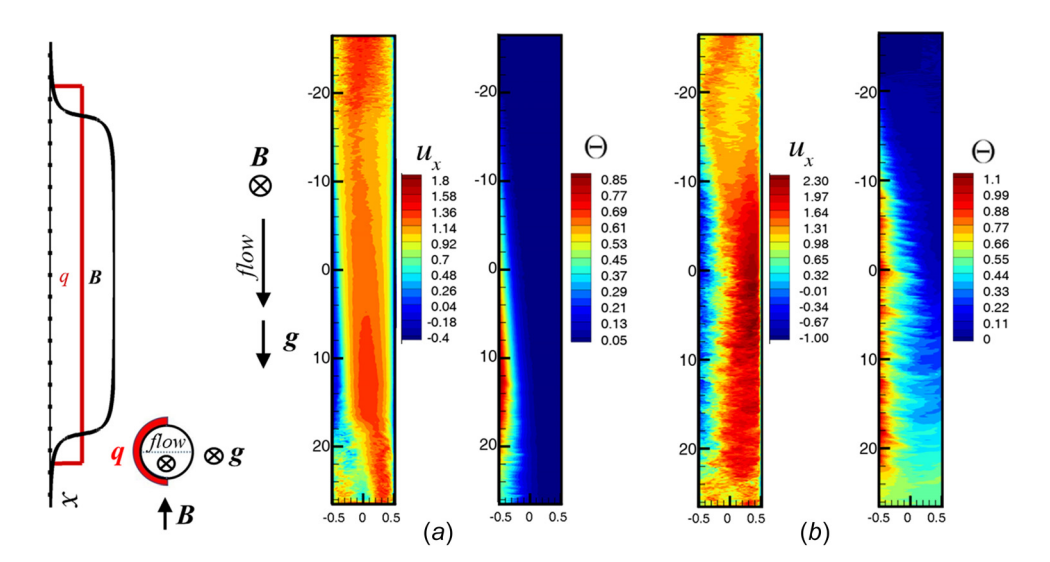


Fig. 16 Results of simulations [207] of downward flow in a pipe with half of the wall heated plotted as in Fig. 14. Snapshots of distributions of axial velocity u_x and temperature θ are shown for two combinations of parameters at which MCFs do not appear. (a) Re = 35,000, Gr = $6 \cdot 10^7$, Ha = 300. MCFs do not appear because Ri = 0.049 is too small. (b) Re = 12,000, Gr = $6 \cdot 10^7$, Ha = 80. MCFs do not appear because Ha is too small. Image copyright of the Elsevier (2016). Reproduced with permission.

geometries. No truly Q2D structures can form in a pipe. There are 3D features of the velocity field that are susceptible to strong magnetic damping even at very high Ha [28,34].

A major remaining question is whether MCFs exist at the values of Gr and Ha typical for a fusion reactor blanket, i.e., the values much larger than those achieved in experiments and shown in Fig. 15. No definitive answer can be given at this moment, but the absence of the constant-Rh cutoff in the 2D simulations of the duct flow performed in the asymptotic limit Ha $\gg 1,\,N\gg 1$ model indicates a positive answer. We note that the parametric range Rh ≤ 1 and Ri ≤ 100 explored in Ref. [122] is much larger than in other studies of the downward flow. While still below the range typical for a blanket, it gives us a basis for a more reliable extrapolation.

Recent experiments [243] indicate an intriguing possibility of intermittent behavior in the vicinity of both upper (less common) and lower (more common) limits of existence of MCFs. Abrupt fluctuations of extremely large amplitude occur every few tens of minutes in an otherwise steady-state flow regime. Such a behavior is difficult to detect and study experimentally or numerically. At the same time, it can create significant risks in fusion reactor applications.

The upward mean flow was studied in experiments [238,244,245] and computations [118,246–249]. It has been confirmed that the principal instability mechanism is similar to that in the downward flows. Transformation of the streamwise velocity profile by buoyancy forces generates inflection points (see Figs. 4(c) and 4(d) for a schematic illustration). This leads to instability in the form of Q2D vortical structures and high-amplitude low-frequency MCFs (see Fig. 17). At the same time, there are evident differences. Since the stratification by the mean-mixed temperature is stable, no elevator modes and no reversed flow zones may appear in the upward flow. The shear is weaker and inflection points form in a smaller range of parameters. This implies a smaller range of existence and a smaller amplitude of MCFs.

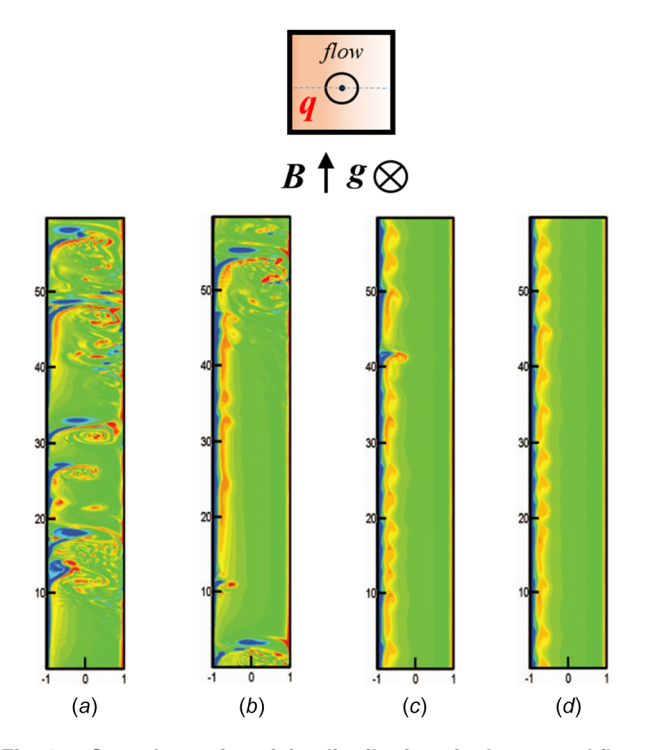


Fig. 17 Snapshots of vorticity distributions in the upward flow in a vertical square duct with asymmetric internal heating [118]. Flows at Re = 10^4 , Gr = $1.6 \cdot 10^9$ and Ha = 50 (a), Ha = 120 (b), Ha = 120 (c), and Ha = 120 (d) are shown (Parameters are recalculated according to the definitions used in this review). Image copyright of the American Institute of Physics (2013). Reproduced with permission.

There are other, subtler differences. For example, 2D simulations [118] show a second instability mode in flows with high Re – the boundary-layer instability near the hotter wall.

An important consequence of this MCF instability is that the secondary flow structures cause additional mixing and strong heat transfer. This occurs at high Ha, at which mixing and heat transfer would be reduced to nearly laminar levels in flows without convection. As an illustration of this effect, Fig. 18 shows the dependence of Nu and the nondimensional standard deviation of temperature fluctuations on Ha at fixed Gr and different values of Re. Experimental data for downward [237] and upward [238] flows in a duct with one wall heated are shown. The Nusselt number is normalized by its value obtained without the magnetic field and shows two different types of behavior in the downward flow. At high Ri and low Re (approximately Ri ≥ 0.25 , Re $\leq 15 \times 10^3$), the heat transfer rate at Ha > 100 tends to its turbulent value (solid lines), while the laminar value is approached at low Ri and high Re (dashed lines). Thus, the joint action of magnetic and buoyancy forces leads to a counterintuitive result - quasi-laminar heat transfer at higher Reynolds numbers and quasi-turbulent at lower ones. The conclusion is supported by the curves of the standard deviation of the fluctuations.

In the upward flow (lower panels of Fig. 18), the dependence of the heat transfer on the magnetic field is weak at any flow rate, while the temperature fluctuations indicate the suppression of the turbulence.

An interesting question is that of the effect of the symmetry of applied heating on MCFs. In addition to the strongly asymmetric heating considered so far, symmetric or mildly asymmetric heating can be realized in experiments by positioning heating elements on the opposite sides of a duct or even on the entire wall of a pipe or a duct, uniformly or nonuniformly. The experimental studies, such as [177,223,234,235,237], show that MCFs appear in such configurations, although their amplitude and the range of existence in the parameter space become smaller as the heating becomes more symmetric. The pattern of MCF signals also changes. For example, a nearly harmonic temperature signal quite unlike the signals in Fig. 13 is found in the downward flow in a duct with symmetric wall heating [237,250].

As another example of an interesting result, Fig. 19 shows the data of the experimental study of the downward flow in a pipe with uniform heating of the walls [177]. Areas of two distinct types of MCF characterized by different distributions of a time-averaged amplitude of temperature fluctuations are clearly visible.

We complete this section by a few summarizing remarks. MCFs appear in a broad range of parameters in all configurations of vertical channels studied so far. It is not proven but is plausible and even likely that they exist at the parameters typical for a fusion reactor blanket. A particularly dangerous situation is anticipated in channels with downward mean flow, in which the amplitude of temperature fluctuations can be spectacularly high.

6.3 Longitudinal magnetic field. A channel with longitudinal (directed along the axis) magnetic field is a key element of the concept of a fusion reactor blanket with toroidal ducts (see Fig. 1(b)). It is also a fascinating system, in which common hydrodynamic mechanisms are profoundly changed, thermal convection may play an exceptionally strong role, and 2D turbulence is a realistic possibility rather than an abstraction.

The first experimental studies of such flows date back to the 1950s and 1960s. The main focus was on the instability of laminar states and the transition to turbulence [251–254] and the effect of a magnetic field on properties of turbulence (flow resistance, mean velocity profile, statistical moments of fluctuations) and heat transfer [255–262]. The main aspects of the magnetic field effect were identified at that time. In particular, it was understood that the magnetic field does not interact with the streamwise mean flow, so there is no MHD pressure drop. The field interacts with velocity fluctuations, directly suppressing longitudinal velocity

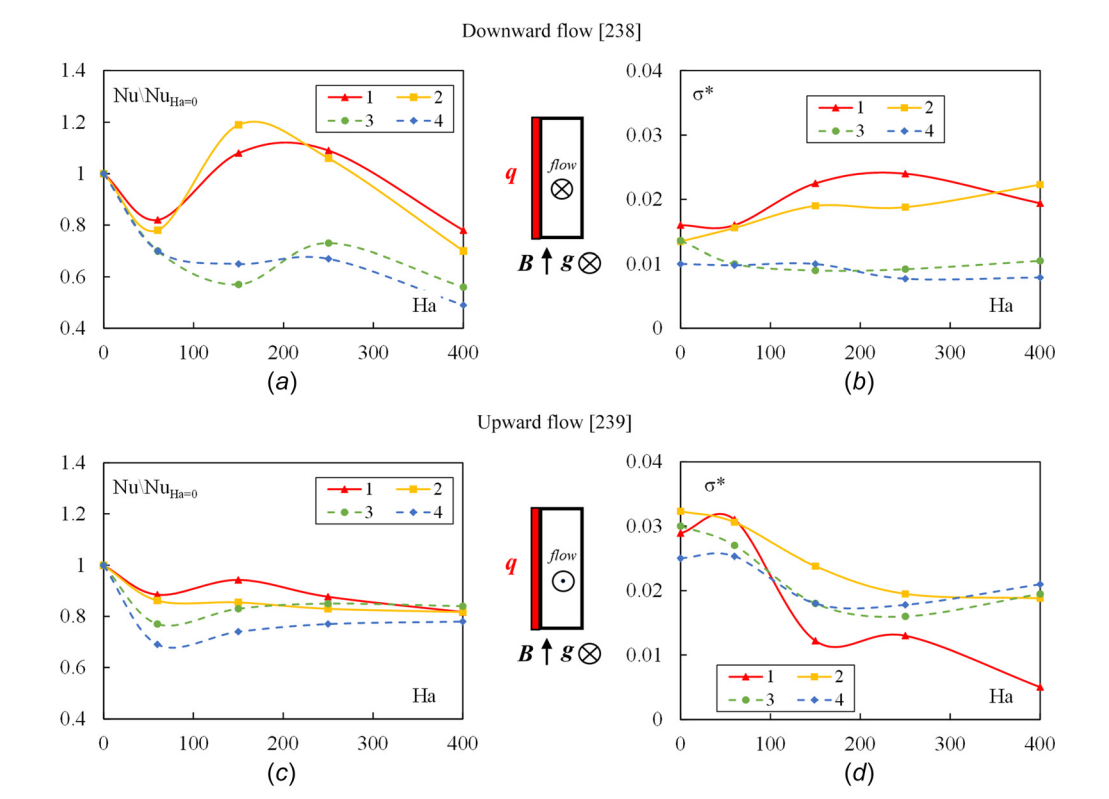


Fig. 18 The normalized local (in the mid-dle of heated side) Nusselt number (a,c) and r.m.s. of temperature fluctuations (b,d) versus Ha for flows in a vertical duct with one side heated and a transverse magnetic field at a distance x/d=40. Experimental results on downward flow (a,b) [237] and upward flow (c,d) [238] are shown for: (1) Re = $10 \cdot 10^3$, Ri = 0.5; (2) Re = $15 \cdot 10^3$, Ri = 0.25; (3) Re = $20 \cdot 10^3$, Ri = 0.12; (4) Re = $25 \cdot 10^3$, Ri = 0.7. (Parameters are recalculated according to the definitions used in this review). Image copyright by Elsevier (2019, 2020). Reproduced with permission.

gradients and indirectly affecting all the other turbulence properties. Turbulent fluctuations become more anisotropic than in hydrodynamic channel flows. The ratios between typical longitudinal and transverse length scales and between amplitudes of longitudinal and transverse velocity components increases with the growing strength of the magnetic field effect (best expressed by the value of N). It is predicted on the basis of theoretical arguments and illustrated in numerical simulations [263–265] that these changes are manifestations of the transformation of coherent

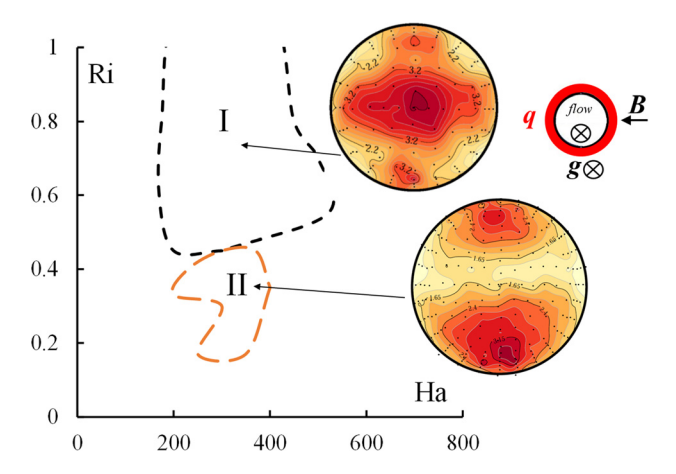


Fig. 19 Domains of existence of two different types of MCFs in the downward flow in a pipe with uniform wall heating [177]. Typical distributions of r.m.s. fluctuation amplitide (in °C) in the pipe cross section are shown.

structures, such as streaks and vortices, which become stabilized and elongated along the magnetic field lines.

An interesting and practically consequential aspect of the effect of a longitudinal magnetic field is the possibility of a purely 2D state of the flow. In theory, such a state is possible when the magnetic field is strong enough to fully suppress velocity gradients along its lines (which requires $Ha \gg 1$ and $N \gg 1$). If the flowdriving parameter, e.g., Re, is large, 2D turbulence may appear. Practically, pure two-dimensionality requires that there are no walls crossing the field lines. This is possible in theoretical models, such as periodic boxes [72] or channels with spanwise or streamwise periodic conditions [86,265], but not in laboratory or technological realizations of straight channel flows. The only practically feasible configuration permitting such purely 2D states is a toroidal duct with a perfectly toroidal magnetic field created by an axial current. This configuration was recently used to study the transition between 3D and 2D flows in a Taylor-Couette arrangement [79]. It was confirmed that purely 2D turbulence is possible in this system, although its realization in laboratory conditions would require very large axial currents so it would inevitably involve effects of nonuniform temperature and imperfect magnetic field.

The configuration of a channel with a longitudinal magnetic field is a central element of the concept of a liquid metal blanket with toroidal ducts [266,267]. The concept was born as an early attempt to solve the problem of the huge MHD pressure drop that appears when a liquid metal is pumped trough a channel with a strong transverse magnetic field and electrically conducting walls [5,34]. Orienting the ducts along the main (toroidal) component of the magnetic field seems to be a good solution to avoid this problem. One can use steel alloys for internal walls and pump the liquid metal with very large flow rates (Re $\sim 10^5$), so the desired

rate of heat transfer can be achieved even in the conditions of turbulence suppressed by the magnetic field.

This logic led to the large-scale effort to develop a blanket with toroidal ducts in the 1980s and 1990s (see the chapter by Bühler in Ref. [161] for a historical review). The concept was abandoned after it was realized that the MHD pressure drop would, in fact, still be large due to the 3D effects in the corners, U-turns, and other nontoroidal elements of the blanket (see, e.g., [268,269]) and that the design would present other complications, such as strong electromagnetic coupling between elements of a blanket module [270]. We now realize that the design was also based on an utterly incorrect assumption – that the effect of natural convection can be ignored so the heat transfer is purely passive.

The more recent experimental research was primarily focused on the effect of a longitudinal magnetic field on heat transfer [166,221,232,271–273]. Flows of mercury in long pipes of different orientations with respect to gravity and with different heating schemes were analyzed. It has been found that the magnetic field changes the behavior at the entrance into the zone of applied heating and the zone of magnetic field. In both cases, the entry length (the distance at which heat transfer coefficients and other statistical properties reach the values of a fully developed flow) grows with the strength of the magnetic field [271,272]. The effect is attributed to stabilization and lengthening of longitudinal velocity structures by the magnetic field. This has serious practical implications for the blanket design, indicating that an analysis based on the characteristics of a fully developed flow can be misleading.

Some of the experiments have been performed with the understanding of potentially significant effects of thermal convection. In particular, it has been found that in the downward flow in a vertical pipe, a longitudinal magnetic field does not suppress thermal convection but leads to stronger convection-induced near-wall jets. Interestingly, indications of what we would now identify as MCFs (high-amplitude, low-frequency temperature fluctuations appearing at strong magnetic fields) were found [232] (see Fig. 20) and confirmed by measurements of velocity fluctuations using fiber-optic sensors [166] (Fig. 21). No serious attention was, however, given to the phenomenon at that time, since it was presumed that the fluctuations would be inevitably suppressed by the much stronger magnetic field in a reactor blanket.

Experiments were also performed to study how longitudinal magnetic fields influence flows in horizontal pipes [273,274]. The main effect consistently found under various heating configurations was the increased asymmetry of the distributions of mean temperature. Some of the experimental data were reproduced with good agreement in the recent numerical simulations [275] (see Fig. 22). The simulations have shown that suppression of turbulent fluctuations and 3D instabilities by the magnetic field leads to stabilization of the convective structures in the form of longitudinal rolls (see Fig. 5). With a sufficiently strong field, the flow becomes steady-state and independent of the longitudinal coordinate and thus not interacting with the magnetic field. No MCFs have been found in the experiments and simulations.

In the remaining part of this subsection, we will review the numerical studies [43,68,276,277] in which the effect of thermal convection was analyzed for several types of 2D and nearly 2D flows forming in a horizontal duct with very strong (Ha ≫ 1, N ≫ 1) longitudinal magnetic field. A fully developed (far from inlet and exit) flow was considered. Internal heating with the volumetric rate decreasing exponentially with the distance from one vertical wall was applied. This heating scheme and the studied configurations were selected to model various effects anticipated in the toroidal ducts of a reactor blanket. The values of Ha and N in such ducts will certainly be large enough to enable transition into a 2D state. The two-dimensionality would be imperfect, since the magnetic field will, in addition to the main toroidal component, have a much weaker but still significant $(\sim 5\%)$ poloidal one. Another reason for imperfection is the finite length of the ducts. There would inevitably be 3D effects near the inlet and exit of each duct (see Fig. 1(b)). At the same time, the

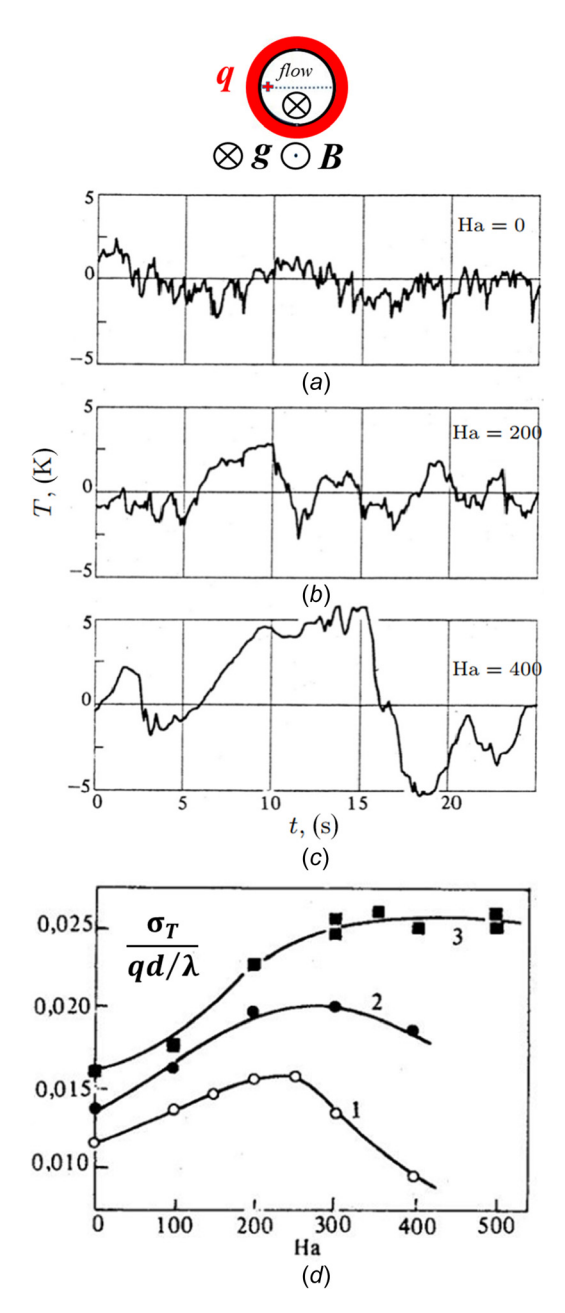


Fig. 20 Signals (a)–(c) and standard deviation (d) of dimensionless temperature fluctuations in a downward flow in a vertical pipe with uniform heated wall and longitudinal magnetic field (see the diagram at the top) [232]. The centered signals recorded at the point indicated by the cross in the diagram and at the axial location 35 pipe diameters downstream from the beginning of the heated section are shown in (a-c) for Re = $7.5 \cdot 10^3$ and various values of Ha. The standard deviation obtained for Re = 10^4 , Gr = 10^7 (curve 1), $2 \cdot 10^7$ (curve 2), and $4 \cdot 10^7$ (curve 3) is shown as a function of Ha in (d).

ratio between the length and width of the ducts is typically sufficiently large, so we can assume existence of a nearly 2D state in the core. Furthermore, curvature of the duct is typically small and can be neglected.

The configuration with zero mean streamwise flow and walls maintained at a constant temperature (an idealized model of a separately cooled blanket, in which the cooling is mostly done by auxiliary heat exchange systems) was analyzed in Ref. [68]. 2D turbulence was found at large Gr (see the top row of Fig. 23). Apart from the evident theoretical interest, this has practical

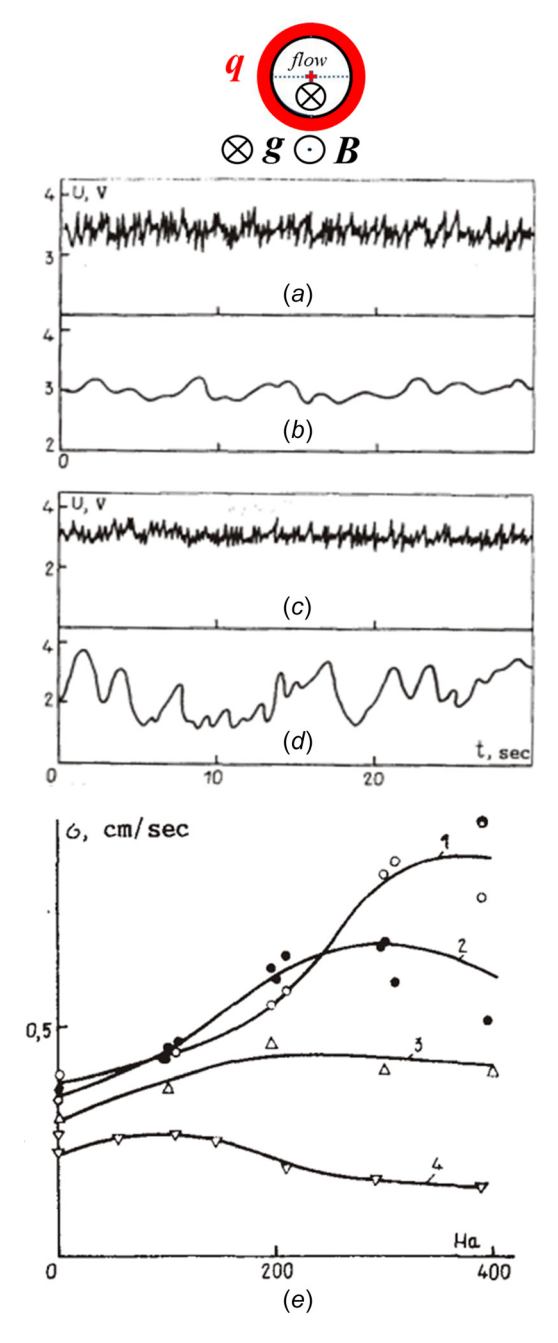


Fig. 21 Signals of streamwise velocity fluctuations (a)–(d) and their standard deviation (e) in a downward flow in a vertical pipe with uniform heated wall (see the diagram at the top). Measurements are performed using the fiber-optic sensors [166]. The signals are recorded at the center point of the pipe and at the axial location 35 pipe diameters downstream from the beginning of the heated section. Results for Re = $7 \cdot 10^3$ are shown in all plots. The other parameters are Gr = 0 (isothermal flow - a,b), Gr = $2.5 \cdot 10^7$ (c,d), Ha = 0 (a,c) and Ha = 300 (b,d). The curves in (e) are for: $1 \cdot \text{Gr} = 2.5 \cdot 10^7$, $2 \cdot \text{Gr} = 1.2 \cdot 10^7$, $3 \cdot \text{Gr} = 5 \cdot 10^6$ and $4 \cdot \text{Gr} = 0$.

implications for fusion reactor blankets. The turbulent mixing and the associated strong heat transfer toward the walls are anticipated to prevent the structurally dangerous strong temperature gradients and MCFs.

The stability of 2D states to 3D perturbations decreases with the longitudinal size of the domain, since the magnetic damping of unstable modes is weaker for modes of larger wavelength along the field lines. The results of [68] indicate that 2D states are likely

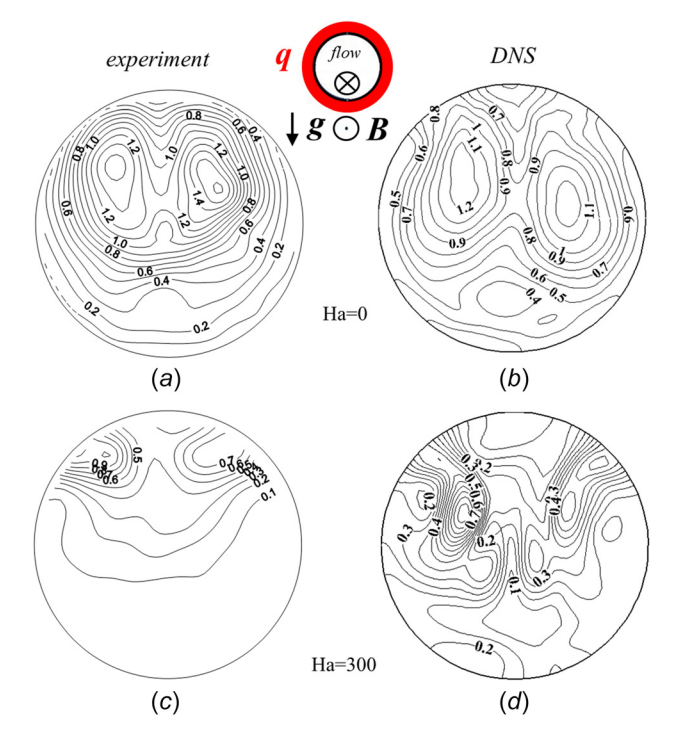


Fig. 22 Standard deviation of temperature fluctuations, in $^{\circ}$ *C*, in the cross section of a horizontal pipe with uniform wall heating and longitudinal magnetic field (see the diagram at the top). The cross section is 37 pipe diameters downstream of the beginning of the heated zone. Results of experiments [273,274] (a), (c) and simulations [275] (b), (d) are shown for Re = 10^4 , Gr = $8 \cdot 10^7$, Ha = 0 (a) and (b) and Ha = 300 (c) and (d). Image copyright is by the Magnetohydrodynamics Journal published by the Institute of Physics, University of Latvia (2019). Reproduced with permission.

to be stable at Gr and Ha and length-to-width ratio typical for ducts in a module of a fusion reactor blanket. It has also been shown in Ref. [68] that even when the 2D states are unstable, 3D perturbations saturate at a low energy level, not more than a few percent of the energy of the 2D flow. The resulting change of the Nusselt number does not exceed 10%.

The analysis was continued in Ref. [276], where the influence of the additional poloidal (vertical in the geometry of [68,276]) component of the magnetic field on 2D states was studied. The effect was found to be strong at the high values of Ha typical for a fusion reactor (see the middle row in Fig. 23 for an illustration). 2D turbulence was suppressed. The flow becomes laminar and steady-state, with its structure dominated by large-scale convection structures. Interestingly, the mixing by these structures is sufficient to achieve the same practical benefits as in the case of a turbulent flow: avoidance of strong temperature gradients and MCFs

A further continuation was the analysis of the effect of strong streamwise flow (Re $\leq 2 \times 10^6$) in the presence of thermally insulated walls [43]. This configuration modeled a toroidal duct of the classical blanket concept shown in Fig. 1(b). The main conclusion of [43] was that the approach adopted in the earlier studies of this concept of ignoring the effect of thermal convection was indeed incorrect. The structure and properties of the flow are practically always dominated by convection. This may happen in two ways. At Gr less than approximately 1.6×10^{10} , convection produces large circulation rolls, which can be steady-state, unsteady, or turbulent depending on the values of Gr and Re. Flows of a completely different type appear at Gr = 1.6×10^{11} and 1.6×10^{12} . The main effect in this case is the buoyancy forces associated with the streamwise growth of mean-mixed temperature, which

causes top-bottom asymmetry of the streamwise velocity profile and stable stratification (see Sec. 3.2). As illustrated in the bottom row of Fig. 23, the stratification suppresses the convection rolls, severely reduces mixing, and leads to extreme temperature variations across the duct. As an example, an estimate made in Ref. [43] predicted that the difference between the average temperatures of the top and bottom walls in a flow of PbLi in a square duct of width $10\,\mathrm{cm}$ at $\mathrm{Gr}=1.6\times10^{12}$ and $\mathrm{Re}=10^6$ would be as high at $322\,\mathrm{K}$. This evidently unrealistic number must be viewed as a warning sign of problems in the blanket development and the analysis of blanket phenomena based on classical hydrodynamic models.

6.4 Inclined channels. The configuration of an inclined channel is of direct significant interest for the design of the liquid metal blankets of fusion reactors. Such channels will be found in the blanket modules located around the torus of the reaction chamber in all but the equatorial and top and bottom areas (see the dashed module positions in Fig. 1(a)). Flows in channels of such modules will be influenced by transverse magnetic fields.

Some concepts of future reactors foresee a blanket in which cooling, shielding, and breeding are done by a liquid metal circulating in long channels surrounding the entire reaction chamber. To minimize the MHD pressure drop, such channels will be coiled so that their axes follow the magnetic field lines. In the context of physical effects considered in this review, this configuration is represented by an inclined channel with a longitudinal magnetic field and strongly asymmetric transverse heat flux. The inclination angle will vary depending on the strength of the poloidal component of the reactor's magnetic field, between 5 and 10 deg in large-scale facilities, such as ITER or DEMO, and up to 40 deg for more compact devices, such as spherical tokamaks.

The available experimental and computational data, which we present below, and general physical reasoning do not give us any reason to doubt that the flow modification by buoyancy and magnetic field is as profound in inclined channels as it is in the vertical and horizontal channels reviewed in Secs. 6.1–6.3. We anticipate modification of streamwise velocity profile (see Sec. 3.2), stable or unstable stratification, formation of inflection points, suppression of turbulent fluctuations, and development of MCFs. New

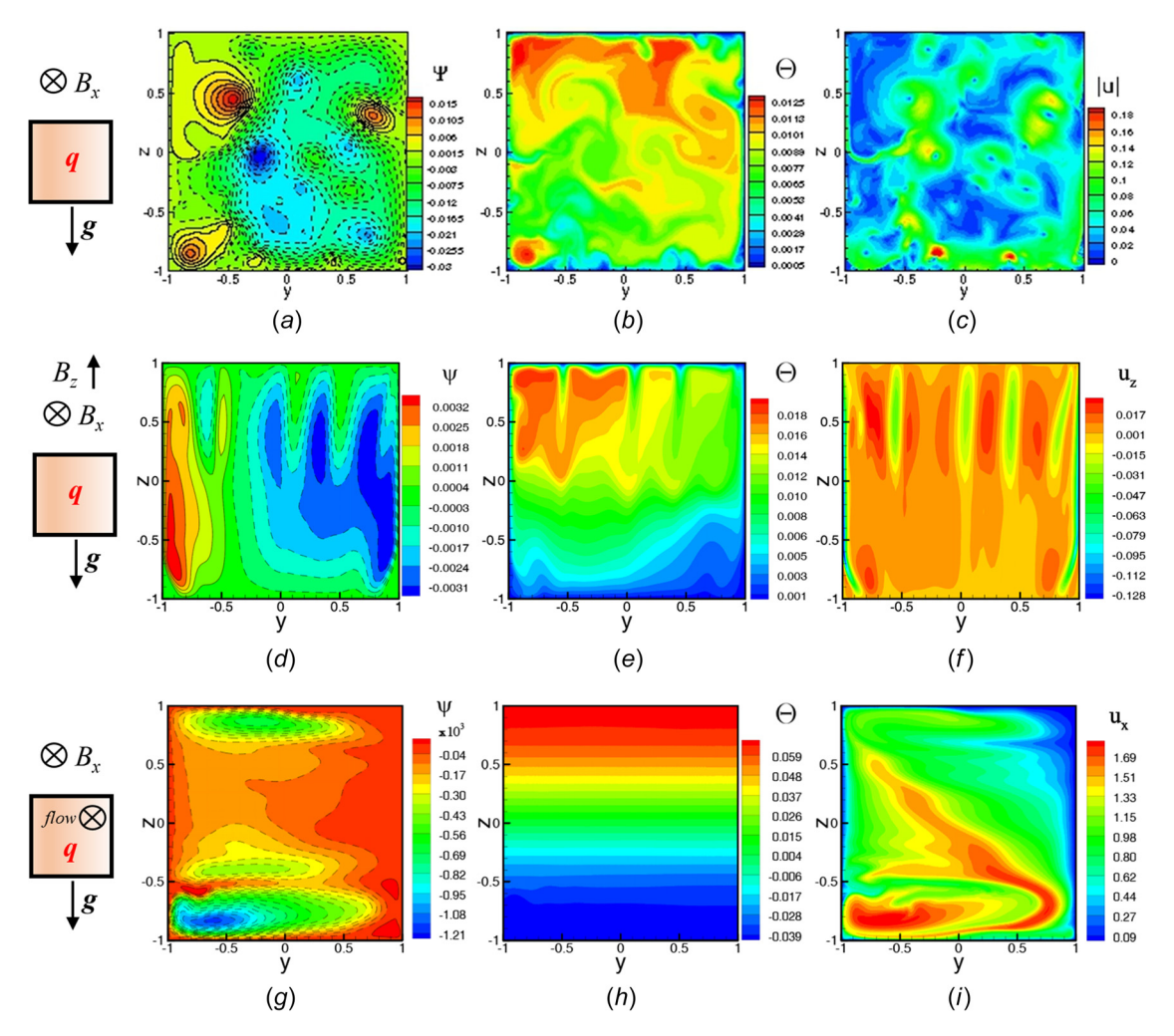


Fig. 23 Computed instantaneous distributions of flow fields in 2D flows in a horizontal duct with strong longitudinal magnetic field at $Gr = 1.6 \cdot 10^{12}$. Internal heating with nondimensional volumetric rate $q = -\exp(-y+1)$ is applied in all cases. Left column: streamfunction (solid and dashed lines indicate, respectively, counterclockwise and clockwise motion); mid-dle column: temperature in excess of the mean-mixed value; right column: velocity magnitude of a component as indicated in the plots. Top row: the case of zero streamwise flow and walls maintained at a constant temperature [68]. Mid-dle row: the same as at the top, but with an additional vertical magnetic field (B_z) of the strength corresponding to the respective Hartmann number $Ha_z = 1000$ [276]. Bothom row: the case with the streamwise flow corresponding to $Re = 10^6$ and thermally insulating walls [43]. Parameters are recalculated according to the definitions used in this review. Images (a)–(i) copyright of the Elsevier (2017). Reproduced with permission.

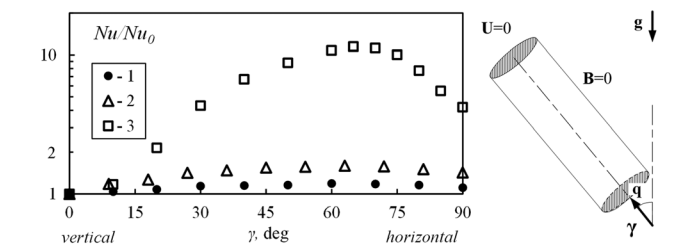


Fig. 24 Normalized Nusselt number versus the tilt angle for natural convection in sodium in cylinders with different aspect ratios: L=D (1 – experiments [279]), L=5D (2 – LES [280]), L=20D (3 – experiments [281]). Note that Nu/Nu₀ is shown in logarithmic scale.

effects not seen in vertical or horizontal channels are also possible. The tilt angle becomes one more (in addition to Re, Gr, and Ha) independent control parameter, which adds complexity to the problem.

As a first illustration of the nonlinear and complex effect of the tilt angle, we will briefly review the recent results obtained for natural convection in inclined cells [52,55,278–281]. It has been found that the cell inclination enhances large-scale circulation and modifies small-scale turbulence, affecting the global convective heat and mass transfer. An extended numerical study [278] of a convection cell of a unit aspect ratio in the range $10^6 \le \text{Ra} \le 10^8$, $0.1 \le \text{Pr} \le 100$ showed that the dependence of Nu on the tilt angle γ is not universal and is strongly influenced by Ra and Pr. At small γ , $\text{Nu}(\gamma)/\text{Nu}(0)$ increases or decreases with γ at, respectively, small or large values of Pr.

Experimental and numerical studies of natural convection in cylindrical cells filled with sodium (Pr = 0.0094) [52,55,279–281] reveal the critical role of the cell's aspect ratio L/D. We see in Fig. 24 that Nu(γ) increases at small γ and reaches the maximum at γ between approximately 60 and 70 deg. The effect is greatly enhanced in taller cells. The largest increase of Nu(γ) is about 20% at L=D, about 50% at L=5D, and more

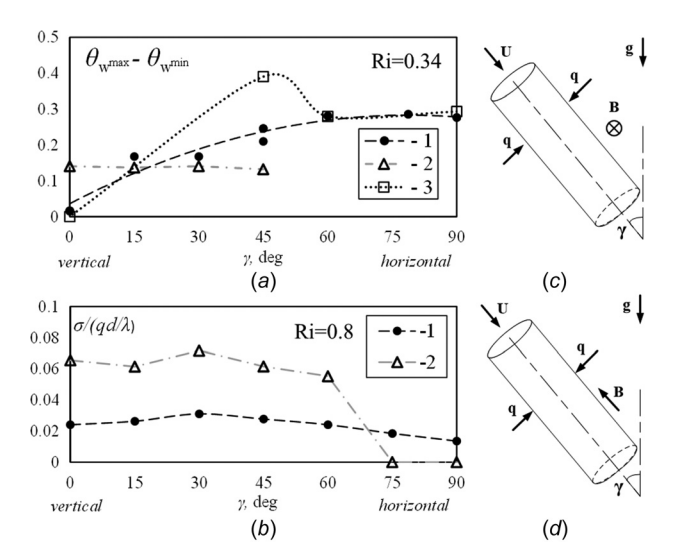


Fig. 25 Experimental data for the downward flow of mercury in an inclined pipe with uniform wall heating and the tilt angle varying between 0° (vertical) and 90° (horizontal). (a) The maximum difference of the dimensionless wall temperature in the pipe's cross section versus the tilt angle and (b) nondimensional standard deviation of temperature fluctuations are shown for Re = 10^4 , and 1—zero magnetic field [283]; 2—transverse magnetic field with Ha = 350 [285]; (c) flow with transverse magnetic field; (d)—flow with longitudinal magnetic field.

than an order of magnitude at L=20D. These data suggest a strong effect of the tilt angle on mixed convection in typically even longer pipes and ducts.

The available data on mixed convection with magnetic field and tilt are, to the best knowledge of the authors, limited to those obtained in the experimental studies of the downward flow of mercury in an inclined pipe [282–285]. Configurations with uniform heating of the entire perimeter of the wall and an either transverse or longitudinal magnetic field were considered. The results are illustrated in Fig. 25(a) by the difference between the maximum and minimum values of the dimensionless temperature at the pipe perimeter $\Delta\theta = \theta_{\rm w}^{\rm max} - \theta_{\rm w}^{\rm min}$. In addition to being of fundamental interest, this characteristic is of practical importance, since it allows us to estimate the thermal stresses anticipated in the walls of the reactor blanket (usually desired to be as small as possible).

Without the magnetic field, $\Delta\theta$ increases with the filt angle γ but tends to an asymptotic constant at $\gamma > 45^{\circ}$ [283].

We see in Fig. 25(a) that the effect of γ becomes remarkably strong in the flow with a longitudinal magnetic field. Such a field does not by itself create variations of flow velocity or temperature in the pipe's cross section. Its main role is to stabilize the streamwise-uniform flow patterns induced by the buoyancy forces, such as the symmetric near-wall streamwise jets in a vertical channel (see Fig. 4(b)) or a pair of longitudinal convection rolls (see Fig. 5(a)) in a horizontal channel. In accordance with this statement, Fig. 25(a) shows a virtually zero value of $\Delta\theta$ at y = 0 and a large value close to that in a nonmagnetic flow at $\gamma = 90$ deg. The nature of the peak around $\gamma = 45$ deg is unclear. We hypothesize that the peak is the result of competition between two effects, both becoming stronger with increasing γ . One is the already mentioned growth of longitudinal convection rolls, which leads to a larger temperature difference between the hot top and cold bottom portions of the pipe. Another is the buoyancy force associated with the growth of the mean-mixed temperature along the channel (see Fig. 3) As we have discussed in Sec. 6.1, the force modifies the streamwise convective heat transfer so that the liquid becomes colder at the top and hotter at the bottom, and the convection rolls are suppressed by stable stratification. The experiments [285] support this explanation and indicate an even more spectacular behavior, which involves a reversed flow in the top portion of the pipe at larger Ri. At the same time, the explanation remains a hypothesis, which needs further analysis, preferably in the form of numerical simulations.

The transverse magnetic field leads to a significant temperature difference, which decreases slowly with γ in the range $0 < \gamma < 45 \text{deg}$ [284] (see Fig. 25(a)). This is similar to other flows with transverse magnetic fields and can be attributed to different rates of heat transfer across the Hartmann and Roberts layers forming at the wall portions perpendicular and parallel to the magnetic field [28,29,34].

MCFs were detected in the inclined pipe flow with the transverse magnetic field [284]. As an illustration, Fig. 25(*b*) shows the nondimensional standard deviation of temperature fluctuations at Re = 10^4 , Ri = 0.8, and Ha = 300. The fluctuation amplitude is about three times larger than in the flows at Ha = 0 and the same Re-and Ri, but only when γ is less than about 60 deg. MCFs disappear at larger γ .

We conclude that inclined channels remain a poorly studied configuration of liquid-metal mixed convection. Further research is necessary to understand the undoubtedly interesting and practically relevant behavior of these flows.

7 Other Effects

In this section, we briefly review the current understanding of the most significant phenomena that affect magnetoconvection in channels but have been omitted so far in our discussion. It must be stressed that understanding the real-life effects, such as those presented below, is far from complete. Further studies are needed, including studies of systems in which these effects are combined in a realistic manner. While technically challenging, such studies are likely to become possible in the near future, as indicated by the recent attempts [202,248,286].

7.1 Effects of Wall Conductivity. No systematic study of the effects of thermal and electrical conductivity of walls on MHD mixed convection is known to the authors. For the thermal conductivity, one can rely on the data accumulated for nonmagnetic flows, especially in their laminar state (see, e.g., [287] for a review). For flows of liquid metals, the effect is usually mild due to the high thermal conductivity and heat capacity of the liquid. It seems plausible that heat conduction within the walls would somewhat reduce temperature nonuniformity, thus damping the buoyancy effects and MCFs.

The effect of finite electric conductivity is more complex and harder to predict. It is known to lead to drastic modification of MHD channels flows, with the results strongly depending on the wall conductance ratio (20) and the distribution of conductivity among walls [27–29,34].

One definitive result on the effect of electric conductivity on mixed convection was obtained in the recent simulations [248,249]. It was shown that the presence of thin conducting walls suppresses the deformation of the streamwise velocity profile and the instability in both upward and downward flows in vertical channels. At the same time, we cannot exclude the possibility that in some configurations and areas of the parameter space, finite thermal and electric conductivity of walls may lead to unanticipated effects, including new instability mechanisms.

It must be noted that this review largely ignores the substantial body of research dealing with natural and low-Re mixed convection in domains with strongly conducting walls. Such studies have been conducted in conjunction with development of the HCLL (helium-cooled lithium-lead) blanket module concept [12] (see Fig. 1(f)). In such a module, circulation of a liquid metal is very slow, and the state of the flow is predominantly determined by the effects of natural convection and magnetic field. The reason for our choice not to discuss such flows is the apparent principal difference between their physics and the phenomena, on which this review is focused. Most importantly, no anomalously strong fluctuations, such as MCFs, have been so far found in systems with strongly conducting walls and a strong imposed magnetic field. There are, however, other interesting features, such as near-wall jets [115,125,288,289] or thermal and electromagnetic coupling through the walls [117,290]. An interested reader can find further information in the just mentioned papers and other works, such as [291-294].

7.2 Internal heating Sources. Another effect is that of internal (volumetric) heating. In the blanket of a fusion reactor, the heating is only partially applied to the wall of a fluid domain. Another, typically larger part is the heating by absorbed neutrons, which is a strongly asymmetric (decreasing rapidly with the distance to the first wall), but still an internal source. This means that the systems with purely wall heating analyzed in many experiments and simulations reviewed above (e.g., [122,177,207, 223,234,235,237,238]), must be considered as approximations, albeit good ones, of the actual blanket systems.

Internal heating cannot be reproduced in MHD experiments but can be modeled in numerical simulations, where one can apply a volumetric heat source of a given distribution (e.g., an exponential decay function, as explained in Ref. [295]). This approach was utilized in studies of both upward and downward flows [118,239,246,248,249]. A particularly interesting recent work in this direction is Ref. [249], where direct comparison between configurations with wall and internal heating is made. While there is no full clarity, we can reliably accept the general conclusion that very similar physical phenomena, including the formation of inflection points and MCFs, are found in flows with wall and strongly asymmetric internal heating.

The differences are more substantial if the internal heating is not strongly asymmetric and thus does not result in a strong unidirectional horizontal heat flux. For example, a uniform internal heating may create inflection points and lead to instability even at zero mean streamwise flow in the channel [296].

7.3 Entry, Exit, and Length Effects. Entry effects, such as those of the flow's entry into a channel, a heated portion of a channel, a sudden expansion or contraction, or a zone of an imposed magnetic field, are inevitable in any practical realization of the flow, be it an experiment or a fusion reactor blanket. The configuration can be very different depending on the type of flow. For example, in a blanket module, a liquid metal flow may enter a duct from a manifold via a 90 deg corner or an expansion in the presence of a constant magnetic field and constant heat flux (see Figs. 1(b)-1(f)). In an experiment, unless it is designed with the specific goal of exactly reproducing a part of a blanket module, the entry is typically a straight segment of a channel, at which heating and the magnetic field start to apply.

Early studies summarized in classical MHD books [28,29,34] convincingly demonstrate that a strong imposed magnetic field changes the nature and increases the significance of the entry effects in comparison with the hydrodynamic case. Common aspects of the change are the suppression of turbulence and formation of special MHD flow patterns often characterized by boundary and internal layers of strong shear.

Unique flow transformations are observed when the channel's geometry and wall properties change abruptly in a strong magnetic field. One example is the flow in a 90 deg corner or a U-turn, where complex 3D laminar flow patterns with thin internal shear layers and Lorentz forces causing a sharp pressure drop have been found (see, e.g., [268–270,297]). Inner shear layers and a complex 3D pattern are also found in sudden expansions of ducts (see the discussions of the classical works in Ref. [28] and more recent works [183,298,299]) or at abrupt changes of the electric conductivity of the channel's walls [116].

Another important entry effect is the transformation of a channel flow entering a zone of imposed transverse magnetic field. A discussion and illustrations can be found in the MHD books, such as [28,29,34], and the classical experimental and theoretical works cited in these books. In the case of electrically insulating walls, the electric current loops forming in the fringe zone of the magnetic field cause Lorentz forces, decelerating the flow in the central part of the channel and accelerating it near the walls parallel to the magnetic field (the sidewalls). More recent computational and experimental studies, such as [300-303], confirm the theory and illustrate the fact that the resulting flow transformation can be quite drastic if the imposed magnetic field is strong. The distribution of streamwise velocity in the channel's cross section acquires the form of a so-called M-shaped velocity profile, with a nearly flat core and sidewall over-speed jets. In the conditions of suppressed turbulent mixing and the stabilizing effect of the magnetic field, the jets survive for a long distance, well into the zone of uniform magnetic field, before they are dissipated by viscosity.

We should also mention the evident effect of the entry flow structures, e.g., of the streamwise velocity profile, on the onset of magnetoconvective instabilities in the main part of the channel. There is also a yet-largely unexplored possibility that the thin shear layers and inflection points associated with the entry flow structures may cause instabilities and high-amplitude velocity and temperature fluctuations on their own.

A related physical effect is that of the length of the channel. It is evident that the realization of the magnetoconvective instabilities presented in Sec. 6 is critically influenced by the length of the segment on which the strong magnetic field and heating are applied. One aspect is that the length must be sufficient for the flow to pass the entry region and attain a fully developed state. Another aspect is that even in this state a certain length is needed for the instability to evolve. In some cases, e.g., in horizontal

channels with bottom heating and a transverse magnetic field (see Sec. 6.1), the distance is required simply to allow the velocity and temperature perturbations to grow to a noticeable level. Sufficiently large lengths are, therefore, critical in experiments and practical implementations [224–228]. In numerical models, segments of fully developed flows as short as one (in linear stability analysis) or several (in nonlinear simulations) typical longitudinal wavelengths are sufficient [40,41]. In other cases, in particular in vertical channels, a large channel length is essential, since only in a long channel is the principal mechanism of the instability (growth of long ascending and descending jets and development of inflection points in the streamwise velocity profile) possible (see Sec. 6.2).

The effect of exit from a channel or a heating zone is usually ignored in the hydrodynamics of incompressible flows. The situation is more complex and less evident in the MHD case. For example, a strong longitudinal magnetic field leads to flow structures that are uniform or nearly uniform along the field lines (see Sec. 6.3), so one should expect strong correlation between the states of the flow at the exit and in the bulk of the channel. Another example is the exit from a zone of strong transverse magnetic field. Similarly to the effects observed near the inlet, this fringing field creates electric current loops and 3D Lorentz forces affecting the flow on both sides of this zone [300,304].

We conclude this section by a rather evident statement that the entry, exit, and length effects have profound influence on the inception and development of the magnetoconvective instabilities. This has to be always taken into account in designing a magnetoconvection experiment or analyzing a blanket module.

7.4 Molten salts. Molten salts, such as FLiNaK or FLiBe (see Table 1 for properties), are considered as possible working fluids for heat transfer applications involving very high heat loads (e.g., in concentrated solar energy) and next-generation nuclear fission technology. They are also considered as potential alternatives to liquid metals as working fluids for blankets of future fusion reactors [5].

In comparison to liquid metals, molten salts have serious disadvantages for use in a reactor blanket. The most important of them are the need to operate at very high temperatures (substantially above the meting point ~450°C) and their chemical aggressiveness. They also have advantages, primarily related to their low electric conductivity. The molten salt flows are characterized by moderate values of Ha (about 100), even in the conditions of the very strong magnetic field present in the blanket (see Fig. 2). This minimizes the MHD pressure drop, thus removing the major problem faced by many liquid-metal concepts. The working fluid can be pumped at a high flowrate. Furthermore, the typical values of Re-and Ha are such that the flow remains turbulent, thus retaining the advantages of turbulent mixing and heat transfer.

Direct MHD experiments with molten salts are very difficult to conduct and, to the best knowledge of the authors, have never been done. Model liquids, such as KOH solutions, are used [178,305,306]. Since the magnetic field in an experiment is inevitably much smaller than in a future reactor blanket, experiments are typically performed at the highest accessible Ha ≈ 30 and Re reduced so as to achieve the same value of N as in the blanket flows. This increases the uncertainty already caused by the uncertain and highly variable values of the thermophysical properties of the liquids (both the model and the salt) and other factors, consideration of which is beyond the scope of this review.

Our understanding of molten salt flows in the presence of magnetic fields is helped by earlier studies of isothermal MHD flows, such as [33,72,74–77,210,211,307–309] (see the discussion in Sec. 4). The studies were primarily focused on the fundamentals of turbulence transformation. Their main conclusion relevant to the subject of this review is that turbulence in molten salt flows in the typical conditions of a fusion reactor blanket is significantly modified by the magnetic field. It is anisotropic and has lower

intensity and steeper energy spectra than its nonmagnetic counterparts at the same Re-and Gr. The transformation of turbulence modifies the properties of the transport of a scalar field, such as temperature [92,149,219,310–312].

While enlightening, the earlier studies of MHD turbulence did not address the key effects considered in this review: the effect of natural convection on channel flows and the possibility of the existence of MCFs or hot and cold spots. A plausible assumption can be made that the presence of turbulence and a higher value of Pr make the effect of natural convection in flows of molten salts less significant than in liquid metals at the same Ri. Further experimental and computational work is needed for more specific and reliable conclusions.

The anticipated turbulent high-Re nature of molten salt flows opens the possibility of using LES and RANS models in numerical analysis. The transformation of turbulence implies that accurate results cannot be obtained with the standard models commonly utilized in engineering CFD (e.g., the classical Smagorinsky or $k-\epsilon$). Modified models taking into account the reduced intensity and anisotropy of turbulent fluctuations must be used [73,77,209–220]. We note that while convincing results on the desired properties and likely composition of such models were obtained for isothermal flows, the question of accurate modeling of turbulent flows with heat transfer and convection remains largely open.

It should also be noted that, as MHD flows at moderately high Ha and high Re in general, the molten salt flows may often be found in a transitional laminar-turbulent state. This makes the results of studies of such transition in channels (see [22] and references therein) directly relevant to the questions of this review.

We conclude by stating that the molten salt flows in channels with magnetic field and heating are still poorly understood and difficult to study. The difficulties primarily stem from the complexity of experiments and lack of properly adapted and verified turbulence models for nonisothermal flows.

7.5 Group and Multiphysics Effects. Considering the implications of magnetoconvection for the operation of the blanket and divertor of a nuclear fusion reactor or another technological device, one must not forget about the effects of geometric and physical complexity. Such effects are beyond the scope of this review and therefore are only presented briefly in this section.

The geometric complexity is illustrated by the blanket module designs presented in Figs. 1(b)-1(f). We see that in each module, the flow of a liquid metal occurs not in an isolated single channel but in a system of channels connected by a manifold. This implies the possibility of significant "group effects," by which flows in individual channels are connected with each other. One such effect is electromagnetic coupling, which can be quite strong, sometimes leading to a complete change of the flow structure [117,161,313,314].

Another group effect is the imbalance of the flow rate and thus the rates of transport of heat and tritium and other admixtures between the parallel channels. Since the MHD flow resistance in each channel is a function of the flow rate, the imbalance is a manifestation of a nonlinear and possibly unsteady dynamics, analysis of which typically requires a numerical solution.

The phenomenon of imbalance has been considered for simplified model geometries and in attempted analyses of entire blanket modules [248,286,315–321]. Interesting and influential results have been obtained. At the same time, the results cannot be considered final, since important physical phenomena affecting the balance have not been considered in these works. In particular, the magnetoconvection has been either ignored or included as a steady-state effect. The results presented in this review clearly show that the buoyancy forces have strong impact on flow resistance and therefore on the distribution of the flow rate among the channels. Moreover, we hypothesize that the fluctuations of temperature, velocity, and pressure generated by an MCF-generating

instability in one channel may penetrate other channels via a manifold. Once there, the strong fluctuations may trigger unanticipated instabilities or change the flow properties in some other way. We cannot exclude the possibility of an entire blanket module being in an unsteady-state dominated by high-amplitude MCFs generated in some of the channels (e.g., vertical channels with downward mean flow, as described in Sec. 6.2).

The group effects are only a part of the general complexity of the processes in a blanket or divertor of an operating fusion reactor. There are other effects that ideally have to be considered together with the MHD and convection effects in a multiphysics analysis. The list of such effects is long. It certainly includes the power deposition by absorbed neutrons and radiation from the reaction chamber, thermal stresses and deformations in the solid components, generation of tritium and its transport and penetration into solids, the effects of corrosion, deposition of solid residue, radiation damage of walls, etc. These effects, considered individually or together in a multiphysics analysis, are subjects of active research that lies outside of the scope of this review. We only mention several works in which the emphasis was on the MHD phenomena [248,288,320–324].

It must be stressed that the complexity of physics and geometry, the very broad ranges of relevant length and time scales, and poor knowledge of physical properties and transport coefficients make the analysis extremely difficult. The analysis can be completed only after drastic simplifying assumptions, some of them barely or not at all justified. As an example, the effects of thermal convection are either ignored or represented by oversimplified steady-state models in such analyses. Another fundamental problem is the lack of proper validation carried out under the true conditions of an operating reactor, which will only become possible when large-scale experimental facilities, such as ITER, DEMO, or FNSF [5,7,16], are built. We conclude that the results of such multiphysics studies must at this moment be considered as preliminary and requiring confirmation in further research.

8 Conclusions

8.1 Summary. The research findings presented in this review demonstrate the unique nature of the channel flows with strong combined effects of thermal convection and magnetic field. Behavior of such flows is profoundly different from anything observed previously in hydrodynamics. It is also surprising and counterintuitive in the sense that it cannot be anticipated on the basis of our understanding of the effects of thermal convection and magnetic fields taken separately. The key features of the flow transformation are the high-amplitude low-frequency magneto-convective fluctuations (MCFs) and exceptionally strong variations of temperature. As an example, temperature fluctuations of an amplitude higher than 50 K and temperature differences between the hot and cold spots exceeding 300 K have been found in experiments and numerical simulations (see Secs. 6.2 and 6.3).

The properties of the transformed flows vary depending on many factors, such as the orientation of the channel with respect to gravity, flow direction, orientation and spatial shape of the imposed magnetic field, heating arrangements, the length of the channel's segments with applied heating and magnetic field, the shape of the channel's cross section, and, of course, the values of the governing parameters: Gr, Ha, and Re. The basic mechanism of the flow transformation, however, consists of the same principal elements in all cases:

- (1) Suppression of turbulence by a strong imposed magnetic field
- (2) Development of a laminar state with very strong temperature gradients and thin boundary or internal shear layers
- (3) If the laminar state is unstable to Q2D perturbations, growth of the perturbations into high-amplitude Q2D structures, typically vortices with their axes along the magnetic field lines. Motion of the structures is manifested by high-

amplitude fluctuations of temperature and velocity (the MCFs).

The flow transformation, should it occur in a blanket or divertor of a fusion reactor, will have profound and far-reaching implications for operation of the system. The most important ones among those identified so far are:

- (1) Changes in the heat and mass transfer. On the one hand, the suppression of turbulence greatly reduces the transfer rates. On the other hand, the MCFs increase the rates, possibly to the levels exceeding those in turbulent nonmagnetic flows, albeit in an anisotropic manner.
- (2) Thermal stresses in the walls created by the oscillations and spatial variations of temperature. The amplitude of these stresses can be enormous, so they potentially threaten the structural integrity of a system already subjected to damage by radiation and high temperature. The possibility is particularly troubling in the case of low-frequency MCF oscillations. It must be stressed that the true extent of the potential damage of the blanket structure is currently unclear and needs further research.
- (3) The effect of strong temperature variations on solubility and transport of admixtures and thus on the chemical composition of the melt. Especially important for fusion technology is the effect on transport of tritium and its diffusion into solid components.
- (4) Effect on corrosion. Many liquid metals (e.g., PbLi) are corrosive to steels. This creates serious problems for technological applications, including operation of liquid-metal components of fusion reactors. The potential effect of magnetoconvection is twofold: higher rate of corrosion in hot zones and deposition of solid steel and its derivatives in cold zones.

We conclude with a statement that may sound evident and even trivial at this stage of the discussion. The effect of magnetoconvection must always be taken into account when a system involving the flow of a liquid metal, heating, and a strong magnetic field is designed or analyzed.

8.2 Open Questions. Our understanding of magnetoconvection in channels is far from complete. There remain serious unanswered questions. The most important of them, listed from the most evident to the most hypothetical, are as follows.

The nature of flow states at very high Gr and Ha remains unclear. This includes the flow behavior at $Gr \sim 10^{10}-10^{12}$, $Ha \sim 10^4$ typical for the conditions of an operating fusion reactor. As we have stressed several times in this review, experiments and full numerical simulations are currently possible only at much smaller values: $Gr \leq 10^9$ and $Ha \leq 10^3$. Preliminary results, in particular those obtained in the numerical models based on the asymptotic high-Ha 2D approximation, suggest that the phenomena of MCFs and strong temperature variations exist and reach extreme amplitudes at high Ha and Gr. The ultimate conclusions can, however, be made only in the future experiments and 3D numerical simulations performed in that parameter range.

Many interesting and practically important configurations are poorly explored. This, in particular, concerns flows in inclined channels and flows in channels with longitudinal magnetic fields (see Secs. 6.4 and 6.3).

The understanding of the effects of magnetoconvection in realistically complex systems is far from complete. Our understanding of the magnetoconvection effects is largely limited to flows in model systems, typically individual ducts and pipes with idealized geometry, heating, magnetic field, and boundary (at the walls, inlet, and exit) conditions. Real flows in fusion reactor components and other technological settings are much more complex, with group, length, and multiphysics effects (see Secs. 7.3 and 7.5).

The possibility and methods of control of magnetoconvection are largely unknown. Predicting the unique magnetoconvection effects in future technological systems is only the first step. The further steps will be toward developing control strategies that will allow us to effectively utilize the positive aspects of the magnetoconvection (e.g., the enhanced mixing) and to avoid the negative aspects where it is necessary. To the best knowledge of the authors, work in this direction has so far been limited to preliminary studies, such as, e.g., the recent exploration of the effect of inlet swirl on the MHD flow in a duct [325].

Role of magnetoconvection in novel concepts of blanket design. All the liquid-metal blanket concepts seriously considered so far have been in the form of compact (\sim 1-2 m) cuboid modules (see Figs. 1(b)-1(f)). The shape and size of such modules are prescribed not as much by considerations of performance as by the space availability for testing in the ITER and DEMO experiments. It is possible and even likely that better technical solutions are to be found if these limitations are removed. A particularity interesting idea is a system of long ducts coiled around the entire blanket so that their axes are aligned with the magnetic field. As we discuss in Secs. 6.3 and 6.4 of this review, this arrangement promises serious advantages of a greatly reduced MHD pressure drop and effective mixing by Q2D convection-induced turbulence. In general, it is the opinion of the authors of this review that the development of liquid metal blankets that starts with clear understanding of magnetoconvection effects (rather than, as is common now, that considers these effects for an already completed design) will lead to simpler, more reliable, and much more efficient concepts.

Acknowledgment

Professor Valentin Sviridov was the key author of this review, with the most extensive experience in the area of MHD-affected heat transfer. Much of the reviewed research was completed with his immediate participation or under his guidance. Regretfully, he passed away on September 28, 2019 and could not participate in the completion of the work, but without him, the review would not have appeared in this form.

Funding Data

- US NSF (No. CBET 1803730; Funder ID: 10.13039/ 100000001).
- The Russian Federation Ministry of Science and Education (No. 14.Z50.31.0042; Funder ID: 10.13039/501100003443).
- Section 5.2 was prepared with financial support from the Russian Science Foundation (No. 20-69-46067; Funder ID: 10.13039/501100006769).

References

- Weiss, N. O., and Proctor, M. R. E., 2014, Magnetoconvection, Cambridge University Press, Cambridge, UK.
- [2] Ozoe, H., 2005, Magnetic Convection, Imperial College Press, London, UK.
- [3] Cukierski, K., and Thomas, B. G., 2008, "Flow Control With Local Electromagnetic Braking in Continuous Casting of Steel Slabs," Met. Mat. Trans. B, 39(1), pp. 94–107.
- [4] Dolan, T. J., Moir, R. W., Manheimer, W., Cadwallader, L. C., and Neumann, M. J., 2013, Magnetic Fusion Technology, Springer, Berlin.
- [5] Abdou, M., Morley, N. B., Smolentsev, S., Ying, A., Malang, S., Rowcliffe, A., and Ulrickson, M., 2015, "Blanket/First Wall Challenges and Required R&D on the Pathway to DEMO," Fusion Eng. Des., 100, pp. 2 –43.
- [6] Giancarli, L. M., Abdou, M., Campbell, D. J., Chuyanov, V. A., Ahn, M. Y., Enoeda, M., Pan, C., Poitevin, Y., Rajendra Kumar, E., Ricapito, I., Strebkov, Y., Suzuki, S., Wong, P. C., and Zmitko, M., 2012, "Overview of the ITER TBM Program," Fusion Eng. Des., 87(5–6), pp. 395–402.
- [7] Giancarli, L. M., Bravo, X., Cho, S., Ferrari, M., Hayashi, T., Kim, B.-Y., Leal-Pereira, A., Martins, J.-P., Merola, M., Pascal, R., Schneiderova, I., Sheng, Q., Sircar, A., Strebkov, Y., van der Laan, J., and Ying, A., 2020, "Overview of Recent ITER TBM Program Activities," Fusion Eng. Des., 158, p. 111674.

- [8] Malang, S., Leroy, P., Casini, G., Mattas, R., and Strebkov, Y., 1991, "Crucial Issues on Liquid Metal Blanket Design," Fusion Eng. Des., 16, pp. 95–109.
- [9] Cha, Y. S., Gohar, Y., Hassanein, A. M., Majumdar, S., Picologlou, B. F., Sze, D. K., and Smith, D. L., 1985, "Design of Self-Cooled, Liquid-Metal Blankets for Tokamak and Tandem Mirror Reactors," Fusion Techn., 8(1P1), pp. 90–113.
- [10] Kovalenko, V. S., Leshukov, A. Y., Tomilov, S. N., Razmerov, A. V., Strebkov, A. V., Sviridenko, M. N., Kirillov, I. R., Obukhov, D. M., Pertsev, D. A., and Vitkovsky, I. V., 2016, "Progress in Design Development and Research Activity on LLCB TBM in Russian Federation," Fusion Eng. Des., 109–111, pp. 521–531.
- [11] Chaudhuri, P., Kumar, E. R., Sircar, A., Ranjithkumar, S., Chaudhari, V., Danani, C., Yadav, B., Bhattacharyay, R., Mehta, V., Patel, R., Vyas, K. N., Singh, R. K., Sarkar, M., Srivastava, R., Mohan, S., Bhanja, K., and Suri, A. K., 2012, "Status and Progress of Indian LLCB Test Blanket Systems for ITER," Fusion Eng. Des., 87(7–8), pp. 1009–1013.
- [12] Forest, L., Aktaa, J., Boccaccini, L. V., Emmerich, T., Eugen-Ghidersa, B., Fondant, G., Froio, A., Puma, A. L., Namburi, H., Neuberger, H., Rey, J., Savoldi, L., Sornin, D., and Vala, L., 2020, "Status of the EU DEMO Breeding Blanket Manufacturing R&D Activities," Fusion Eng. Des., 152, p. 111420.
- [13] Aiello, G., De Dinechin, G., Forest, L., Gabriel, F., Puma, A. L., Rampal, G., Rigal, E., Salavy, J., and Simon, H., 2011, "HCLL TBM Design Status and Development," Fusion Eng. Des., 86(9–11), pp. 2129–2134.
- [14] Smolentsev, S., Morley, N. B., Abdou, M. A., and Malang, S., 2015, "Dual-Coolant Lead-Lithium (DCLL) Blanket Status and R&D Needs," Fusion Eng. Des., 100, pp. 44–54.
- [15] Ling, Q., and Wang, G., 2020, "A Research and Development Review of Water-Cooled Breeding Blanket for Fusion Reactors," Ann. Nucl. Energy, 145, p. 107541.
- [16] Kessel, C. E., Blanchard, J. P., Davis, A., El-Guebaly, L., Ghoniem, N., Humrickhouse, P. W., Malang, S., Merrill, B. J., Morley, N. B., Neilson, G. H., Rensink, M. E., Rognlien, T. D., Rowcliffe, A. F., Smolentsev, S., Snead, L. L., Tillack, M. S., Titus, P., Waganer, L. M., Ying, A., Young, K., and Zhai, Y., 2015, "The Fusion Nuclear Science Facility, the Critical Step in the Pathway to Fusion Energy," Fusion Sci. Techn., 68(2), pp. 225–236.
- way to Fusion Energy," Fusion Sci. Techn., 68(2), pp. 225–236.

 [17] Miyazawa, J., Goto, T., Murase, T., Ohgo, T., Yanagi, N., Tanaka, H., Tamura, H., Tanaka, T., Masuzaki, S., Sakamoto, R., Yagi, J., and Sagara, A., 2017, "Conceptual Design of a Liquid Metal Limiter/Divertor System for the FFHR-d1," Fusion Eng. Des., 125, pp. 227–238.
- [18] Ruzic, D. N., Xu, W., Andruczyk, D., and Jaworski, M. A., 2011, "Lithium-Metal Infused Trenches (LiMIT) for Heat Removal in Fusion Devices," Nucl. Fusion, 51(10), p. 102002.
- [19] Evtikhin, V. A., Lyublinski, I. E., Vertkov, A. V., Yezhov, N. I., Khripunov, B. I., Sotnikov, S. M., Mirnov, S. V., and Petrov, V. B., 2000, "Energy Removal and MHD Performance of Lithium Capillary-Pore Systems for Divertor Target Application," Fusion Eng. Des., 49–50, pp. 195–199.
 [20] Meng, Z., Zhang, S., Jia, J., Chen, Z., and Ni, M., 2018, "A K-Epsilon RANS
- [20] Meng, Z., Zhang, S., Jia, J., Chen, Z., and Ni, M., 2018, "A K-Epsilon RANS Turbulence Model for Incompressible MHD Flow at High Hartmann Number in Fusion Liquid Metal Blankets," Int. J. Energy Res., 42(1), pp. 314–320.
- [21] Smolentsev, S., Moreau, R., Bühler, L., and Mistrangelo, C., 2010, "MHD Thermofluid Issues of Liquid-Metal Blankets: Phenomena and Advances," Fusion Eng. Des., 85(7–9), pp. 1196–1205.
- [22] Zikanov, O., Krasnov, D., Boeck, T., Thess, A., and Rossi, M., 2014, "Laminar-Turbulent Transition in Magnetohydrodynamic Duct, Pipe, and Channel Flows," ASME Appl. Mech. Rev., 66(3), p. 030802.
- Channel Flows," ASME Appl. Mech. Rev., 66(3), p. 030802. [23] Gray, D. D., and Giorgini, A., 1976, "The Validity of the Boussinesq Approximation for Liquids and Gases," Int. J. Heat Mass Trans., 19(5), pp. 545–551.
- [24] Ahlers, G., Brown, E., Araujo, F. F., Funfschilling, D., Grossmann, S., and Lohse, D., 2006, "Non-Oberbeck-Boussinesq Effects in Strongly Turbulent Rayleigh-Bénard Convection," J. Fluid Mech., 569, p. 409.
- [25] Schulz, B., 1991, "Thermophysical Properties of the Li(17)Pb(83) Alloy," Fusion Eng. Des., 14(3-4), pp. 199-205.
 [26] Mas de Les Valls, E., Sedano, L., Batet, L., Ricapito, I., Aiello, A., Gastaldi,
- [26] Mas de Les Valls, E., Sedano, L., Batet, L., Ricapito, I., Aiello, A., Gastaldi, O., and Gabriel, F., 2008, "Lead-Lithium Eutectic Material Database for Nuclear Fusion Technology," J. Nucl. Mater., 376(3), pp. 353–357.
- [27] Branover, G., and Tsinober, A., 1970, Magnetohydrodynamics of Incompressible Fluids(in Russian), Nauka, Fys.Mat.Lit, Moscow, Russia.
- [28] Branover, H., 1978, Magnetohydrodynamic Flow in Ducts, Wiley, Hoboken, NJ.
- [29] Moreau, R., 1990, Magnetohydrodynamics, Kluwer Academic Publishers, Dordrecht, The Netherlands.
- [30] Davidson, P. A., 2016, Introduction to Magnetohydrodynamics, Cambridge University Press, Cambridge, UK.
 [31] Roberts, P. H., 1967, An Introduction to Magnetohydrodynamics, Longmans,
- [51] Roberts, P. H., 1907, An introduction to magnetonyarodynamics, Longmans, Green, New York.
- [32] Noskov, V., Denisov, S., Stepanov, R., and Frick, P., 2012, "Turbulent Viscosity and Turbulent Magnetic Diffusivity in a Decaying Spin-Down Flow of Liquid Sodium," Phys. Rev. E, 85(1), p. 016303.
- [33] Knaepen, B., Kassinos, S., and Carati, D., 2004, "Magnetohydrodynamic Turbulence at Moderate Magnetic Reynolds Number," J. Fluid Mech., 513, pp. 199–220.
- [34] Müller, U., and Bühler, L., 2001, Magnetohydrodynamics in Channels and Containers, Springer, Berlin.
- [35] Smolentsev, S., Cuevas, S., and Beltrán, A., 2010, "Induced Electric Current-Based Formulation in Computations of Low Magnetic Reynolds Number Magnetohydrodynamic Flows," J. Comp. Phys., 229(5), pp. 1558–1572.

- [36] Votyakov, E. V., Kassinos, S. C., and Albets-Chico, X., 2009, "Analytic Models of Heterogenous Magnetic Fields for Liquid Metal Flow Simulations, Theor. Comp. Fluid Dyn., 23(6), pp. 571–578.
- [37] Smolentsev, S., 2009, "MHD Duct Flows Under Hydrodynamic "Slip" Con-
- dition," Theor. Comp. Fluid Dyn., 23(6), pp. 557–570.
 [38] Alboussière, T., Garandet, J. P., and Moreau, R., 1993, "Buoyancy-Driven Convection With a Uniform Magnetic Field. Part 1. Asymptotic Analysis," Fluid Mech., 253(1), pp. 545-563.
- [39] Lyubimova, T. P., Lyubimov, D. V., Morozov, V. A., Scuridin, R. V., Hadid, H. B., and Henry, D., 2009, "Stability of Convection in a Horizontal Channel Subjected to a Longitudinal Temperature Gradient. Part 1. Effect of Aspect Ratio and Prandtl Number," J. Fluid Mech., 635, pp. 275-296.
- [40] Zikanov, O., Listratov, Y., and Sviridov, V. G., 2013, "Natural Convection in Horizontal Pipe Flow With Strong Transverse Magnetic Field," J. Fluid Mech., 720, pp. 486–516.
- [41] Zhang, X., and Zikanov, O., 2014, "Mixed Convection in a Horizontal Duct With Bottom Heating and Strong Transverse Magnetic Field," J. Fluid Mech., 757, pp. 33-56.
- [42] Lv, X., and Zikanov, O., 2014, "Mixed Convection in Horizontal Duct Flow With Transverse Magnetic Field and Heating of Side Wall," Phys. Fluids, 26(9), p. 097106.
- [43] Zhang, X., and Zikanov, O., 2017, "Thermal Convection in a Toroidal Duct of a Liquid Metal Blanket. Part II. Effect of Axial Mean Flow," Fusion Eng. Des., 116, pp. 40-46.
- [44] Birikh, R. V., 1966, "On Thermocapillary Convection in a Horizontal Layer of Fluid," J. Appl. Mech. Tech. Phys., 7(3), pp. 69-72.
- [45] Ahlers, G., Grossmann, S., and Lohse, D., 2009, "Heat Transfer and Large Scale Dynamics in Turbulent Rayleigh-Bénard Convection," Rev. Mod. Phys., 81(2), pp. 503-537.
- [46] Horanyi, S., Krebs, L., and Müller, U., 1999, "Turbulent Rayleigh-Benard Convection in Low Prandtl-Number Fluids," Int. J. Heat Mass Transfer, 42(21), pp. 3983-4003.
- Takeshita, T., Segawa, T., Glazier, J. A., and Sano, M., 1996, "Thermal Turbulence in Mercury," Phys. Rev. Lett., 76(9), pp. 1465–1468.
 [48] Cioni, S., Ciliberto, S., and Sommeria, J., 1997, "Strongly Turbulent Rayleigh
- Bénard Convection in Mercury: Comparison With Results at Moderate Prandtl
- Number," J. Fluid Mech., 335, pp. 111–140. [49] King, E., and Aurnou, J., 2013, "Turbulent Convection in Liquid Metal With and Without Rotation," Proc. Natl. Acad. Sci., 110(17), pp. 6688-6693.
- [50] Zürner, T., Schindler, F., Vogt, T., Eckert, S., and Schumacher, J., 2019, 'Combined Measurement of Velocity and Temperature in Liquid Metal Convection," J. Fluid Mech., 876, pp. 1108-1128.
- [51] Glazier, J. A., Segawa, T., Naert, A., and Sano, M., 1999, "Evidence Against Ultrahard' Thermal Turbulence at Very High Rayleigh Numbers," Nat., 398(6725), pp. 307-310.
- [52] Zwirner, L., Khalilov, R., Kolesnichenko, I., Mamykin, A., Mandrykin, S., Pavlinov, A., Shestakov, A., Teimurazov, A., Frick, P., and Shishkina, O., 2020, "The Influence of the Cell Inclination on the Heat Transport and Large-Scale Circulation in Liquid Metal Convection," J. Fluid Mech., 884, p. A18
- [53] Akhmedagaev, R., Zikanov, O., Krasnov, D., and Schumacher, J., 2020, 'Turbulent Convection in Strong Vertical Magnetic Field," J. Fluid Mech., 895, p. R4.
- Scheel, J. D., and Schumacher, J., 2017, "Predicting Transition Ranges to Fully Turbulent Viscous Boundary Layers in Low Prandtl Number Convection Flows," Phys. Rev. Fluids, 2(12), p. 123501.
- Mandrykin, S. D., and Teimurazov, A. S., 2018, "Turbulent Convection of Liquid Sodium in an Inclined Cylinder of Unit Aspect Ratio," Comp. Cont. Mech., 11(4), pp. 417–428.in russian).
- [56] Shishkina, O., Stevens, R. J., Grossmann, S., and Lohse, D., 2010, "Boundary Layer Structure in Turbulent Thermal Convection and Its Consequences for the Required Numerical Resolution," New J. Phys., 12(7), p. 075022
- [57] Frick, P., Khalilov, R., Kolesnichenko, I., Mamykin, A., Pakholkov, V., Pavlinov, A., and Rogozhkin, S. A., 2015, "Turbulent Convective Heat Transfer in a Long Cylinder With Liquid Sodium," Europhys. Lett., **109**(1), p. 14002.
- [58] Mamykin, A., Frick, P., Khalilov, R., Kolesnichenko, I., Pakholkov, V., Rogozhkin, S., and Vasiliev, A., 2015, "Turbulent Convective Heat Transfer in an Inclined Tube With Liquid Sodium," Magnetohydrodynamics, 51(2), pp.
- [59] Petukhov, B. S., Polyakov, A., and Launder, B. E., 1988, Heat Transfer in Turbulent Mixed Convection, Hemisphere Publishing Corporation.
- [60] Jackson, J., Axcell, B., and Walton, A., 1994, "Mixed-Convection Heat Transfer to Sodium in a Vertical Pipe," Exp. Heat Transfer, 7(1), pp.
- [61] Kim, W., He, S., and Jackson, J., 2008, "Assessment by Comparison With DNS Data of Turbulence Models Used in Simulations of Mixed Convection, Int. J. Heat Mass Transfer, **51**(5–6), pp. 1293–1312. [62] Hering, W., and Jaeger, W., 2018, "Mixed Convection With Liquid Metals:
- Review of Experiments and Model Development," Advances in Thermal Hydraulics (ATH2018), Orlando, FL, Nov. 11–15, pp. 846–859.
- [63] Batchelor, G. K., and Nitsche, J. M., 1991, "Instability of Stationary Unbounded Stratified Fluid," J. Fluid Mech., 227, pp. 357–391
- [64] Calzavarini, E., Doering, C. R., Gibbon, J. D., Lohse, D., Tanabe, A., and Toschi, F., 2006, "Exponentially Growing Solutions of Homogeneous Rayleigh-Bénard Flow," Phys. Rev. E, 73(3), p. R035301.
 [65] Liu, L., and Zikanov, O., 2015, "Elevator Mode Convection in Flows With
- Strong Magnetic Fields," Phys. Fluids, 27(4), p. 044103.

- [66] Armenio, V., and Sarkar, S., 2002, "An Investigation of Stably Stratified Turbulent Channel Flow Using Large-Eddy Simulation," J. Fluid Mech., 459, pp. 1-42.
- [67] Garcia-Villalba, M., and del Alamo, J. C., 2011, "Turbulence Modification by Stable Stratification in Channel Flow," Phys. Fluids, 23(4), p. 045104.
- [68] Zhang, X., and Zikanov, O., 2015, "Two-Dimensional Turbulent Convection in a Toroidal Duct of a Liquid Metal Blanket of a Fusion Reactor," J. Fluid Mech., 779, pp. 36-52.
- [69] Nicolas, X., Luijkx, J., and Platten, J., 2000, "Linear Stability of Mixed Convection Flows in Horizontal Rectangular Channels of Finite Transversal Extension Heated From Below," Int. J. Heat Mass Transfer, 43(4), pp. 589-610.
- [70] Moffatt, K., 1967, "On the Suppression of Turbulence by a Uniform Magnetic Field," J. Fluid Mech., 28(03), pp. 571–592.
- [71] Sommeria, J., and Moreau, R., 1982, "Why, How and When MHD-Turbulence Becomes Two-Dimensional," J. Fluid Mech., 118(1), pp. 507-518.
- [72] Zikanov, O., and Thess, A., 1998, "Direct Numerical Simulation of Forced MHD Turbulence at Low Magnetic Reynolds Number," J. Fluid Mech., 358, pp. 299-333.
- [73] Knaepen, B., and Moin, P., 2004, "Large-Eddy Simulation of Conductive Flows at Low Magnetic Reynolds Number," Phys. Fluids, 16(5), pp. 1255-1261.
- [74] Burattini, P., Zikanov, O., and Knaepen, B., 2010, "Decay of Magnetohydrodynamic Turbulence at Low Magnetic Reynolds Number," J. Fluid Mech., **657**, pp. 502–538.
- [75] Zikanov, O., Krasnov, D., Boeck, T., and Sukoriansky, S., 2019, "Decay of Turbulence in a Liquid Metal Duct Flow With Transverse Magnetic Field," J. Fluid Mech., 867, pp. 661–690. [76] Schumann, U., 1976, "Numerical Simulation of the Transition From Three- to
- Two-Dimensional Turbulence Under a Uniform Magnetic Field," J. Fluid Mech., 74(1), pp. 31–58.
- [77] Vorobev, A., Zikanov, O., Davidson, P. A., and Knaepen, B., 2005, "Anisotropy of Magnetohydrodynamic Turbulence at Low Magnetic Reynolds Number," Phys. Fluids, 17(12), p. 125105. [78] Thess, A., and Zikanov, O., 2007, "Transition From Two-Dimensional to
- Three-Dimensional Magnetohydrodynamic Turbulence," J. Fluid Mech., 579, pp. 383-412.
- [79] Zhao, Y., Tao, J., and Zikanov, O., 2014, "Transition to Two-Dimensionality in Magnetohydrodynamic Turbulent Taylor-Couette Flow," Phys. Rev. E, 89(3), p. 033002.
- [80] Hartmann, J., 1937, "Hg-Dynamics I: Theory of the Laminar Flow of an Electrically Conductive Liquid in a Homogeneous Magnetic Field," K. Dan. Vidensk. Selsk. Mat. Fys. Medd., 15(6), pp. 1–28.
- [81] Hartmann, J., and Lazarus, F., 1937, "Hg-Dynamics II: Experimental Investigations on the Flow of Mercury in a Homogeneous Magnetic Field," K. Dan. idensk. Selsk. Mat. Fys. Medd., 15(7), pp. 1-45.
- [82] Hunt, J., 1965, "Magnetohydrodynamic Flow in Rectangular Ducts," J. Fluid Mech., 21(4), pp. 577–590.
- [83] Roberts, P. H., 1967, "Singularities of Hartmnann Layers," Proc. Roy. Soc. A, 300(1460), pp. 94-107.
- [84] Kinet, M., Knaepen, B., and Molokov, S., 2009, "Instabilities and Transition in Magnetohydrodynamic Flows in Ducts With Electrically Conducting Walls," Phys. Rev. Lett., 103(15), p. 154501.
- [85] Priede, J., Aleksandrova, S., and Molokov, S., 2010, "Linear Stability of Hunt's Flow," J. Fluid Mech., 649, pp. 115–134.
- [86] Krasnov, D., Zikanov, O., Schumacher, J., and Boeck, T., 2008, 'Magnetohydrodynamic Turbulence in a Channel With Spanwise Magnetic Field," Phys. Fluids, 20(9), p. 095105.
- [87] Vorobev, A., and Zikanov, O., 2007, "Instability and Transition to Turbulence in a Free Shear Layer Affected by a Parallel Magnetic Field," J. Fluid Mech., **574**, pp. 131–154.
- [88] Krasnov, D., Rossi, M., Zikanov, O., and Boeck, T., 2008, "Optimal Growth and Transition to Turbulence in Channel Flow With Spanwise Magnetic Field," J. Fluid Mech., **596**, pp. 73–101.
- [89] Krasnov, D., Zikanov, O., Rossi, M., and Boeck, T., 2010, "Optimal Linear Growth in Magnetohydrodynamic Duct Flow," J. Fluid Mech., 653, pp.
- [90] Boeck, T., Krasnov, D., Thess, A., and Zikanov, O., 2008, "Large-Scale Intermittency of Liquid-Metal Channel Flow in a Magnetic Field," Phys. Rev. Lett., **101**(24), p. 244501.
- [91] Duguet, Y., Schlatter, P., and Henningson, D., 2010, "Formation of Turbulent Patterns Near the onset of transition in plane Couette flow," J. Fluid Mech., 650, pp. 119-129
- [92] Dey, P., and Zikanov, O., 2012, "Scalar Transport and Perturbation Dynamics in Intermittent Magnetohydrodynamic Flow," Phys. Fluids, 24(8), p. 084104.
- [93] Krasnov, D. S., Zikanov, O., and Boeck, T., 2012, "Numerical Study of Magnetohydrodynamic Duct Flow at High Reynolds and Hartmann Numbers," Fluid Mech., 704, pp. 421–446.
- [94] Krasnov, D., Thess, A., Boeck, T., Zhao, Y., and Zikanov, O., 2013, Patterned Turbulence in Liquid Metal Flow: Computational Reconstruction of the Hartmann Experiment," Phys. Rev. Lett., 110(8), p. 084501. [95] Zikanov, O., Krasnov, D., Li, Y., Boeck, T., and Thess, A., 2014, "Patterned
- Turbulence in Spatially Evolving Magnetohydrodynamic Tube Flows," Theor. Comp. Fluid Dyn., 28(3), pp. 319–334.
- [96] Chandrasekhar, S., 1961, Hydrodynamic and Hydromagnetic Stability, Clarendon Press, Oxford, UK.

- [97] Yanagisawa, T., Yamagishi, Y., Hamano, Y., Tasaka, Y., and Takeda, Y., 2011, "Spontaneous Flow Reversals in Rayleigh-Bénard Convection of a Liquid Metal," Phys. Rev. E, 83(3), p. 036307.
- [98] Yanagisawa, T., Hamano, Y., Miyagoshi, T., Yamagishi, Y., Tasaka, Y., and Takeda, Y., 2013, "Convection Patterns in a Liquid Metal Under an Imposed Horizontal Magnetic Field," Phys. Rev. E, 88(6), p. 063020.
- Vogt, T., Ishimi, W., Yanagisawa, T., Tasaka, Y., Sakuraba, A., and Eckert, S., 2018, "Transition Between Quasi-Two-Dimensional and Three-Dimensional Rayleigh-Bénard Convection in a Horizontal Magnetic Field," Phys. Rev. Fluids, 3(1), p. 013503.
- [100] Yan, M., Calkins, M. A., Maffei, S., Julien, K., Tobias, S. M., and Marti, P., 2019, "Heat Transfer and Flow Regimes in Quasi-Static Magnetoconvection With a Vertical Magnetic Field," J. Fluid Mech., 877, pp. 1186-1206.
- [101] Cioni, S., Chaumat, S., and Sommeria, J., 2000, "Effect of a Vertical Magnetic Field on Turbulent Rayleigh-Bénard Convection," Phys. Rev. E, 62(4), pp. R4520-R4523.
- [102] Burr, U., and Müller, U., 2001, "Rayleigh-Bénard Convection in Liquid Metal Layers Under the Influence of a Vertical Magnetic Field," Phys. Fluids, 13(11), pp. 3247-3257.
- [103] Zürner, T., Schindler, F., Vogt, T., Eckert, S., and Schumacher, J., 2020, "Flow Regimes of Rayleigh-Bénard Convection in a Vertical Magnetic Field," J. Fluid Mech., 894, p. A21.
- [104] Houchens, B. C., Witkowski, L. M., and Walker, J. S., 2002, "Rayleigh Bénard Instability in a Vertical Cylinder With a Vertical Magnetic Field," Fluid Mech., 469(1), pp. 189-207.
- [105] Busse, F. H., 2008, "Asymptotic Theory of Wall-Attached Convection in a Horizontal Fluid Layer With a Vertical Magnetic Field," Phys. Fluids, 20(2), pp. 024102-024102-4.
- [106] Lim, Z. L., Chong, K. L., Ding, G., and Xia, K., 2019, "Quasistatic Magnetoconvection: Heat Transport Enhancement and Boundary Layer Crossing," J. Fluid Mech., 870, pp. 519-542.
- [107] Liu, W., Krasnov, D., and Schumacher, J., 2018, "Wall Modes in Magnetoconvection at High Hartmann Numbers," J. Fluid Mech., 849, p. R2.
- [108] Akhmedagaev, R., Zikanov, O., Krasnov, D., and Schumacher, J., 2020, "Rayleigh-Bénard Convection in Strong Vertical Magnetic Field: Flow Struc-ture and Verification of Numerical Method," Magnetohydrodynamics, **56**(2-3), pp. 157-165.
- [109] Kulikovskii, A., 1971, "Slow Steady Flows of a Conducting Fluid at Large Hartmann Numbers," Fluid Dyn., 3(2), pp. 1–5. [110] Hua, T., and Walker, J., 1989, "Three-Dimensional Mhd Flow in Insulating
- Circular Ducts in Non-Uniform Transverse Magnetic Fields," Int. J. Eng. Sci., 27(9), pp. 1079-1091.
- [111] Moon, T. J., and Walker, J., 1990, "Liquid Metal Flow Through a Sharp Elbow in the Plane of a Strong Magnetic Field," J. Fluid Mech., 213(1), pp.
- [112] Di Piazza, I., and Ciofalo, M., 2002, "MHD Free Convection in a Liquid-Metal Filled Cubic Enclosure. I. Differential Heating," Int. J. Heat Mass Trans., 45(7), pp. 1477–1492.
- [113] Di Piazza, I., and Ciofalo, M., 2002, "MHD Free Convection in a Liquid-Metal Filled Cubic Enclosure. II. Internal Heating," Int. J. Heat Mass Trans., 45(7), pp. 1493-1511.
- [114] Bühler, L., and Mistrangelo, C., 2017, "MHD Flow and Heat Transfer in Model Geometries for WCLL Blankets," Fusion Eng. Des., 124, pp. 919-923.
- [115] de Les Valls, E. M., Batet, L., de Medina, V., and Sedano, L. A., 2012, "MHD Thermofluid Flow Simulation of Channels With a Uniform Thermal Load as Applied to HCLL Breeding Blankets for Fusion Technology," Magnetohydrodynamics, 48(1), pp. 157–168.
- [116] Mistrangelo, C., and Bühler, L., 2015, "Magnetohydrodynamic Flow in Ducts With Discontinuous Electrical Insulation," Fusion Eng. Des., 98-99, pp. 1833-1837.
- [117] Mistrangelo, C., and Bühler, L., 2016, "Electro-Magnetic Flow Coupling for Liquid Metal Blanket Applications," Fusion Eng. Des., 109-111, pp. 1452-1457.
- [118] Vetcha, N., Smolentsev, S., Abdou, M., and Moreau, R., 2013, "Study of Instabilities and Quasi-Two-Dimensional Turbulence in Volumetrically Heated Magnetohydrodynamic Flows in a Vertical Rectangular Duct," Phys. Fluids, 25(2), p. 024102.
- [119] Gelfgat, A. Y., and Molokov, S., 2011, "Quasi-Two-Dimensional Convection in a Three-Dimensional Laterally Heated Box in a Strong Magnetic Field Normal to Main Circulation," Phys. Fluids, 23(3), p. 034101.
- [120] Bühler, L., 1996, "Instabilities in Quasi-Two-Dimensional Magnetohydrodynamic Flows," J. Fluid Mech., 326, pp. 125-150.
- [121] Cuevas, S., Smolentsev, S., and Abdou, M. A., 2006, "On the Flow Past a Magnetic Obstacle," J. Fluid Mech., 553(1), pp. 227-252.
- Zhang, X., and Zikanov, O., 2018, "Convection Instability in a Downward Flow in a Vertical Duct With Strong Transverse Magnetic Field," Phys. Fluids, 30(11), p. 117101.
- [123] Potherat, A., Sommeria, J., and Moreau, R., 2000, "An Effective Two-Dimensional Model for MHD Flows With Transverse Magnetic Field," J. Fluid Mech., 424, pp. 75–100.
- [124] Pothérat, A., Sommeria, J., and Moreau, R., 2005, "Numerical Simulations of an Effective Two-Dimensional Model for Flows With a Transverse Magnetic Field," J. Fluid Mech., **534**, pp. 115–143.
- [125] Burr, U., and Müller, U., 2002, "Rayleigh-Bénard Convection in Liquid Metal Layers Under the Influence of a Horizontal Magnetic Field," J. Fluid Mech., **453**, pp. 345–369.

- [126] Aristov, S. N., and Frik, P. G., 1988, "Advective Flows in a Plane Rotating
- Layer of a Conducting Fluid," Magnetohydrodynamics, 24(1), pp. 10–16. [127] Aristov, S. N., and Frik, P. G., 1990, "Nonlinear Effect in the Interaction of Convective Vortices and a Magnetic Field in a Thin Layer of a Conducting Fluid," Magnetohydrodynamics, 26(1), pp. 71-77.
- [128] Coen, V., 1985, "Lithium-Lead Eutectic as Breeding Material in Fusion Reactors," J. Nucl. Mater., 133-134, pp. 46-51.
- [129] Kirillov, P., Terentieva, M., and Deniskina, N., 2007, Thermophysical Properties of Materials for Nuclear Engineering, 2nd ed., IzdAt, Moscow, Russia (in Russian).
- [130] Grigoriev, I., and Meilikhov, E., eds., 1991, Physical Quantities, Handbook, Energoatomizdat, Moscow, Russia.
- [131] Adams, P. D., and Leach, J. S. L., 1967, "Resistivity of Liquid Lead-Tin Alloys," Phys. Rev., 156(1), pp. 178-183.
- [132] Sobolev, V., 2011, "Database of Thermophysical Properties of Liquid Metal Coolants for GEN-IV," Scientific Report No. SCK-CEN-BLG-1069
- [133] Dobosz, A., Plevachuk, Y., Sklyarchuk, V., Sokoliuk, B., and Gancarz, T., 2018, "Thermophysical Properties of the Liquid Ga-Sn-Zn Eutectic Alloy," Fluid Phase Equilibr., **465**(3), pp. 1–9.
- [134] Plevachuk, Y., Sklyarchuk, V., Eckert, S., Gerbeth, G., and Novakovic, R., 2014, "Thermophysical Properties of the Liquid Ga-in-Sn Eutectic Alloy," J. Chem. Eng. Data, 59(3), pp. 757–763.
- [135] Sohal, M. S., Ebner, M. A., Sabharwall, P., and Sharpe, P., 2010, "Engineering Database of Liquid Salt Thermophysical and Thermochemical Properties Idaho National Laboratory (INL), Idaho Falls, ID, Report No. INL/EXT-10-
- [136] Uchiyama, Y., and Kawamura, K., 1981, "Measurement of the Electrical Conductivities of Molten Sodium Nitrate-Potassium Nitrate-Sodium Nitrite and Molten Lithium Fluoride-Sodium Fluoride-Potassium Fluoride by Displacing the Positions of Electrodes," J. Chem. Eng. Data, 26(4), pp. 407-410.
- [137] Serrano-López, R., Fradera, J., and Cuesta-López, S., 2013, "Molten Salts Database for Energy Applications," Chem. Eng. Process., 73, pp. 87-102.
- [138] Gierszowski, P., Mikic, B., and Todreas, N., 1980, "Property Correlations for Lithium, Sodium, Helium, Flibe and Water in Fusion Reactor Applications
- [139] Gilliam, R., Graydon, J., Kirk, D., and Thorpe, S., 2007, "A Review of Specific Conductivities of Potassium Hydroxide Solutions for Various Concentrations and Temperatures," Int. J. Hydrog. Energy, 32(3), pp. 359-364.
- [140] Le Bideau, D., Mandin, P., Benbouzid, M., Kim, M., and Sellier, M., 2019, "Review of Necessary Thermophysical Properties and Their Sensivities With Temperature and Electrolyte Mass Fractions for Alkaline Water Electrolysis Multiphysics Modelling," Int. J. Hydrog. Energy, 44(10), pp. 4553–4569.
 [141] Freilich, M. B., and Petersen, R. L., 2014, *Potassium Compounds*, Kirk-
- Othmer Encyclopedia of Chemical Technology, Kluwer, Amsterdam, The Netherlands, pp. 1-35.
- [142] Beznosov, A., Novozhilova, O., Savinov, S. Y., Yarmonov, M., and Alekseev, R., 2013, "The Magnetic Field Effect on Heat-Exchange Characteristics and MHD Resistance of Lead-Bismuth Eutectic Flow in the Tokamak Blanket Heat-Sink Systems," Magnetohydrodynamics, 49(1-2), pp. 237-248.
- [143] Chen, H., Zhou, T., Yang, Z., Lü, R., Zhu, Z., and Ni, M., 2010, 'Magnetohydrodynamic Experimental Design and Program for Chinese Liquid Metal LiPb Experimental Loop DRAGON-IV," Fusion Eng. Des., **85**(10–12), pp. 1742–1746.
- [144] Ivanov, S., Shishko, A., Flerov, A., Platacis, E., Romanchuks, A., and Zik, A., 2014, "MHD PbLi Loop at IPUL," In 9th PAMIR International Conference on Fundamental and Applied MHD, pp. 76-80.
- [145] Meng, Z., Zhu, Z., He, J., and Ni, M., 2015, "Experimental Studies of MHD Pressure Drop of PbLi Flow in Rectangular Pipes Under Uniform Magnetic Field," J. Fusion Energ., 34(4), pp. 759–764.
- [146] Courtessole, C., Smolentsev, S., Sketchley, T., and Abdou, M., 2016, "MHD PbLi Experiments in MaPLE Loop at UCLA," Fusion Eng. Des., 109-111, pp. 1016-1021.
- [147] Hon, A. Y., Kirillov, I., Komov, K., Kovalchuk, O., Lancetov, A., Obukhov, D., Pertsev, D., Pugachev, A., Rodin, I. Y., and Zapretilina, E., 2017, "Lead-Lithium Facility With Superconducting Magnet for MHD/HT Tests of Liquid Metal Breeder Blanket," Fusion Eng. Des., 124, pp. 832-836.
- [148] Kumar, M., Patel, A., Jaiswal, A., Ranjan, A., Mohanta, D., Sahu, S., Saraswat, A., Rao, P., Rao, T. S., Mehta, V., Ranjith Kumar, S., Bhattacharyay, R., Rajendrakumar, E., Malhotra, S., and Satyamurthy, P., 2019, "Engineering Design and Development of Lead Lithium Loop for Thermo-Fluid Mhd Studies," Fusion Eng. Des., 138, pp. 1-5.
- [149] Takahashi, M., Aritomi, M., Inoue, A., and Matsuzaki, M., 1998, "MHD Pressure Drop and Heat Transfer of Lithium Single-Phase Flow in a Rectangular Channel Under Transverse Magnetic Field," Fusion Eng. Des., 42(1-4), pp. 365-372.
- [150] Grinberg, G., Kavdze, M., and Lielavsis, O., 1985, "Local MHD Resistances on a Liquid Sodium Circuit With a Superconducting Magnet," Magnetohydrodynamics, 21(1), pp. 99-104.
- [151] Eckert, S., Gerbeth, G., Witke, W., and Langenbrunner, H., 2001, "MHD Turbulence Measurements in a Sodium Channel Flow Exposed to a Transverse Magnetic Field," Int. J. Heat Fluid Flow, 22(3), pp. 358–364.
- [152] Evtushenko, I., Sidorenkov, S., and Shishko, A. Y., 1993, "Experimental Studies of Magnetohydrodynamic Processes in Slotted Channels Within a Strong Magnetic Field," Magnetohydrodynamics, 28(2), pp. 182–192.
- [153] Buhler, L., Mistrangelo, C., and Koehly, C., 2012, "Layout of an Experimental Liquid-Metal Circuit Based on MHD Considerations," IEEE Trans. Plasma Sci., 40(3), pp. 590–595.

- [154] Miyazaki, K., Kotake, S., Yamaoka, N., Inoue, S., and Fujii-E, Y., 1983, 'MHD Pressure Drop of NaK Flow in Stainless Steel Pipe," Nucl. Technol.-Fusion, 4(2P2), pp. 447–452.
- [155] Bühler, L., Horanyi, S., and Arbogast, E., 2007, "Experimental Investigation of Liquid-Metal Flows Through a Sudden Expansion at Fusion-Relevant Hart-
- mann Numbers," Fusion Eng. Des., 82(15–24), pp. 2239–2245.

 [156] Satyamurthy, P., Swain, P., Tiwari, V., Kirillov, I., Obukhov, D., and Pertsev, D., 2015, "Experiments and Numerical MHD Analysis of LLCB TBM Test-Section With NaK at 1 T Magnetic Field," Fusion Eng. Des., 91, pp. 44-51.
- [157] Batenin, V., Belyaev, I., Sviridov, V., Sviridov, E., and Listratov, Y. I., 2015, "Modernization of the Experimental Base for Studies of MHD Heat Exchange at Advanced Nuclear Power Facilities," High Temp., 53(6), pp. 904-907.
- [158] Bühler, L., Mistrangelo, C., Konys, J., Bhattacharyay, R., Huang, Q., Obukhov, D., Smolentsev, S., and Utili, M., 2015, "Facilities, Testing Program and Modeling Needs for Studying Liquid Metal Magnetohydrodynamic Flows in Fusion Blankets," Fusion Eng. Des., 100, pp. 55-64.
- [159] Sagara, A., Tanaka, T., Yagi, J., Takahashi, M., Miura, K., Yokomine, T., Fukada, S., and Ishiyama, S., 2015, "First Operation of the Flinak/LiPb Twin Loop OROSH2I-2 With a 3T SC Magnet for R&D of Liquid Blanket for Fusion Reactor," Fusion Sci. Technol., 68(2), pp. 303-307.
- [160] Blum, É. Y., Mikhailov, Y. A., and Ozols, R. Y., 1980, Heat and Mass Exchange in a Magnetic Field, Zinatne, Riga, USSR (in Russian).
- [161] Molokov, S., Moreau, R., and Moffatt, H. K., 2007, Magnetohydrodynamics: Historical Evolution and Trends, Springer, Berlin.
- [162] Schulenberg, T., and Stieglitz, R., 2010, "Flow Measurement Techniques in Heavy Liquid Metals," Nucl. Eng. Des., 240(9), pp. 2077–2087.
- [163] Eckert, S., Buchenau, D., Gerbeth, G., Stefani, F., and Weiss, F.-P., 2011, 'Some Recent Developments in the Field of Measuring Techniques and Instrumentation for Liquid Metal Flows," J. Nucl. Sci. Technol., 48(4), pp. 490-498
- [164] Roelofs, F., 2018, Thermal Hydraulics Aspects of Liquid Metal Cooled Nuclear Reactors, Woodhead Publishing, Cambridge, UK.
- [165] Zhilin, V., Zvyagin, K., Ivochkin, Y. P., and Oksman, A., 1989, "Diagnostics of Liquid Metal Flows Using Fibre-Optic Velocity Sensor," Liquid Metal Magnetohydrodynamics, Springer, Berlin/Heidelberg, Germany, pp. 373-379.
- [166] Kovalev, S., Ogorodnikov, V., Osipov, V., Sviridov, V., and Tsoi, V., 1993, Velocity Fluctuation Measurements in a Nonisothermal Liquid Metal Flow in a Longitudinal Magnetic Field," Magnetohydrodynamics, 28(3), pp. 300-304.
- [167] Eckert, S., Witke, W., and Gerbeth, G., 2000, "A New Mechano-Optical Technique to Measure Local Velocities in Opaque Fluids," Flow Meas. Inst., 11(2),
- [168] Belyaev, I., Razuvanov, N., Sviridov, V., and Zagorsky, V., Temperature Correlation Velocimetry Technique in Liquid Metals," Flow Meas. Inst., 55, pp. 37-43.
- [169] Zhang, J., and Li, N., 2007, "Analysis on Liquid Metal Corrosion-Oxidation Interactions," Corros. Sci., 49(11), pp. 4154–4184.
 [170] Yaskiv, O., and Fedirko, V., 2014, "Oxidation/Corrosion Behaviour of Ods
- Ferritic/Martensitic Steels in pb Melt at Elevated Temperature," Int. J. Nucl. Energy, 2014, pp. 1-8.
- [171] Courouau, J., Lorentz, V., Tabarant, M., Bosonnet, S., and Balbaud-Célérier, F., 2013, "Corrosion by Oxidation and Carburization in Liquid Sodium at 550°C of Austenitic Steels for Sodium Fast Reactors," International Conference on Fast Reactors and Related Fuel Cycles (FR13), Paris, France, Mar., pp. 1-12.
- [172] Thess, A., Votyakov, E. V., and Kolesnikov, Y., 2006, "Lorentz Force Velocimetry," Phys. Rev. Lett., 96(16).
- [173] Thess, A., Votyakov, E., Knaepen, B., and Zikanov, O., 2007, "Theory of the Lorentz Force Flowmeter," New J. Phys., 9(8), pp. 299–299.
 [174] Stefani, F., Gundrum, T., and Gerbeth, G., 2004, "Contactless Inductive Flow
- Tomography," Phys. Rev. E, **70**(5), p. 056306.
- [175] Franke, S., Lieske, H., Fischer, A., Büttner, L., Czarske, J., Räbiger, D., and Eckert, S., 2013, "Two-Dimensional Ultrasound Doppler Velocimeter for Flow Mapping of Unsteady Liquid Metal Flows," Ultrason., 53(3), pp. 691–700.
- [176] Belyaev, I., Biryukov, D., Pyatnitskaya, N. Y., Razuvanov, N., Sviridov, E., and Sviridov, V., 2019, "A Technique for Scanning Probe Measurement of Temperature Fields in a Liquid Flow," Therm. Eng., 66(6), pp. 377–387.

 [177] Belyaev, I., Frick, P., Razuvanov, N., Sviridov, E., and Sviridov, V., 2018,
- Temperature Fluctuations in a Nonisothermal Mercury Pipe Flow Affected by a Strong Transverse Magnetic Field," Int. J. Heat Mass Transfer, 127, pp. 566-572.
- [178] Belyaev, I., Biryukov, D., Kotlyar, A., Belavina, E., Sardov, P., and Sviridov, V., 2019, "Heat Transfer During Mixed Convection of a Molten Salt in the Presence of Magnetic Fields," Tech. Phys. Lett., 45(5), pp. 499-502.
- Li, L., and Zheng, W., 2017, "A Robust Solver for the Finite Element Approximation of Stationary Incompressible Mhd Equations in 3D," J. Comp. Phys., 351, pp. 254-270.
- [180] Planas, R., Badia, S., and Codina, R., 2011, "Approximation of the Inductionless Mhd Problem Using a Stabilized Finite Element Method," J. Comp. Phys., 230(8), pp. 2977–2996.
- [181] Artemov, V., Yan'kov, G., Karpov, V., and Makarov, M., 2000, "Computer Simulation of Heat and Mass Exchanges in the Elements of Heat-Engineering
- and Power Equipment," Thermal Eng., No. 7, pp. 52–59. [182] Di Piazza, I., and Bühler, L., 2000, "A General Computational Approach for Magnetohydrodynamic Flows Using the CFX Code: Buoyant Flow Through a Vertical Square Channel," Fusion Techn., 38(2), pp. 180-189.

- [183] Mistrangelo, C., 2005, "Three-Dimensional MHD Flow in Sudden Expansions," Ph.D. thesis, TU Karlsruhe, Karlsruhe, Germany.
 [184] Mistrangelo, C., and Bühler, L., 2011, "Development of a Numerical Tool to
- Simulate Magnetohydrodynamic Interactions of Liquid Metals With Strong Applied Magnetic Fields," Fusion Sci. Technol., 60(2), pp. 798-803.
- [185] Kim, S. H., Kim, M. H., Lee, D. W., and Choi, C., 2012, "Code Validation and Development for MHD Analysis of Liquid Metal Flow in Korean TBM,' Fusion Eng. Des., **87**(7–8), pp. 951–955.
- [186] Feng, J., Chen, H., He, Q., and Ye, M., 2015, "Further Validation of Liquid Metal MHD Code for Unstructured Grid Based on OpenFOAM," Fusion Eng. Des., 100, pp. 260-264.
- [187] Smolentsev, S., Courtessole, C., Abdou, M., Sharafat, S., Sahu, S., and Sketchley, T., 2016, "Numerical Modeling of First Experiments on PbLi MHD Flows in a Rectangular Duct With Foam-Based SiC Flow Channel Insert," Fusion Eng. Des., 108, pp. 7-20.
- [188] Meng, Z., Ni, M., Jiang, J., Zhu, Z., and Zhou, T., 2016, "Code Validation for Magnetohydrodynamic Buoyant Flow at High Hartmann Number," J. Fusion Energ., 35(2), pp. 148-153.
- [189] Belyaev, I., Listratov, Y., Melnikov, I., Razuvanov, N., Sviridov, V., and Sviridov, E., 2016, "Engineering Approach to Numerical Simulation of MHD Heat Transfer," Magnetohydrodynamics, 52(3), p. 287.
- [190] Tassone, A., Caruso, G., Del Nevo, A., and Di Piazza, I., 2017, "CFD Simulation of the Magnetohydrodynamic Flow Inside the WCLL Breeding Blanket Module," Fusion Eng. Des., 124, pp. 705-709.
- [191] Sahu, S., and Bhattacharyay, R., 2018, "Validation of COMSOL Code for Analyzing Liquid Metal Magnetohydrodynamic Flow," Fusion Eng. Des. 127, pp. 151-159.
- [192] Belyaev, I. A., Razuvanov, N. G., and Sviridov, V. G., 2018, "A Method to Calculate Mixed MHD Convention in a Vertical Channel," High Temp., **56**(5), pp. 767–773.
- [193] Smolentsev, S., Rhodes, T., Yan, Y., Tassone, A., Mistrangelo, C., Bühler, L., and Urgorri, F., 2020, "Code-to-Code Comparison for a PbLi Mixed-Convection MHD Flow," Fusion Sci. Technol., pp. 1–17.
- [194] Huang, P., Chhabra, R., Munipalli, R., Pulugundla, G., Kawczynski, C., and Smolentsev, S., 2017, "A Comprehensive High Performance Predictive Tool for Fusion Liquid Metal Hydromagnetics," HyPerComp Inc., Westlake Village, CA, Report No. HPC-DOE-P2SBIR-FINAL-2017.
- [195] Smolentsev, S., Badia, S., Bhattacharyay, R., Bühler, L., Chen, L., Huang, Q., Jin, H.-G., Krasnov, D., Lee, D.-W., de Les Valls, E. M., Mistrangelo, C., Munipalli, R., Ni, M.-J., Pashkevich, D., Patel, A., Pulugundla, G., Satyamurthy, P., Snegirev, A., Sviridov, V., Swain, P., Zhou, T., and Zikanov, O., 2015, "An Approach to Verification and Validation of MHD Codes for Fusion Applications," Fusion Eng. Des., 100, pp. 65-72.
- [196] Ni, M.-J., Munipalli, R., Huang, P., Morley, N. B., and Abdou, M. A., 2007, "A Current Density Conservative Scheme for Incompressible MHD Flows at a Low Magnetic Reynolds Number. Part I: On a Rectangular Collocated Grid System," J. Comp. Phys., 227(1), pp. 174-204.
- [197] Ni, M.-J., Munipalli, R., Huang, P., Morley, N. B., and Abdou, M. A., 2007, "A Current Density Conservative Scheme for Incompressible MHD Flows at a Low Magnetic Reynolds Number. Part II: On an Arbitrary Collocated Mesh," J. Comp. Phys., 227(1), pp. 205–228.
- [198] Vantieghem, S., and Knaepen, B., 2011, "Numerical Simulation of Magnetohydrodynamic Flow in a Toroidal Duct of Square Cross-Section," Int. J. Heat Fluid Flow, 32(6), pp. 1120-1128.
- [199] Krasnov, D., Zikanov, O., and Boeck, T., 2011, "Comparative Study of Finite Difference Approaches to Simulation of Magnetohydrodynamic Turbulence at Low Magnetic Reynolds Number," Comp. Fluids, 50(1), pp. 46-59.
- [200] Ni, M.-J., and Li, J.-F., 2012, "A Consistent and Conservative Scheme for Incompressible MHD Flows at a Low Magnetic Reynolds Number. Part III: On a Staggered Mesh," J. Comp. Phys., 231(2), pp. 281–298. [201] Gelfgat, A. Y., and Zikanov, O., 2018, "Computational Modeling of Magneto-
- convection: Effects of Discretization Method, Grid Refinement and Grid Stretching," Comput. Fluids, 175, pp. 66-82.
- [202] Chen, L., Smolentsev, S., and Ni, M.-J., 2020, "Toward Full Simulations for a Liquid Metal Blanket: MHD Flow Computations for a PbLi Blanket Prototype at Ha ~ 10⁴," Nucl. Fusion, **60**(7), p. 076003. [203] Morinishi, Y., Lund, T. S., Vasilyev, O. V., and Moin, P., 1998, "Fully Con-
- servative Higher Order Finite Difference Schemes for Incompressible Flow," J. Comp. Phys., **143**(1), pp. 90–124.
- [204] Zhao, Y., Zikanov, O., and Krasnov, D., 2011, "Instability of Magnetohydrodynamic Flow in an Annular Channel at High Hartmann Number," Phys. Fluids, 23(8), p. 084103.
- [205] Zhao, Y., and Zikanov, O., 2012, "Instabilities and Turbulence in Magnetohydrodynamic Flow in a Toroidal Duct Prior to Transition in Hartmann Layers," J. Fluid Mech., **692**, pp. 288–316.
- [206] Zhang, J., and Ni, M.-J., 2014, "A Consistent and Conservative Scheme for MHD Flows With Complex Boundaries on an Unstructured Cartesian Adaptive System," J. Comp. Phys., 256, pp. 520–542.
 [207] Zikanov, O., and Listratov, Y., 2016, "Numerical Investigation of MHD Heat
- Transfer in a Vertical Round Tube Affected by Transverse Magnetic Field," Fusion Eng. Des., 113, pp. 151–161.
- [208] Patel, A., Pulugundla, G., Smolentsev, S., Abdou, M., and Bhattacharyay, R., 2018, "Validation of Numerical Solvers for Liquid Metal Flow in a Complex Geometry in the Presence of a Strong Magnetic Field," Theor. Comp. Fluid Dyn., 32(2), pp. 165–178.

- [209] Sarris, I. E., Kassinos, S. C., and Carati, D., 2007, "Large-Eddy Simulations of the Turbulent Hartmann Flow Close to the Transitional Regime," Phys. Fluids, 19(8), p. 085109.
- [210] Kobayashi, H., 2006, "Large Eddy Simulation of Magnetohydrodynamic Turbulent Channel Flows With Local Subgrid-Scale Model Based on Coherent Structures," Phys. Fluids, 18(4), p. 045107.
- [211] Kobayashi, H., 2008, "Large Eddy Simulation of Magnetohydrodynamic Turbulent Duct Flows," Phys. Fluids, 20(1), p. 015102.
- [212] Viré, A., Krasnov, D., Boeck, T., and Knaepen, B., 2011, "Modeling and Discretization Errors in Large Eddy Simulations of Hydrodynamic and Magnetohydrodynamic Channel Flows," J. Comp. Phys., 230(5), pp. 1903–1922.
- [213] Artemov, V. I., Makarov, M. V., Minko, K. B., and Yankov, G. G., 2020, "Assessment of Performance of Subgrid Stress Models for a Les Technique for Predicting Suppression of Turbulence and Heat Transfer in Channel Flows Under the Influence of Body Forces," Int. J. Heat Mass Transfer, 146, p. 118822.
- [214] Vorobev, A., and Zikanov, O., 2008, "Smagorinsky Constant in LES Modeling of Anisotropic MHD Turbulence," Theor. Comp. Fluid Dyn., 22(3–4), pp. 317–325.
- [215] Widlund, O., Zahrai, S., and Bark, F. H., 1998, "Development of a Reynolds Stress Closure for Modeling of Homogeneous MHD Turbulence," Phys. Fluids, 10(8), pp. 1987–1996.
- [216] Widlund, O., 2000, "Modeling of Magnetohydrodynamic Turbulence," Ph.D. thesis, Royal Institute of Technology, Stockholm, Sweden.
- [217] Kenjerec, S., and Hanjalic, A., 2000, "On the Implementation of Effects of Lorentz Force in Turbulence Closure Models," Int. J. Heat Fluid Flow, 21, pp. 329–337.
- [218] Kenjeres, S., Hanjalic, K., and Bal, D., 2004, "A Direct-Numerical-Simulation-Based Second-Moment Closure for Turbulent Magnetohydrodynamic Flows," Phys. Fluids, 16(5), pp. 1229–1241.
- [219] Yamamoto, Y., Kunugi, T., Satake, S-I., and Smolentsev, S., 2008, "DNS and k-Epsilon Model Simulation of MHD Turbulent Channel Flows With Heat Transfer," Fusion Eng. Des., 83(7–9), pp. 1309–1312.
- [220] Yamamoto, Y., Osawa, N., and Kunugi, T., 2017, "A New RANS Model in Turbulent Channel Flow Imposed Wall-Normal Magnetic Field With Heat Transfer," Fusion Sci. Technol., 72(4), pp. 601–608.
- [221] Genin, L., Kovalev, S., and Sviridov, V., 1987, "Convective Heat Transfer for a Liquid Metal in a Pipe in a Longitudinal Magnetic Field," Magnetohydrodynamics, 23(4), pp. 374–378.
- [222] Miyazaki, K., Yamashita, S., and Yamaoka, N., 1987, "Natural Convection Heat Transfer of Liquid Lithium Under Transverse and Parallel Magnetic Fields," J. Nucl. Sci. Technol., 24(5), pp. 409–414.
- [223] Belyaev, I., Sardov, P., Melnikov, I., and Frick, P., 2021, "Limits of Strong Magneto-Convective Fluctuations in Liquid Metal Flow in a Heated Vertical Pipe Affected by a Transverse Magnetic Field," Int. J. Therm. Sci., 161, p. 106773.
- [224] Kirillov, I. R., and Muraviev, E. V., 1997, "Review of Liquid Metal Divertor Concepts for Tokamak Reactors," *Fusion Technology* 1996, Elsevier, Amsterdam, The Netherlands, pp. 251–254.
- [225] Sviridov, V. G., Razuvanov, N. G., Ivochkin, Y. P., Listratov, Y. I., Sviridov, E. V., Genin, L. G., Zhilin, V. G., and Belyaev, I. A., 2010, "Liquid Metal Heat Transfer Investigations Applied to Tokamak Reactor," ASME Paper No. IHTC14-22369.
- [226] Genin, L. G., Zhilin, V. G., Ivochkin, Y. P., Razuvanov, N. G., Belyaev, I. A., Listratov, Y. I., and Sviridov, V. G., 2011, "Temperature Fluctuations in a Heated Horizontal Tube Affected by Transverse Magnetic Field," Proc. Eighth PAMIR Conf. Fund. Appl. MHD, Borgo, Corsica, France, Sept., pp. 37–41.
- [227] Belyaev, I., Ivochkin, Y. P., Listratov, Y. I., Razuvanov, N., and Sviridov, V., 2015, "Temperature Fluctuations in a Liquid Metal MHD-Flow in a Horizontal Inhomogeneously Heated Tube," High Temp., 53(5), pp. 734–741.
- [228] Sahu, S., Courtessole, C., Ranjan, A., Bhattacharyay, R., Sketchley, T., and Smolentsev, S., 2020, "Thermal Convection Studies in Liquid Metal Flow Inside a Horizontal Duct Under the Influence of Transverse Magnetic Field," Phys. Fluids, 32(6), p. 067107.
- [229] Listratov, Y., Ognerubov, D., Zikanov, O., and Sviridov, V., 2018, "Numerical Simulations of Mixed Convection in Liquid Metal Flow Within a Horizontal Pipe With Transverse Magnetic Field," Fluid Dyn. Res., 50(5), p. 051407.
- [230] Vo, T., Pothérat, A., and Sheard, G. J., 2017, "Linear Stability of Horizontal, Laminar Fully Developed, Quasi-Two-Dimensional Liquid Metal Duct Flow Under a Transverse Magnetic Field and Heated From Below," Phys. Rev. Fluids, 2(3), p. 033902.
- [231] Genin, L., Zhilin, V. G., Ivochkin, Y. P., Listratov, Y. I., Razuvanov, N., Sarvin, R., and Sviridov, V., 2006, "Experimental Investigation of Heat Transfer Along the Length of a Horizontal Tube During Liquid Metal Heat-Carrier Flow in a Transverse Magnetic Field," Heat Trans. Res., 37(3), pp. 247–258.
- [232] Belyaev, I., Genin, L., Listratov, Y. I., Melnikov, I., Sviridov, V., Sviridov, E., Ivochkin, Y. P., Razuvanov, N., and Shpansky, Y. S., 2013, "Specific Features of Liquid Metal Heat Transfer in a Tokamak Reactor," Magnetohydrodynamics, 49(1-2), pp. 177–190.
- [233] Giancarli, L. M., Ahn, M.-Y., Bonnett, I., Boyer, C., Chaudhuri, P., Davis, W., Dell'Orco, G., Iseli, M., Michling, R., Neviere, J.-C., Pascal, R., Poitevin, Y., Ricapito, I., Schneiderova, I., Sexton, L., Tanigawa, H., Tonqueze, Y. L., van der Laan, J. G., Wang, X., and Yoshino, R., 2018, "ITER TBM Program and Associated System Engineering," Fusion Eng. Des., 136, pp. 815–821.
- Associated System Engineering," Fusion Eng. Des., 136, pp. 815–821.

 [234] Melnikov, I., Sviridov, E., Sviridov, V., and Razuvanov, N., 2016,
 "Experimental Investigation of Mhd Heat Transfer in a Vertical Round Tube
 Affected by Transverse Magnetic Field," Fusion Eng. Des., 112, pp. 505–512.

- [235] Kirillov, I. R., Obukhov, D. M., Genin, L. G., Sviridov, V. G., Razuvanov, N. G., Batenin, V. M., Belyaev, I. A., Poddubnyi, I. I., and Pyatnitskaya, N. Y., 2016, "Buoyancy Effects in Vertical Rectangular Duct With Coplanar Magnetic Field and Single Sided Heat Load," Ensign Eng. Des. 104, pp. 1–8.
- Magnetic Field and Single Sided Heat Load," Fusion Eng. Des., 104, pp. 1–8.

 [236] Listratov, Y., Melnikov, I., Razuvanov, N., Sviridov, V., and Zikanov, O., 2016, "Convection Instability and Temperature Fluctuations in a Downward Flow in a Vertical Pipe With Strong Transverse Magnetic Field," Proceedings of 10th PAMIR Conference Fundamental and Applied MHD, Cagliari, Italy, June, pp. 112–116.
- [237] Razuvanov, N., Frick, P., Belyaev, I., and Sviridov, V., 2019, "Experimental Study of Liquid Metal Heat Transfer in a Vertical Duct Affected by Coplanar Magnetic Field: Downward Flow," Int. J. Heat Mass Transf., 143, p. 118529.
- [238] Razuvanov, N., Pyatnitskaya, N., Frick, P., Belyaev, I., and Sviridov, V., 2020, "Experimental Study of Liquid Metal Heat Transfer in a Vertical Duct Affected by Coplanar Magnetic Field: Upward Flow," Int. J. Heat Mass Transf., 156, p. 119746.
- [239] Vetcha, N., Smolentsev, S., and Abdou, M., 2011, "Stability Analysis for Buoyancy-Opposed Flows in Poloidal Ducts of the DCLL Blanket," Fusion Sci. Technol., 60(2), pp. 518–522.
- [240] Kolesnikov, Y. B., 1972, "Two-Dimensional Turbulent Flow in a Channel With Inhomogeneous Electrical Conductivity of the Walls," Magnetohydrodynamics, 8(3), pp. 308–312.
- [241] Burr, U., Barleon, L., Müller, U., and Tsinober, A., 2000, "Turbulent Transport of Momentum and Heat in Magnetohydrodynamic Rectangular Duct Flow With Strong Sidewall Jets," J. Fluid Mech., 406, pp. 247–279.
- [242] Andreev, O., Kolesnikov, Y., and Thess, A., 2006, "Experimental Study of Liquid Metal Channel Flow Under the Influence of a Nonuniform Magnetic Field," Phys. Fluids, 18(6), p. 065108.
- [243] Belyaev, I., Biryukov, D., Pyatnitskaya, N. Y., Razuvanov, N., and Sviridov, V., 2018, "Temperature Fluctuations Accompanying MHD Heat Transfer of Liquid Metal Downflow in a Pipe," Fluid Dyn. Res., 50(5), p. 051403.
- [244] Kirillov, I., Obukhov, D., Sviridov, V., Razuvanov, N., Belyaev, I., Poddubnyi, I., and Kostichev, P., 2018, "Buoyancy Effects in Vertical Rectangular Duct With Coplanar Magnetic Field and Single Sided Heat Load–Downward and Upward Flow," Fusion Eng. Des., 127, pp. 226–233.
 [245] Luchinkin, N., Razuvanov, N., Belyaev, I., and Sviridov, V., 2020, "Heat
- [245] Luchinkin, N., Razuvanov, N., Belyaev, I., and Sviridov, V., 2020, "Heat Transfer in Liquid Metal at an Upward Flow in a Pipe in Transverse Magnetic Field," High Temp., 58(3), pp. 400–409.
- [246] Vetcha, N., Smolentsev, S., and Abdou, M., 2009, "Theoretical Study of Mixed Convection in Poloidal Flows of DCLL Blanket," Fusion Sci. Technol., 56(2), pp. 851–855.
- [247] Smolentsev, S., Vetcha, N., and Abdou, M., 2013, "Effect of a Magnetic Field on Stability and Transitions in Liquid Breeder Flows in a Blanket," Fusion Eng. Des., 88(6–8), pp. 607–610.
- [248] Liu, Z.-H., Chen, L., Ni, M.-J., and Zhang, N.-M., 2019, "Effects of Magneto-hydrodynamic Mixed Convection on Fluid Flow and Structural Stresses in the DCLL Blanket," Int. J. Heat Mass Transf., 135, pp. 847–859.
- [249] Rhodes, T. J., Pulugundla, G., Smolentsev, S., and Abdou, M., 2020, "3D Modelling of MHD Mixed Convection Flow in a Vertical Duct With Transverse Magnetic Field and Volumetric or Surface Heating," Fusion Eng. Des., 160, p. 111834.
- [250] Belyaev, I., Krasnov, D., Kolesnikov, Y., Biryukov, D., Chernysh, D., Zikanov, O., and Listratov, Y., 2020, "Effects of Symmetry on Magnetohydrodynamic Mixed Convection Flow in a Vertical Duct," Phys. Fluids, 32(9), p. 094106.
- [251] Stuart, J. T., 1954, "On the Stability of Viscous Flow Between Parallel Planes in the Presence of a Co-Planar Magnetic Field," Proc. Roy. Soc. London. Ser. A. Math. Phys. Sci., 221, pp. 189 –206.
- [252] Globe, S., 1961, "The Effect of a Longitudinal Magnetic Field on Pipe Flow of Mercury," J. Heat Trans., 83(4), pp. 445–453.
- [253] Hunt, J. C. R., 1966, "On the Stability of Parallel Flows With Parallel Magnetic Fields," Proc. Roy. Soc. London. Ser. A. Math. Phys. Sci., 293, pp. 342–358
- [254] Fraim, F. W., and Heiser, W. H., 1968, "The Effect of a Strong Longitudinal Magnetic Field on the Flow of Mercury in a Circular Tube," J. Fluid Mech., 33(02), pp. 397–413.
- [255] Kovner, D. S., Krasil'nikov, E. Y., Nikolaenko, V. S., and Panevin, I. G., 1971, "Experimental Study of the Effect of a Longitudinal Magnetic Field on Convective Heat Transfer in a Turbulent Tube Flow of Conducting Liquid," Magnetohydrodynamics, 3(2), pp. 60–63.
- [256] Levin, V. B., and Chinenkov, I. A., 1966, "Experimental Investigations of the Turbulent Flow of an Electrically Conducting Fluid in a Tube in a Longitudinal Magnetic Field," Magnetohydrodynamics, 2(4), pp. 89–90.
- [257] Branover, G. G., 1967, "Suppression of Turbulence in Pipes With Transverse and Longitudinal Magnetic Fields," Magnetohydrodynamics, 3(2), pp. 106 –107.
- [258] Genin, L., Zhilin, V., and Manchkha, S., 1970, "Effect of a Longitudinal Magnetic Field on Stability of Flow of an Electrically Conducting Liquid," Teplofiz. Vys. Temp, 8(2), p. 428.
- [259] Genin, L. G., Manchkha, S. P., and Sviridov, V. G., 1973, "Effect of a Longitudinal Magnetic Field on the Statistical Properties of Turbulent Temperature Fluctuations in Mercury Flow in a Circular Pipe," Magnetohydrodynamics, 9(4), pp. 462–467.
- [260] Krasilnikov, E. I., Lushchik, V. G., Nikolaenko, V. S., Panevin, I., Platnieks, I., and Tsinober, A. B., 1975, "Experimental Investigation of the Pulsation

- Characteristics of Turbulent Flow of a Conducting Fluid in a Tube in a Longitudinal Magnetic Field," Docl. Phys, **225**, pp. 1281–1283.
- [261] Genin, L. G., Manchkha, S. P., and Sviridov, V. G., 1978, "Turbulent Transfer Coefficients in the Case of the Flow of a Liquid Metal in a Tube in a Longitudinal Magnetic Field," Magnetohydrodynamics, 14(2), pp. 179–183.
- [262] Genin, L., and Krasnoshchekova, T., 1982, "Flow of an Electrically Conducting Liquid in a Pipe With a Longitudinal Magnetic Field," Magnetohydrodynamics, 18(3), pp. 258–262.
- [263] Lee, D., and Choi, H., 2001, "Magnetohydrodynamic Turbulent Flow in a Channel at Low Magnetic Reynolds Number," J. Fluid Mech., 439, pp. 367–394.
- [264] Dey, P., and Zikanov, O., 2012, "Turbulent Flow and Transport of Passive Scalar in Magnetohydrodynamic Channel Flows With Different Orientations of Magnetic Field," Int. J. Heat Fluid Flow, 36, pp. 101–117.
- [265] Dong, S., Krasnov, D., and Boeck, T., 2012, "Secondary Energy Growth and Turbulence Suppression in Conducting Channel Flow With Streamwise Magnetic Field," Phys. Fluids, 24(7), p. 074101.
- [266] Hunt, J. C. R., and Hancox, R., 1971, "The Use of Liquid Lithium as Coolant in a Toroidal Fusion Reactor," Technical Report CLM-R 115, Culham Lab., 11K
- [267] Malang, S., Arheidt, K., and Barleon, L., 1988, "Self-Cooled Liquid-Metal Blanket Concept," Fusion Technol., 14(3), pp. 1343–1356.
- [268] Molokov, S., and Bühler, L., 1994, "Liquid Metal Flow in a U-Bend in a Strong Uniform Magnetic Field," J. Fluid Mech., 267, pp. 325–352.
- [269] Stieglitz, R., Barleon, L., Bühler, L., and Molokov, S., 1996, "Magnetohydrodynamic Flow in a Right-Angle Bend in a Strong Magnetic Field," J. Fluid Mech., 326, pp. 91–123.
- [270] Stieglitz, R., and Molokov, S., 1997, "Experimental Study of Magnetohydrodynamic Flows in Electrically Coupled Bends," J. Fluid Mech., 343, pp. 1–28.
- [271] Genin, L., and Sviridov, V. G., 1983, "Heat Transfer and Temperature Distribution in the Initial Thermal Section of a Flow of Liquid Metal in a Longitudinal Magnetic Field," Magnetohydrodynamics, 19(2), pp. 140–145.
- nal Magnetic Field," Magnetohydrodynamics, 19(2), pp. 140–145.

 [272] Genin, L., Ninh, K. B., Pakhotin, Y. A., and Sviridov, V. G., 1983, "Heat Exchange of a Liquid Metal in a Tube in the Longitudinal Magnetic Field of a Solenoid With Account Taken of End Effects," Magnetohydrodynamics, 19(3), pp. 268–273.
- [273] Sviridov, V. G., and Shpanskii, Y. S., 1994, "Effect of the Thermogravitational Convection and a Longitudinal Magnetic Field on the Heat Exchange in Liquid Metal Flow Trough a Horizontal Pipe," Magnetohydrodynamics, 30(1), pp. 75–83.
- [274] Sviridov, V., Shpanskii, Y., and Razuvanov, N., 1997, "Experimental Investigation of Liquid Metal Heat Transfer Under Conditions, Approximating Those in a Real Tokamak Reactor," Magnetohydrodynamics, 33(4), pp. 418–421.
- [275] Akhmedagaev, R., Listratov, Y., and Belyaev, I., 2019, "Numerical Study of Secondary Flows in Liquid Metal in a Pipe Affected by a Longitudinal Magnetic Field," Magnetohydrodynamics, 55(4), pp. 475–490.
 [276] Zhang, X., and Zikanov, O., 2017, "Thermal Convection in a Toroidal Duct of
- [276] Zhang, X., and Zikanov, O., 2017, "Thermal Convection in a Toroidal Duct of a Liquid Metal Blanket. Part I. Effect of Poloidal Magnetic Field," Fusion Eng. Des., 116, pp. 52–60.
- [277] Zhang, X., and Zikanov, O., 2017, "Thermal Convection in a Duct With Strong Axial Magnetic Field," Magnetohydrodynamics, 53(1), pp. 213–220.
- Strong Axial Magnetic Field," Magnetohydrodynamics, **53**(1), pp. 213–220. [278] Shishkina, O., and Horn, S., 2016, "Thermal Convection in Inclined Cylindrical Containers," J. Fluid Mech., **790**, p. R3.
- [279] Khalilov, R., Kolesnichenko, I., Pavlinov, A., Mamykin, A., Shestakov, A., and Frick, P., 2018, "Thermal Convection of Liquid Sodium in Inclined Cylinders," Phys. Rev. Fluids, 3(4), p. 043503.
- [280] Teimurazov, A., and Frick, P., 2017, "Thermal Convection of Liquid Metal in a Long Inclined Cylinder," Phys. Rev. Fluids, 2(11), p. 113501.
- [281] Vasil'ev, A. Y., Kolesnichenko, I. V., Mamykin, A. D., Frick, P. G., Khalilov, R. I., Rogozhkin, S. A., and Pakholkov, V. V., 2015, "Turbulent Convective Heat Transfer in an Inclined Tube Filled With Sodium," Techn. Phys., 60(9), pp. 1305–1309.
- [282] Belyaev, I. A., Listratov, Y. I., Razuvanov, N. G., and Sviridov, V. G., 2011, "Liquid Metal Heat Transfer in Inclined Tube Affected by Longitudinal Magnetic Field," Proc. 8th PAMIR Conf. Fund. Appl. MHD, Borgo, Corsica, France, Sept., pp. 43–47.
- [283] Belyaev, I., Biryukov, D., and Chernysh, D. Y., 2018, "Channel Inclination Influence on MHD-Heat Transfer of Liquid Metal Downflow in a Pipe," Fluid Dyn. Res., 50(5), p. 051417.
- [284] Belyaev, I. A., Chernysh, D. Y., Luchinkin, N., and Razuvanov, N., 2018, "Influence of Channel Inclination on Heat Transfer of Liquid Metal Flow," *Int. Heat Transf. Conf. Digital Lib*, Begel House, Danbury, CT, pp. 3061–3067.
- [285] Belyaev, I., Razuvanov, N., Sviridov, V., and Zagorsky, V., 2015, "Liquid Metal Downflow in an Inclined Heated Tube Affected by a Longitudinal Magnetic Field," Magnetohydrodynamics, 51(4), pp. 673–683.
- [286] Mistrangelo, C., Bühler, L., and Klüber, V., 2020, "Three-Dimensional Magneto Convective Flows in Geometries Relevant for DCLL Blankets," Fusion Eng. Des., 159, p. 111686.
- [287] Shah, R. K., and London, A. L., 2014, Laminar Flow Forced Convection in Ducts: A Source Book for Compact Heat Exchanger Analytical Data, Academic Press, Cambridge, MA.
- [288] Mistrangelo, C., and Buehler, L., 2014, Magnetoconvection in HCLL Blankets, 7672, KIT Scientific Publishing, Karlsruhe, Germany.
- [289] Bühler, L., 1998, "Laminar Buoyant Magnetohydrodynamic Flow in Vertical Rectangular Ducts," Phys. Fluids, 10(1), pp. 223–236.

- [290] Mistrangelo, C., and Bühler, L., 2013, "Magneto-Convective Flows in Electrically and Thermally Coupled Channels," Fusion Eng. Des., 88(9–10), pp. 2323–2327.
- [291] Mistrangelo, C., and Bühler, L., 2009, "Influence of Helium Cooling Channels on Magnetohydrodynamic Flows in the HCLL Blanket," Fusion Eng. Des., 84(7-11), pp. 1323-1328.
- [292] Mistrangelo, C., and Bühler, L., 2012, "Numerical Study of Fundamental Magnetoconvection Phenomena in Electrically Conducting Ducts," IEEE Trans. Plasma Sci., 40(3), pp. 584–589.
- [293] Mistrangelo, C., Bühler, L., and Aiello, G., 2014, "Buoyant-Mhd Flows in Hcll Blankets Caused by Spatially Varying Thermal Loads," IEEE Trans. Plasma Sci., 42(5), pp. 1407–1412.
- [294] Mistrangelo, C., and Bühler, L., 2015, "Magneto Convective Instabilities Driven by Internal Uniform Volumetric Heating," Magnetohydrodynamics, 51(2), pp. 303–310.
- [295] Smolentsev, S., Morley, M., and Abdou, M., 2006, "MHD and Thermal Issues of the SiCf/SiC Flowchannel Insert," Fusion Sci. Technol., 50(1), pp. 107–119.
- [296] Hudoba, A., and Molokov, S., 2016, "Linear Stability of Buoyant Convective Flow in a Vertical Channel With Internal Heat Sources and a Transverse Magnetic Field," Phys. Fluids, 28(11), p. 114103.
- [297] He, Q., Feng, J., and Chen, H., 2016, "Numerical Analysis and Optimization of 3D Magnetohydrodynamic Flows in Rectangular U-Bend," Fus. Eng. Des., 109–111, pp. 1313–1317.
- [298] Mistrangelo, C., 2011, "Topological Analysis of Separation Phenomena in Liquid Metal Flow in Sudden Expansions. Part 2. Magnetohydrodynamic Flow," J. Fluid Mech., 674, pp. 132–162.
- [299] Kim, C. N., 2013, "Computational Analysis of a Liquid Metal Magnetohydrodynamic Flow in a Manifold Under a Uniform Magnetic Field," Fusion Sci. Tech., 64(4), pp. 787–799.
- [300] Albets-Chico, X., Radhakrishnan, H., Kassinos, S., and Knaepen, B., 2011, "Numerical Simulation of a Liquid-Metal Flow in a Poorly Conducting Pipe Subjected to a Strong Fringing Magnetic Field," Phys. Fluids, 23(4), p. 047101.
- [301] Li, F.-C., Sutevski, D., Smolentsev, S., and Abdou, M., 2013, "Experimental and Numerical Studies of Pressure Drop in Pbli Flows in a Circular Duct Under Non-Uniform Transverse Magnetic Field," Fusion Eng. Des., 88(11), pp. 3060–3071.
- [302] Li, Y., and Zikanov, O., 2013, "Laminar Pipe Flow at the Entrance Into Transverse Magnetic Field," Fusion Eng. Des., 88(4), pp. 195–201.
- [303] Pulugundla, G., Smolentsev, S., Rhodes, T., Kawczynski, C., and Abdou, M., 2015, "Transition to a Quasi-Fully Developed MHD Flow in an Electrically Conducting Pipe Under a Transverse Non-Uniform Magnetic Field," Fusion Sci. Techn., 68(3), pp. 684–689.
- [304] Reed, C., Picologlou, B., Hua, T., and Walker, J., 1987, "ALEX Results: A Comparison of Measurements From a Round and a Rectangular Duct With 3-D Code Predictions," Argonne National Laboratory, Lemont, IL, Report No. CONF-871007-90.
- [305] Takeuchi, J., Ichi Satake, S., Morley, N. B., Kunugi, T., Yokomine, T., and Abdou, M. A., 2008, "Experimental Study of MHD Effects on Turbulent Flow of FLIBE Simulant Fluid in Circular Pipe," Fusion Eng. Des., 83(7–9), pp. 1082–1086.
- [306] Takeuchi, J., Satake, S., Miraghaie, R., Yuki, K., Yokomine, T., Kunugi, T., Morley, N., and Abdou, M., 2006, "Study of Heat Transfer Enhancement/Suppression for Molten Salt Flows in a Large Diameter Circular Pipe: Part I: Benchmarking," Fusion Eng. Des., 81(1-7), pp. 601-606.
- Benchmarking," Fusion Eng. Des., 81(1–7), pp. 601–606.

 [307] Knaepen, B., and Moreau, R., 2008, "Magnetohydrodynamic Turbulence at Low Magnetic Reynolds Number," Ann. Rev. Fluid Mech., 40(1), pp. 25–45.
- [308] Satake, S., Kunugi, T., and Smolentsev, S., 2002, "Direct Numerical Simulations of Turbulent Pipe Flow in a Transverse Magnetic Field," J. Turb., 3, pp. 27–29.
- [309] Satake, S., Kunugi, T., Takase, K., and Ose, Y., 2006, "Direct Numerical Simulation of Turbulent Channel Flow Under a Uniform Magnetic Field for Large-Scale Structures at High Reynolds Number," Phys. Fluids, 18(12), p. 125106.
- [310] Nakaharai, H., Takeuchi, J., Yokomine, T., Kunugi, T., Satake, S-I., Morley, N., and Abdou, M., 2007, "The Influence of a Magnetic Field on Turbulent Heat Transfer of a High Prandtl Number Fluid," Exp. Therm. Fluid Sci., 32(1), pp. 23–28.
- [311] Satake, S.-I., Yoshida, N., Kunugi, T., Takase, K., Ose, Y., and Kano, T., 2008, "DNS of Turbulent Heat Transfer Under a Uniform Magnetic Field at High Reynolds Number," Fusion Eng. Des., 83(7–9), pp. 1092–1096.
- [312] Kassinos, S. C., Knaepen, B., and Carati, D., 2007, "The Transport of a Passive Scalar in Magnetohydrodynamic Turbulence Subjected to Mean Shear and Frame Rotation," Phys. Fluids, 19(1), p. 015105.
- [313] Chen, H., Meng, Z., Feng, J., and He, Q., 2014, "Effect of Electromagnetic Coupling on Mhd Flow in the Manifold of Fusion Liquid Metal Blanket," Fusion Eng. Des., 89(7–8), pp. 1406–1410.
- [314] Bluck, M. J., and Wolfendale, M. J., 2015, "An Analytical Solution to Electromagnetically Coupled Duct Flow in MHD," J. Fluid Mech., 771, pp. 595–623.
- [315] Ni, W., Qiu, S., Su, G., Tian, W., and Wu, Y., 2012, "Numerical Investigation of Buoyant Effect on Flow and Heat Transfer of Lithium-Lead Eutectic in DFLL-TBM," Progr. Nucl. En., 58, pp. 108-115.
- [316] Kim, C. N., 2014, "Numerical Examination of Liquid Metal Magnetohydrodynamic Flow in Multiple Channels in the Plane Perpendicular to the Magnetic Field," J. Mech. Sci. Technol., 28(12), pp. 4959–4968.

- [317] Mistrangelo, C., and Bühler, L., 2014, "Liquid Metal Magnetohydrodynamic Flows in Manifolds of Dual Coolant Lead Lithium Blankets," Fusion Eng. Des., 89(7–8), pp. 1319–1323.
- [318] Rhodes, T. J., Smolentsev, S., and Abdou, M., 2018, "Magnetohydrodynamic Pressure Drop and Flow Balancing of Liquid Metal Flow in a Prototypic Fusion Blanket Manifold," Phys. Fluids, 30(5), p. 057101.
- [319] Rhodes, T. J., Smolentsev, S., and Abdou, M., 2018, "Effect of the Length of the Poloidal Ducts on Flow Balancing in a Liquid Metal Blanket," Fusion Eng. Des., 136, pp. 847–851.
- [320] Swain, P. K., Shishko, A., Mukherjee, P., Tiwari, V., Ghorui, S., Bhattacharyay, R., Patel, A., Satyamurthy, P., Ivanov, S., Platacis, E., and Ziks, A., 2018, "Numerical and Experimental Mhd Studies of Lead-Lithium Liquid Metal Flows in Multichannel Test-Section at High Magnetic Fields," Fusion Eng. Des., 132, pp. 73–85.
- [321] Swain, P., Koli, P., Ghorui, S., Mukherjee, P., and Deshpande, A., 2020, "Thermofluid MHD Studies in a Model of Indian LLCB TBM at

- High Magnetic Field Relevant to ITER," Fusion Eng. Des., 150, p. 111374.
- [322] Liu, Z.-H., Ni, M.-J., and Zhang, N.-M., 2019, "Numerical Study of MHD Mixed Convection Under Volumetric Heat Source in Vertical Square Duct With Wall Effects," Theor. Appl. Mech. Lett., 9(3), pp. 152–160.
- [323] Smolentsev, S., Saedi, S., Malang, S., and Abdou, M., 2013, "Numerical Study of Corrosion of Ferritic/Martensitic Steels in the Flowing PbLi With and Without a Magnetic Field," J. Nucl. Mat., 432(1-3), pp. 294-304.
- [324] Spagnuolo, G. A., Chiovaro, P., Di Maio, P. A., and Favetti, R., 2019, "A Multi-Physics Integrated Approach to Breeding Blanket Modelling and Design," Fusion Eng. Des., 143, pp. 35–40.
- [325] Krasnov, D., Kolesnikov, Y. B., Belyaev, I., Listratov, Y. I., and Zikanov, O., 2020, "Liquid Metal Swirling Flow Affected by Transverse Magnetic Field," Magnetohydrodynamics, 56(2–3), pp. 121–129.